

**Cellular and molecular mechanisms of sebaceous
gland morphogenesis and sebaceous tumour
formation**

Inaugural Dissertation

zur

Erlangung des Doktorgrades

der Mathematisch-Naturwissenschaftlichen Fakultät

der Universität zu Köln

vorgelegt von

Daniela Frances

aus Kassel

Köln 2013

Berichterstatter

Prof. Dr. Matthias Hammerschmidt

Prof. Dr. Carien Niessen

Tag der mündlichen Prüfung: 14.06.2012

Table of Contents

1) Introduction.....	1
1.1) The structure of the skin.....	1
1.2) The interfollicular epidermis	2
1.3) The hair follicle	3
1.3.1) Morphogenesis of the HF	4
1.3.2) Cyclic regeneration of the HF	7
1.3.3) Stem cells of the HF bulge region.....	8
1.3.3.1) Lineage tracing of HF bulge stem cells (in K15CreER(G)T2 mice)	9
1.3.3.2) Expression of bulge stem cell marker Keratin 15 in the skin	10
1.3.4) Non-bulge stem and progenitor cell populations of the HF	12
1.4) The sebaceous gland.....	12
1.4.1) Morphogenesis of the SG.....	14
1.4.2) Homeostasis and regeneration of the SG.....	15
1.5) Impaired Wnt / β -Catenin signalling leads to skin tumour formation	16
1.5.1) Canonical Wnt signalling	16
1.5.2) Impact of Wnt / β -Catenin signalling in skin	18
1.5.3) K14 Δ NLef1 mouse model.....	18
1.5.4) K14 Δ NLef1/L61Rac1 double transgenic mice	19
1.6) Aims	20
2) Material and Methods.....	21
2.1) Chemicals and reagents	21
2.1.1) Chemicals.....	21
2.1.2) Solutions and buffers.....	22
2.1.3) Antibodies.....	23
2.1.4) Kits	23
2.2) Mouse experiments.....	24
2.2.1) Mouse models	24
2.2.2) Activation of Cre recombinase.....	24
2.2.3) BrdU / EdU injections	25
2.2.4) Tissue preparation.....	25
2.2.4.1) Tissue preparation for paraffin and cryo embedding.....	25
2.2.4.2) Preparation of epidermal whole mounts.....	26
2.3) Tissue analysis and histology.....	26
2.3.1) Deparaffinisation.....	26
2.3.2) Haematoxylin and eosin staining	26
2.3.3) Immunofluorescence stainings	27
2.3.3.1) Immunofluorescence stainings of epidermal whole mounts.....	27
2.3.3.2) Immunofluorescence stainings of paraffin sections.....	27
2.3.3.3) Immunofluorescence stainings of cryo sections.....	28
2.3.3.4) Immunofluorescence staining of cells	28
2.3.4) Immunohistochemistry (IHC)	29

2.3.5) Alkaline Phosphatase reaction (AP)	29
2.3.6) OilRedO staining	30
2.4) Micro dissection	30
2.5) Molecular Biology	32
2.5.1) Genotyping of experimental mice	32
2.5.1.1) Isolation of genomic DNA (gDNA).....	32
2.5.2) Polymerase Chain Reaction (PCR)	32
2.5.3) Agarose gel electrophoresis	34
2.5.4) Quantitative real-time-PCR.....	34
2.5.5) mRNA isolation and cDNA synthesis.....	35
2.5.6) cDNA-library-generation	35
2.5.7) Oligonucleotid array analysis.....	39
2.6) Cell biology	40
2.6.1) Isolation of primary keratinocytes	40
2.6.2) Cultivation of J2-3T3 fibroblasts and primary keratinocytes.....	40
2.6.3) Fluorescence activated cell sorting.....	41
2.6.4) Colony forming assay	42
3) Results.....	43
3.1) Analysis of SG and HF morphogenesis in mouse tail skin	43
3.1.1) HFs in mouse tail skin develop in two waves.....	43
3.1.2) HF morphogenesis in tail skin is delayed compared to back skin.....	45
3.1.3) Different HF patterning in back and tail skin	46
3.1.4) Two SGs emerge from one cluster of sebocytes	48
3.1.5) Proliferation during HF morphogenesis is not confined to a distinct region of the HF	49
3.1.6) Spatio-temporal analysis of stem and progenitor cell populations during HF morphogenesis	50
3.1.7) Dynamic expression of stem cell markers Lrig1 and Sox9 during HF and SG morphogenesis	52
3.2) Cellular mechanisms of SG morphogenesis	54
3.2.1) Sebocytes emerge adjacent to Lrig1 expressing cells.....	54
3.2.2) Lrig1 positive stem cells generate sebocytes by asymmetric cell fate decision	56
3.2.3) Proliferating Lrig1 positive cells give rise to sebocytes.....	58
3.3) Origin of cells forming HF and SG.....	61
3.3.1) Individual cells are labelled in tail IFE upon embryonic Tam treatment	62
3.3.2) Cells originating in the IFE contribute to HF and SG formation	63
3.3.3) K15 derived progeny display high proliferative capacity in vitro.....	66
3.4) Influence of Rac1 on sebocyte differentiation in skin tumours	69
3.4.1) L61Rac1 alters proliferation and sebocyte differentiation in skin tumours.....	70
3.4.2) Isolation and transcriptional profiling of distinct cell populations from sebaceous tumours	72
3.4.3) Verification of selected candidate genes	75

3.4.3.1) Down regulation of Scd1, Elov3 and Elov4 in cells of K14ΔNLef1/L61Rac1 carcinoma	76
3.4.3.2) Decreased expression of 24-Dehydrocholesterol-reductase in K14ΔNLef1/L61Rac1 tumours.....	77
3.4.3.3) Reduced Nuclear protein1 expression in cells of K14ΔNLef1/L61Rac1 carcinoma	78
4. Discussion.....	80
4.1) Differences in HF morphogenesis in mouse back and tail skin	80
4.2) Formation of HF progenitor compartments	82
4.3) Cellular and molecular mechanisms of SG morphogenesis.....	84
4.3.1) A cluster of sebocytes generates two SGs in mouse tail skin.....	86
4.3.2) Lrig1 positive stem cells generate sebocytes	88
4.4) Origin of cells forming HF and SG.....	89
4.4.1) Specific targeting of individual IFE cells during skin morphogenesis	90
4.4.2) Progeny of K15 positive IFE cells contribute to HF and SG morphogenesis	91
4.4.3) Test for proliferative capacity of K15 derived progeny	93
4.5) Role of Rac1 in tumour formation.....	93
4.5.1) Activation of Rac1 leads to decreased sebocyte differentiation in skin tumours.....	94
4.5.2) Gene expression profile is altered in cells of K14ΔNLef1/L61Rac1 carcinomas	95
4.6) Perspectives.....	98
5) Summary	100
6) Zusammenfassung	102
7) References	104
8) Figure index.....	118
9) Table index	120
10) List of abbreviations	121
11) Annex.....	123
12) Curriculum vitae	127

1) Introduction

1.1) The structure of the skin

The skin constitutes the largest organ of the body and protects the organism against environmental assaults such as UV irradiation, pathogens and mechanical stress. Balancing water and electrolyte influx and efflux, the skin prevents the body from dehydration. In addition, the skin has thermoregulatory and sensory function (Lüllmann-Rauch, 2003).

Mammalian skin is a complex organ consisting of several layers (Fig. 1). The epidermis is the outermost layer creating a barrier against the environment. It comprises interfollicular epidermis (IFE) with associated hair follicles (HFs) and sebaceous glands (SGs). The underlying dermis provides nutrients to the epidermis and stimulates proliferation. The subcutis contains adipocytes and serves as nutrient storage for epidermis and dermis (Montagna, 1974b).

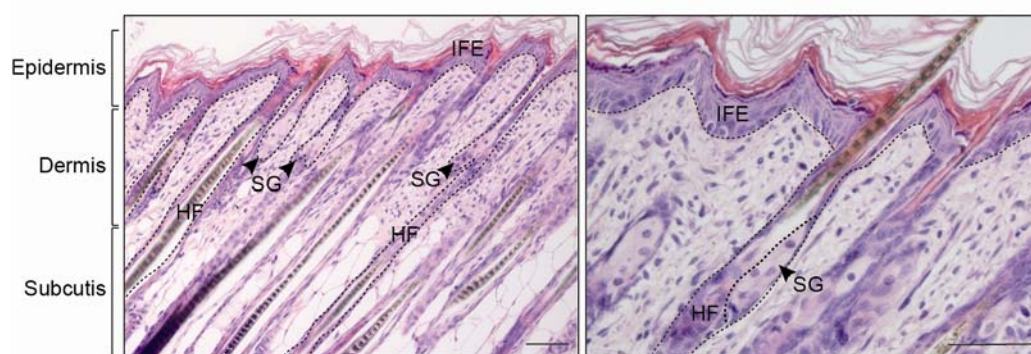


Fig. 1) The structure of the skin. Epidermis, dermis and subcutis are the three main layers of the skin. IFE = interfollicular epidermis, SG = sebaceous gland, HF = hair follicle. Arrowheads point to sebaceous glands. Scale bar = 50 μ m.

1.2) The interfollicular epidermis

The IFE renews constantly throughout life. Cells originating from the basal layer transit the different layers of the epithelium. A tight balance has to be maintained between proliferation in the basal layer and cell death in the cornified layer.

The multilayered stratified epithelium of the IFE is separated from the dermis by a basement membrane (Fig. 2). The basement membrane consists of proteins secreted by epidermal keratinocytes and dermal fibroblasts (Burgeson and Christiano, 1997; McMillan et al., 2003). Undifferentiated, proliferatively active keratinocytes are attached to the basement membrane constituting the stratum basale (Simpson et al., 2011). Basal keratinocytes express the intermediate filaments Keratin (K) 5 and K14. During early postnatal development also K15 expression can be detected (Liu et al., 2003; Nelson and Sun, 1983). Upon terminal differentiation, keratinocytes stop proliferation and detach from the basement membrane and are moved into the stratum spinosum (Fig. 2). Keratin expression switches from K5 and K14 to K1 and K10 forming a stronger intermediate filament network (Fuchs and Green, 1980). Cells of the stratum granulosum express further structural proteins like filaggrin and loricrin. These are deposited beneath the plasma membrane functioning as scaffold for lipid bilayers important for maintaining the barrier function of the IFE (Blanpain and Fuchs, 2009; Candi et al., 2005). Finally, cells of the stratum granulosum form the outermost layer of the IFE, the stratum corneum (cornified layer). These cornified dead cells are eventually shed off.

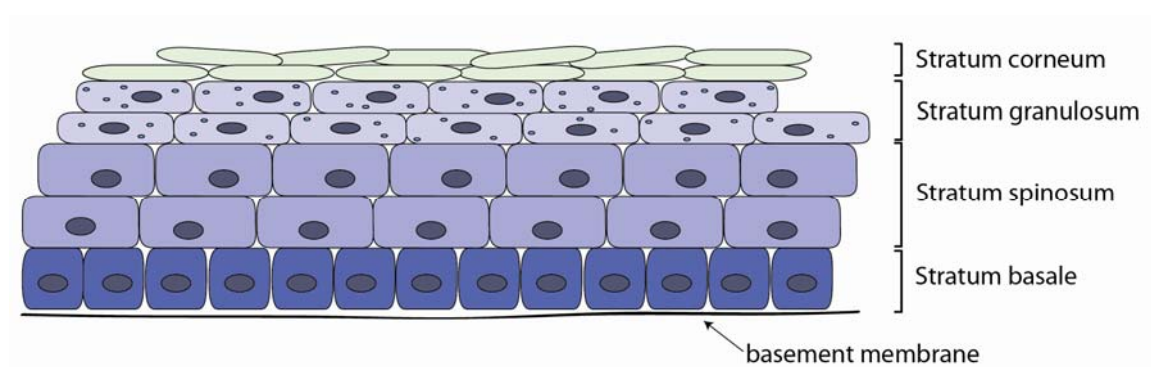


Fig. 2) The interfollicular epidermis. The IFE comprises four different cell layers (stratum basale, stratum spinosum, stratum granulosum, stratum corneum).

1.3) The hair follicle

The HF (Fig. 3 A) is an appendage of the IFE. In general, it comprises a hair shaft and one or two SGs, depending on the type of HF. HFs comprise their own stem cell population localised in the permanent part of the follicle in a region called bulge.

The non-permanent part of the HF undergoes cycles of growth (anagen), regression (catagen) and rest (telogen) (Lavker et al., 2003; Muller-Rover et al., 2001) (see 1.3.2 and Fig. 3) and regenerates in a cyclic manner throughout adult life (Hardy, 1992).

Like the IFE, the HF consists of different cellular layers (Fig. 3 B). The outer root sheath (ORS) contains proliferating basal keratinocytes. In the so called bulb at the lower part of the HF, proliferating transit amplifying cells are localised giving rise to cells of the 4 layers of the inner root sheath (IRS) and the 3 layers of the hair shaft (Krause and Foitzik, 2006; Rogers, 2004; Schneider et al., 2009). Cell type specification of the different cell layers of the IRS and the hair shaft occurs at the basis of the HF.

In mouse pelage fur, four types of HFs exist (Sundberg, 1994). Guard HF make up 1-3 % of the mouse fur and produce long tylotrich hairs that have also sensory function. Awl hairs constitute about 30 % of the mouse coat and are approximately half as long as the guard hairs. The most abundant hair type in the mouse coat are zigzag hairs (65 -70%). Zigzag hairs are as long as awl hairs but contain up to four bends. Auchene hairs are present at a very low frequency in mouse fur (0.1 %). They contain two to four medulla columns (innermost layer of the hair shaft) like awl hairs and are bended once resembling zigzag hairs (Duverger and Morasso, 2009).

The HF is formed during embryogenesis and early postnatal development in mice (Hardy, 1992).

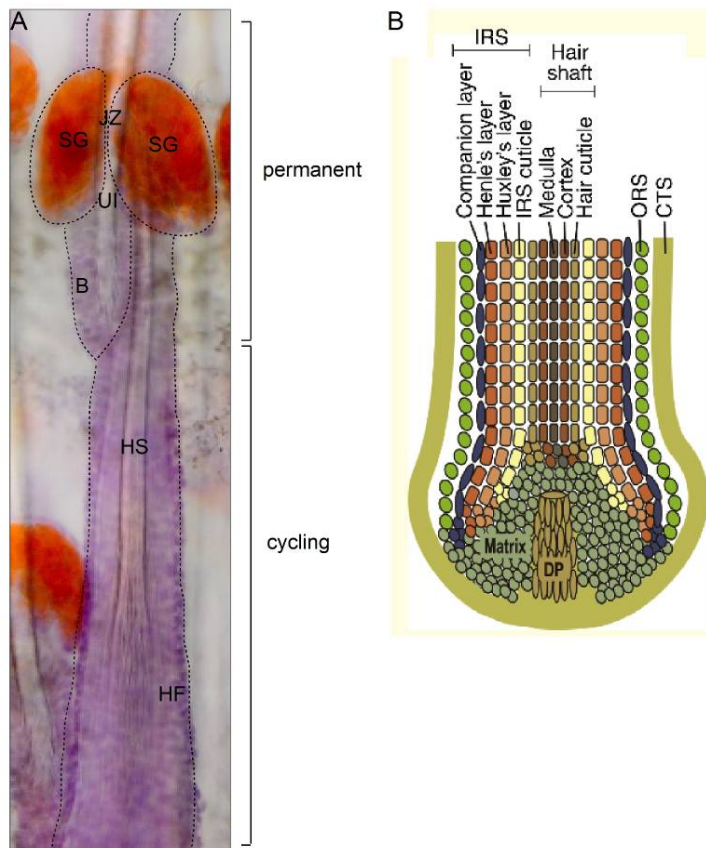


Fig. 3) The hair follicle. A) epidermal whole mount preparation stained with haematoxylin and OilRedO; different compartments are shown: B = bulge, HF = hair follicle, HS = hair shaft, JZ = junctional zone, SG = sebaceous gland, UI = upper isthmus. B) Different cell layers of the HF, IRS = inner root sheath, ORS = outer root sheath, CTS = connective tissue sheath. From Schneider et al, 2009.

1.3.1) Morphogenesis of the HF

Morphogenesis of the HF starts during embryonic development around embryonic day (E) 14.5 (Duverger and Morasso, 2009). A series of signals exchanged between the epidermis and the underlying mesenchyme is preceding the formation of HFs (Fuchs, 2007; Hardy, 1992; Millar, 2002). A first mesenchymal signals including FGFs and BMP inhibitory factors (Botchkarev et al., 1999; Petiot et al., 2003) defines were epidermal thickenings, so called placodes are formed. The epidermis emits Wnt signals back to the mesenchyme inducing the assembly of dermal cells (dermal condensate) beneath the placode (DasGupta and Fuchs, 1999; Gat et al., 1998). The dermal condensate sends a second dermal signal to the placode initiating down growth of the epithelium into the dermis to form a HF.

HF morphogenesis can be sub divided into distinct stages. Each stage describes morphological and histological events (Hardy, 1951; Hardy, 1992; Paus et al., 1999). At stage 0 of HF morphogenesis, no thickening can be seen in the epidermis (Fig. 4 A). However, expression of TGF β RII at future sites of HF formation can be visualized by immunohistochemistry (Paus et al., 1999). Stage 1 of HF morphogenesis is marked by condensation of epidermal keratinocytes forming a placode (Fig. 4 B). The dermal condensate can be visualized below the placode by alkaline phosphatase reaction (see 2.3.5). HFs at stage 2 of morphogenesis are clearly distinguishable as an elongation of the epithelium into the mesenchyme forming the hair germ (Fig. 4 C). The dermal condensate forms a cap like structure below the hair germ. When the HF enters stage 3 of morphogenesis, keratinocytes of the lower part enclose the dermal condensate forming the dermal papillae (DP) (Fig. 4 D). At stage 4 of HF morphogenesis the DP is longer than wide (Fig. 4 E). Above the DP, formation of the IRS starts (IRS cone, Fig. 4 E). HFs at stage 5 of morphogenesis display an elongated IRS and melanin granules are visible at the precortex (Fig. 4 F). The DP is almost completely enclosed by keratinocytes of the HF. First lipid producing sebocytes of the future SG can be visualised by staining with OilRedO. At stage 6 of HF morphogenesis, a cluster of sebocytes can be seen at the upper part of the HF (Fig. 4 G). The hair canal becomes visible at the transition of the HF and the IFE (infundibulum) and a hair shaft is formed within the IRS. In HFs at stage 7 of morphogenesis the tip of the hair shaft reaches the hair canal (Fig. 4 H). At the last stage of HF morphogenesis (stage 8), the hair shaft emerges through the IFE and the HF attains its maximal length.

In murine back skin, four different types of HFs (1.3) are formed in three distinct waves of HF morphogenesis (Duverger and Morasso, 2009). Placodes forming guard hairs are first detected at E14.5. Awl and Auchene HFs are induced at E16.5 and zigzag HFs are the last to be formed at E18.5. Thus, back skin of mice at postnatal (P) 0.5 or P1.5 displays a mixture of HFs at different stages of development.

Once HF morphogenesis is completed, the lower part of the HF enters the cyclic renewal and undergoes phases of regression (catagen), rest (telogen) and growth (anagen). These phases are tightly controlled by diverse signalling events.

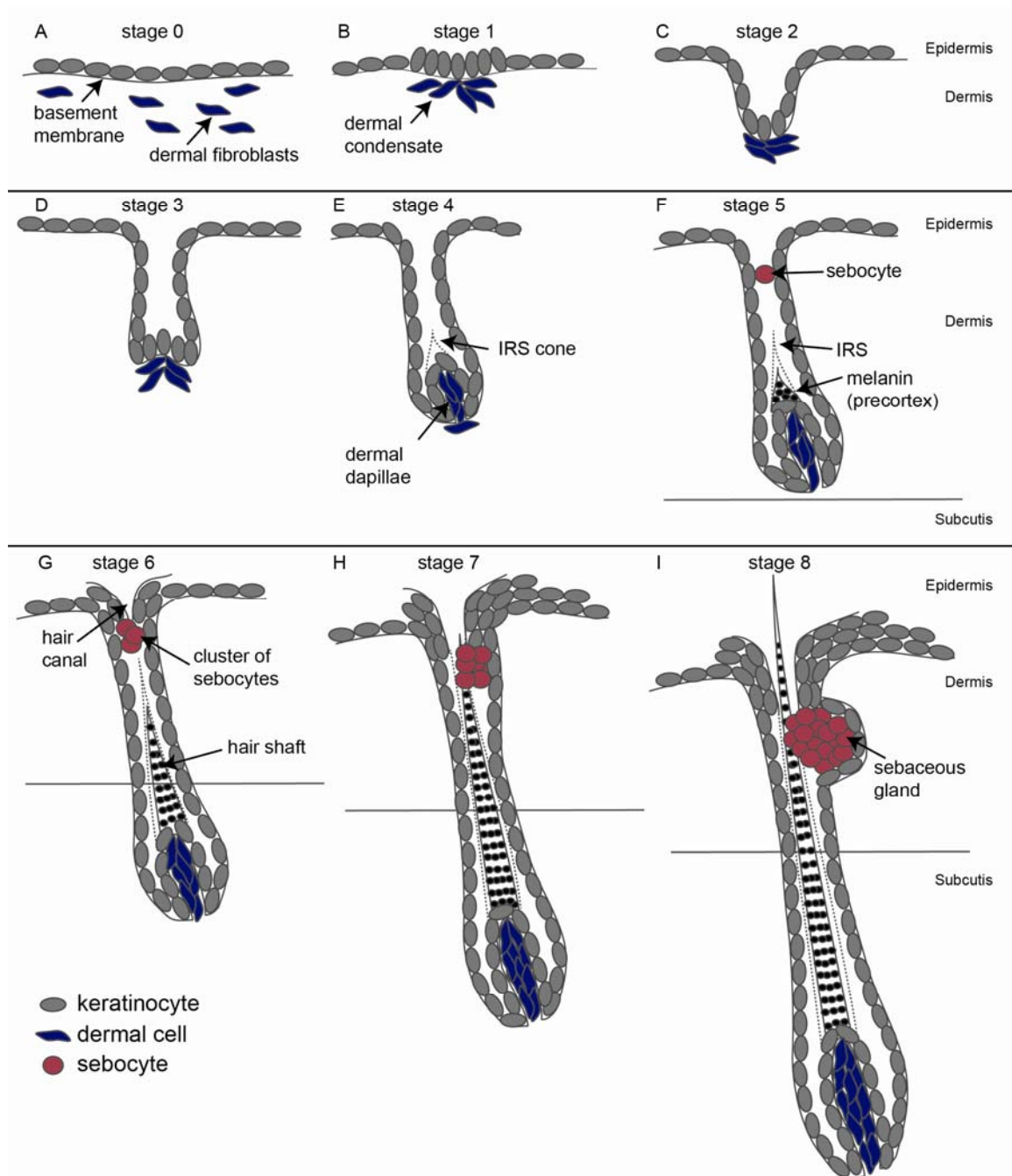


Fig. 4) Morphogenesis of the HF. (modified from Paus, 1999). A-I) Stage 0 to stage 8 of HF morphogenesis. Keratinocytes are marked in grey, dermal fibroblasts are shown in blue and sebocytes are depicted in red. IRS = inner root sheath.

1.3.2) Cyclic regeneration of the HF

Following morphogenesis, the HF enters the regression phase (catagen) (Fig. 5). Cells of the lower portion of the HF undergo apoptosis; the HF shortens and becomes reduced to an epithelial strand. Due to degeneration of the HF, the DP is brought in close proximity to the HF bulge. At the end of catagen, a cell population called the secondary hair germ (sHG) becomes visible between the bulge and the DP (Lyle et al., 1999; Muller-Rover et al., 2001; Panteleyev et al., 2001).

Once catagen is completed, the HF remains in a resting phase (telogen) where HF stem cells are thought to be quiescent. By the end of telogen, HF stem cells become activated by mesenchymal Wnt- and TGF β -signals from the DP (Enshell-Seijffers et al., 2010; Greco et al., 2009; Oshimori and Fuchs, 2012; Rendl et al., 2008). It has been shown that cells of the sHG respond faster to mesenchymal signals and start proliferation to generate cells for the formation of a new HF. With a delay of several days, cells of the bulge become eventually activated at the beginning of a new growth phase (anagen) (Greco et al., 2009; Hsu et al., 2011; Jaks et al., 2008). During anagen, HF stem cells give rise to transit-amplifying cells possessing the ability to undergo a limited number of cell divisions. SC progeny moves to the matrix at the basis of the HF to provide cells of the different layers of the HF (Fig. 3). Once matrix cells cease to proliferate, a new catagen phase starts followed by telogen. With the next anagen phase, the hair cycle starts again.

Clearly, BMP- and Wnt- signalling regulate quiescence and activation of HF stem cells. During telogen, active BMP signalling keeps the HF stem cells in a quiescent state. The repression of BMP signalling and active Wnt signalling leads to activation of HF stem cells (Blanpain et al., 2004; Horsley et al., 2008; Kobiela et al., 2007; Rendl et al., 2008). More recently, it has been proposed that cells of the DP emit TGF β 2 repressing active BMP signalling and thus, leading to activation of sHG cells (Oshimori and Fuchs, 2012). For induction of catagen, FGF5 was shown to play a key role (Hebert et al., 1994; Paus and Foitzik, 2004; Stenn and Paus, 2001).

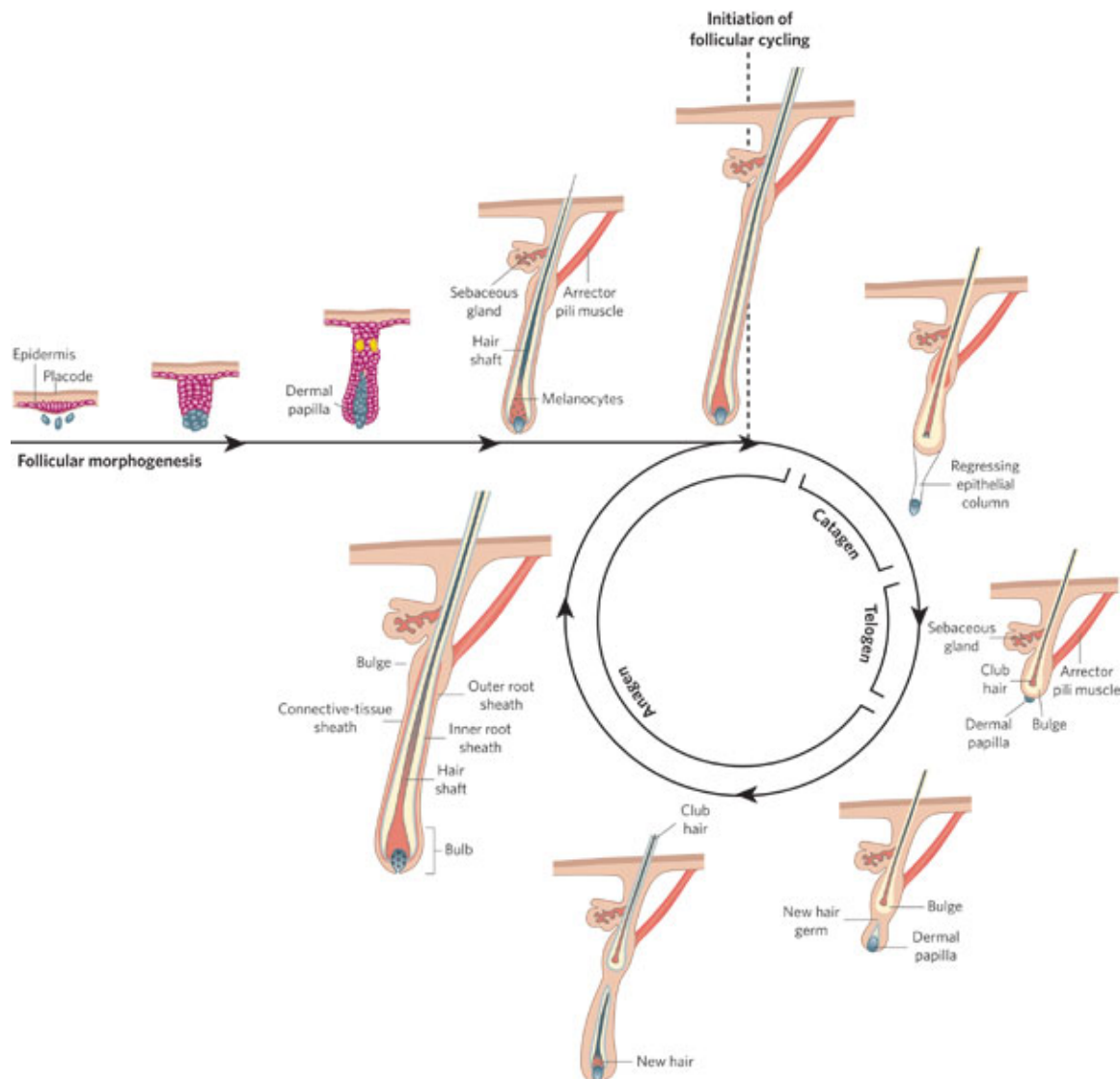


Fig. 5) The hair cycle. Adult HFs undergo cycles of growth (anagen), regression (catagen) and rest (telogen). From Fuchs, 2007.

1.3.3) Stem cells of the HF bulge region

The best characterised HF stem cell compartment is the bulge region located in the upper non cycling part of the HF. Bulge stem cells have the ability to retain a BrdU label over a long period of time, indicating their slow cycling character (label retaining cells, LRC) (Cotsarelis et al., 1990; Lavker et al., 2003; Tumber et al., 2004). Furthermore, several molecules including K15 (Keratin 15), CD34, Lhx2 (LIM/homeobox protein2), Sox9 (SRY box9), Tcf3 (T-cell factor3) and NFATc1 (Nuclear factor of activated T-cells, cytoplasmic1), have been described to be expressed by cells in the bulge region of HFs (Fig. 7) (Horsley et al., 2008;

Liu et al., 2003; Lyle et al., 1998; Merrill et al., 2001; Nguyen et al., 2006; Nowak et al., 2008; Rhee et al., 2006; Trempus et al., 2003; Vidal et al., 2005). A sub population of the telogen bulge and the sHG expresses Lgr5 (leucine-rich repeat-containing G-protein coupled receptor) (Jaks et al., 2008).

Bulge stem cells have been isolated by FAC-sorting via CD34+/Igtα6high expression. In transplantation assays, the isolated HF stem cells were able to regenerate all epidermal lineages, including HF, SG and IFE (Blanpain et al., 2004). Moreover, it could be demonstrated that HF stem cells contribute to IFE in wounding experiments (Ito et al., 2005; Levy et al., 2007).

Altogether, these studies demonstrate that the bulge region of the HF contains multipotent stem cells able to reconstitute all lineages of the epidermis.

1.3.3.1) Lineage tracing of HF bulge stem cells (in K15CreER(G)T2 mice)

Lineage tracing provides a powerful tool to study the progeny of stem cells within a tissue. Therefore, stem cells are labelled with a stable marker that is transmitted to the progeny of the originally labelled cell (Kretzschmar and Watt, 2012).

During the past years, it was demonstrated by several lineage tracing approaches that stem cells of the HF are able to reconstitute HF and the SG (Morris et al., 2004; Panteleyev et al., 2000; Petersson et al., 2011; Snippert et al., 2010b; Taylor et al., 2000).

Previously, it had been demonstrated that cells in the HF bulge express K15 protein (Lloyd et al., 1995; Lyle et al., 1998; Lyle et al., 1999). Moreover, expression of the K15 regulatory promoter sequence could be specifically localised to the bulge region in adult mice (Liu et al., 2003; Morris et al., 2004). To perform lineage tracing of HF bulge stem cells, this promoter region was used to drive an inducible Cre recombinase, fused to a modified ligand binding domain of the human oestrogen receptor carrying a triple mutation in G400V/M543A/L544A (CreER(G)T2) (Forde et al., 2002; Indra et al., 1999; Petersson et al., 2011). Upon application of the oestrogen analogue Tamoxifen (Tam) cytoplasmic Cre recombinase in K15 positive cells translocates to the nucleus and becomes active.

K15CreER(G)T2 mice were crossed to R26REYFP-reporter mice (Srinivas et al., 2001). In these mice, a floxed STOP-cassette is localised ahead of the EYFP- (enhanced yellow fluorescent protein) gene within the Rosa26 locus. Cre recombinase activity deletes the STOP-cassette leading to constitutive expression of EYFP in cells expressing Cre (Fig. 6). As the deletion is irreversible, not only the K15 positive cells but also all daughter cells constitutively express EYFP. Upon treatment of K15CreER(G)T2/R26REYFP mice with a low dose of Tam, individual YFP positive cells can be detected in the bulge region of the HF (Pettersson et al., 2011). By performing lineage tracing for different periods of time, it was demonstrated that cells originating in the HF bulge contributed to regeneration of the SG. This occurred independently from hair cycling (Pettersson et al., 2011).

Thus, this mouse model constitutes a useful tool to study HF stem cell dynamics in adult mouse skin.

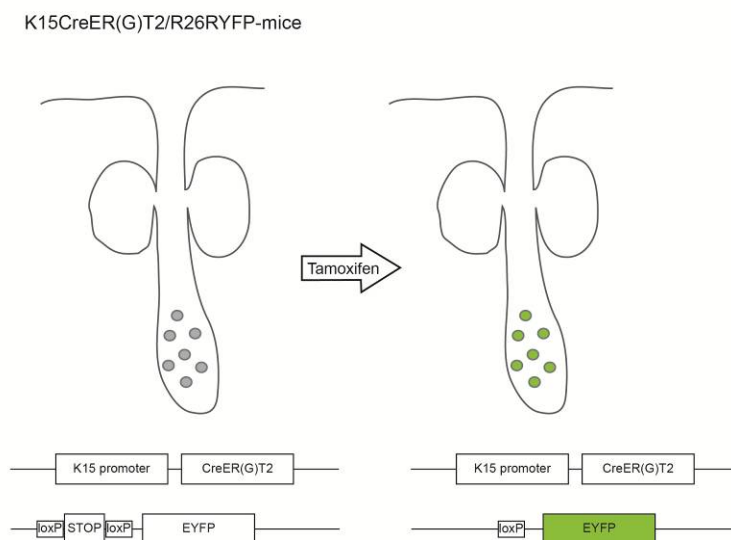


Fig. 6) K15CreER(G)T2 mouse model. Cre recombinase can be activated in individual bulge stem cells upon treatment with Tamoxifen.

1.3.3.2) Expression of bulge stem cell marker Keratin 15 in the skin

K15 expression is not confined to the bulge at all time points during skin morphogenesis and homeostasis. It was shown that the K15 promoter fragment used for the generation of K15CreER(G)T2/R26REYFP mice was also

expressed in cells of the epidermis during neonatal development (Liu et al., 2003). Expression of LacZ, driven by the K15 promoter, could be detected at P2.5 and 3.5 within the epidermis. At P5.5, LacZ expression diminished and was no longer detectable in the epidermis by P16.5. However, LacZ expression was specifically localised in the bulge region by P16.5 (Liu et al., 2003).

Interestingly, K15 protein could first be detected at E15.5 in mouse back skin (Nöbel, 2009). Detection of K15 protein during embryogenesis indicates that the K15 promoter is already active as early as E15.5 and potentially even before in mouse back skin. Therefore, K15CreER(G)T2/R26REYFP mice could be used for lineage tracing analyses during HF and SG morphogenesis.

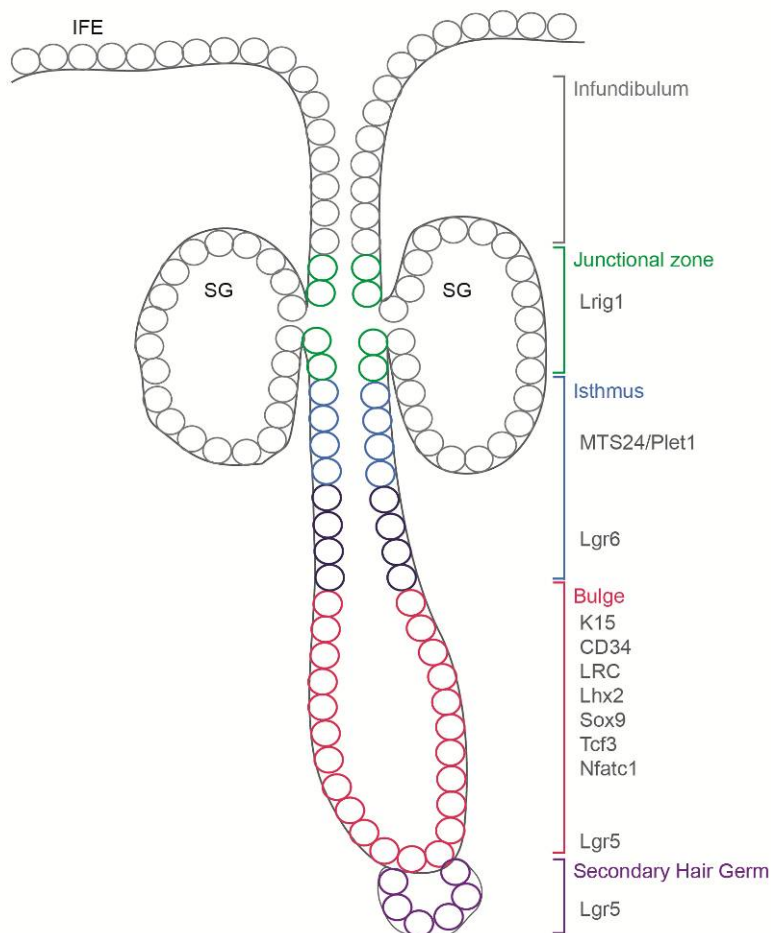


Fig. 7) Stem and progenitor cell populations of the adult HF. The junctional zone (green), the isthmus (blue/dark blue), the bulge region (red) and the secondary hair germ (violet) contain stem and progenitor cells implicated in regeneration of the HF and the SG

1.3.4) Non-bulge stem and progenitor cell populations of the HF

Besides the bulge, other progenitor compartments have been described during the past years (Fig. 7). The HF region above the bulge and below the SG is termed upper isthmus. Cells located in this area are recognised by the MTS24-antibody (mouse thymic stroma24) (Nijhof et al., 2006). Recently, the corresponding antigen, Plet1 (placenta-expressed transcript 1 protein), has been discovered (Depreter et al., 2008). Cells of the upper isthmus were clonogenic in culture and their gene expression profile showed overlap with bulge stem cells (Jensen et al., 2008b). Another stem cell population, marked by the expression of Lgr6 (leucine-rich repeat-containing G protein-coupled receptor 6) also locates to the isthmus region. Lineage tracing showed that these cells were capable of regenerating IFE and SG (Snippert et al., 2010b).

A further stem cell population was described residing in the region next to the SG, the so called junctional zone. Cells in this area of the HF express Lrig1. It was suggested that Lrig1 positive cells were able to reconstitute IFE and SG (Jensen et al., 2009).

1.4) The sebaceous gland

The SG is a holocrine gland mostly attached to HFs (Montagna, 1974a). In skin, SGs are generally associated with HFs and localise to the upper, permanent part (Schneider et al., 2009). In mouse skin, HFs of different regions of the body contain either one or two SGs. In mouse tail skin, two large SGs are attached to each HF, whereas most back skin HFs harbour one SG (Duverger and Morasso, 2009).

Furthermore, specialised SGs, not associated with HFs, exist. For example Meibomian glands in the eyelid have been described (Knop et al., 2009; Knop and Knop, 2009; Thody and Shuster, 1989).

To date, the function of the SG is not completely understood. It is known that SGs produce lipids preventing the skin from dehydration and to maintain an intact epidermal barrier (Schneider and Paus, 2009; Thody and Shuster, 1989). Moreover, analyses of SG deficient (asebia) mouse models have demonstrated

that HFs are destroyed in absence of functional SGs (Josefowicz and Hardy, 1978; Sundberg et al., 2000). This is also observed in human patients with scarring alopecia which characteristically start with SG ablation (Sundberg et al., 2000). These observations suggest that SGs have important function in maintenance of the pilosebaceous unit consisting of HF and SG.

SGs consist of three distinct cellular regions, the peripheral, the maturation and the necrosis zone (Fig. 8). Small, proliferatively active cells are located in the peripheral zone of the gland (PZ, Fig. 8). These are attached to a basement membrane. Constantly, cells from the periphery of the gland are being displaced towards the centre of the gland, thereby starting differentiation. Sebocytes of the maturation zone (MZ, Fig. 8) produce lipids being stored in the cytoplasm. Consequently, the cells increase in size. Once the size reaches a maximum, cells of the necrosis zone disintegrate and release their cytoplasmic content (NZ, Fig. 8) (Niemann, 2009; Schneider and Paus, 2009; Thiboutot, 2004). The mixture of lipids and cellular debris, termed sebum, is transported via the sebaceous duct (SD) into the hair canal and to the skin surface (Fig. 8). Sebum serves as protection against dehydration and pathogens (Schneider and Paus, 2009; Thody and Shuster, 1989).

Several components have been described to play a role in regulating the function of the SG. For instance Stearoyl CoA Desaturase 1 (Scd1), an enzyme of the fatty acid metabolism, has key functions in maintenance and proper development of the gland (Binczek et al., 2007; Miyazaki et al., 2001; Sampath et al., 2009; Sundberg et al., 2000; Zheng et al., 1999). Moreover, Scd1 is already expressed during early SG development and constitutes a reliable marker for sebocytes (Fehrenschild et al., 2012; Frances and Niemann, 2012). Besides Scd1, mature sebocytes express MC5R (Melanocortin 5 Receptor) and PPAR γ (Peroxisome proliferator activator-receptor γ) (Zhang et al., 2006). MC5R influences the production and secretion of lipids by sebocytes. Depletion of MCR5 resulted in skin barrier defects (Chen et al., 1997). PPAR γ stimulates lipid production of sebocytes (Rosenfield et al., 1998; Rosenfield et al., 1999). Gene knock-out studies suggested that PPAR γ is necessary for sebocyte differentiation (Rosen et al., 1999).

The lipids produced by mature sebocytes can be visualised by staining with lipophilic dyes such as OilRedO and Nile Red.

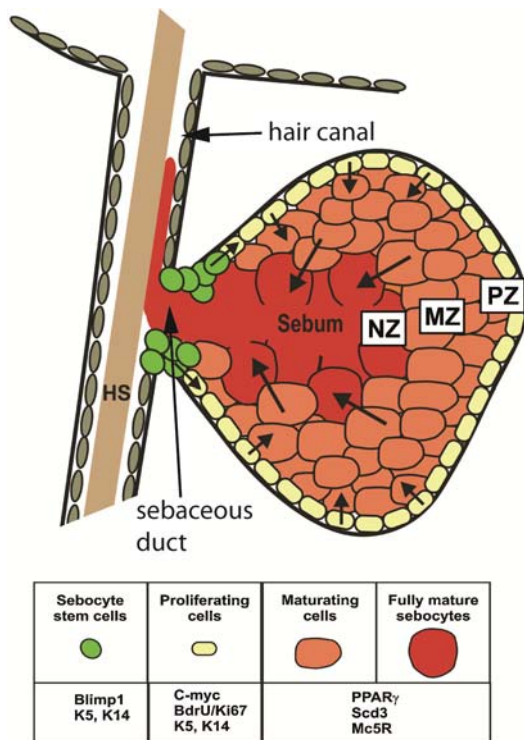


Fig. 8) The Sebaceous gland (SG). The SG contains a proliferative basal layer (PZ), more mature sebocytes in the maturation zone (MZ) and degenerating cells in the necrotic zone (NZ). HS = hair shaft. (modified from Schneider and Paus, 2009).

1.4.1) Morphogenesis of the SG

SG morphogenesis occurs in association with HF development. The SG develops around P0 as an outgrowth of the ORS of the HF. It has been described that first sebocytes are visible at stage 5 of mouse pelage HF morphogenesis (Paus et al., 1999). During the first postnatal days, a cluster of sebocytes is formed. Around P3 - P4, the glandular structure of the SG, including proliferating basal cells surrounding more differentiated cells becomes visible. Upon completion of HF morphogenesis, the SG attains its maximal size.

To date, the molecular mechanisms regulating SG morphogenesis are not clear. It has been demonstrated that Sox9 which is necessary for the specification of early HF stem cells is also required for SG formation. In absence of Sox9 during HF morphogenesis, neither the HF stem cell region nor SGs were formed (Nowak et al., 2008). In addition, it was shown in a lineage tracing approach that Lgr6 positive cells labelled in hair pegs during HF morphogenesis gave rise to cells of the SGs (Snippert et al., 2010b). Moreover, it was proposed that

unipotent progenitor cells expressing the transcription factor Blimp1 are located at the SD. It was suggested that this cell population is established prior sebocyte maturation at the upper developing HF during embryogenesis and early postnatal development (Horsley et al., 2006).

In contrast to the regulation of SG morphogenesis, diverse signalling pathways including Wnt and Hedgehog (HH) have been identified playing a crucial role in the maintenance and regeneration of the gland in adult mouse skin (Allen et al., 2003; Merrill et al., 2001; Niemann et al., 2002; Niemann et al., 2003).

1.4.2) Homeostasis and regeneration of the SG

During the past years, several signalling pathways have been shown to be implicated in homeostasis and differentiation of the SG. It was demonstrated that disturbed Wnt / β -Catenin signalling in basal keratinocytes leads to increased differentiation towards the sebocyte lineage (Merrill et al., 2001; Niemann et al., 2002). C-myc was also shown to be important for proper SG differentiation and maintenance. Proliferating cells of normal human skin express c-myc (Gandarillas and Watt, 1995; Hurlin et al., 1995). However, over expression of c-myc in mouse keratinocytes was shown to result in stimulation of sebocyte differentiation (Arnold and Watt, 2001; Waikel et al., 2001). Enhanced sebocyte differentiation resulting in increased size and number of SGs, was also described by over expressing an activated version of the HH receptor smoothened. In contrast, inhibition of HH signalling by expressing a dominant negative form of the transcription factor Gli2, results in suppression of sebocyte development (Allen et al., 2003; Gu and Coulombe, 2008). Furthermore, analyses of the HH ligand Indian Hedgehog (IHH) in human and mouse epidermis and sebaceous tumours suggested that IHH regulates proliferation and differentiation of sebocytes (Niemann et al., 2003).

To preserve the epidermal barrier function, the cells of the SG constantly differentiate and disintegrate generating sebum. To cope with the resulting high cellular turn over in the gland, sebocytes need to be replenished. To date, it is not fully understood how SGs are regenerated and which cellular compartments of the epidermis play a role in this process. Two hypotheses are currently

discussed. One assumption is that progenitor cells reside in the gland itself to assure the replenishment of cells (Ghazizadeh and Taichman, 2001; Horsley et al., 2006). It was proposed that unipotent progenitor cells marked by the expression of Blimp1 reside at the sebaceous duct (Horsley et al., 2006). However, analyses in human SGs showed that Blimp1 was expressed by more mature cells of the SG. Therefore, it is debated if Blimp1 marks SG progenitor cells, at least in the human system (Sellheyer and Krahl, 2009).

Another hypothesis describes multipotent HF stem or progenitor cells that migrate upwards and repopulate the SG (Blanpain et al., 2004; Jensen et al., 2009; Morris et al., 2004; Snippert et al., 2010b; Taylor et al., 2000). Indeed it was elegantly shown by lineage tracing analysis following the fate of bulge stem cell progeny. It was demonstrated that cells of the bulge region were able to regenerate the SG (Pettersson et al., 2011) (see 1.3.3.1).

1.5) Impaired Wnt / β -Catenin signalling leads to skin tumour formation

1.5.1) Canonical Wnt signalling

A central component of the canonical Wnt / β -Catenin signalling pathway is β -Catenin. Within the cell, β -Catenin is either localised in the cytoplasm or associated with the members of the cadherin family in the adherens junctions of the cell membrane (Huber et al., 1997; Huelsken et al., 1994). Nuclear localisation of β -Catenin is a sign of active Wnt-signalling (Nusse, 2005).

In the absence of the Wnt ligand, cytoplasmic β -Catenin is phosphorylated and targeted for proteasomal degradation by a protein complex comprising Axin1, APC, CK1- α and GSK3 β (Fig. 9). If a Wnt ligand is present and binds to the receptor frizzled and its coreceptor LRP, dishevelled gets activated and recruits the degradation complex to the membrane by interacting with Axin1. As a consequence, β -Catenin cannot be phosphorylated and is not targeted for proteasomal degradation. Stabilised β -Catenin accumulates in the cytoplasm and eventually translocates into the nucleus. Here, β -Catenin can bind to members of the transcription factor family TCF/Lef, displacing transcriptional repressors like Groucho or CBP. The β -Catenin-TCF/Lef complex acts as a

transcriptional activator. Upon binding of β -Catenin to TCF/Lef transcription factors, target genes like c-Myc, Cyclin-D1 and E-Cadherin are expressed (Clevers, 2006; Nusse, 2005).

Besides Wnt-ligands, other molecules can activate the pathway. For example R-spondin was shown to potentiate Wnt-signalling (Kazanskaya et al., 2004; Kim et al., 2008). However, it remained unclear which receptor was implicated in active Wnt signalling mediated by R-spondin. Recently, it was shown that R-spondin can bind to Lgr5, Lgr6 and Lgr4 (Carmon et al., 2012; de Lau et al., 2011; Glinka et al., 2011). This family of molecules marks stem cells in different tissues including skin (Barker et al., 2007; Barker et al., 2010; Jaks et al., 2008; Snippert et al., 2010b). Lgr4 and Lgr5 associate with frizzled/LRP receptor complexes, upon binding of R-spondin, Wnt signalling is enhanced.

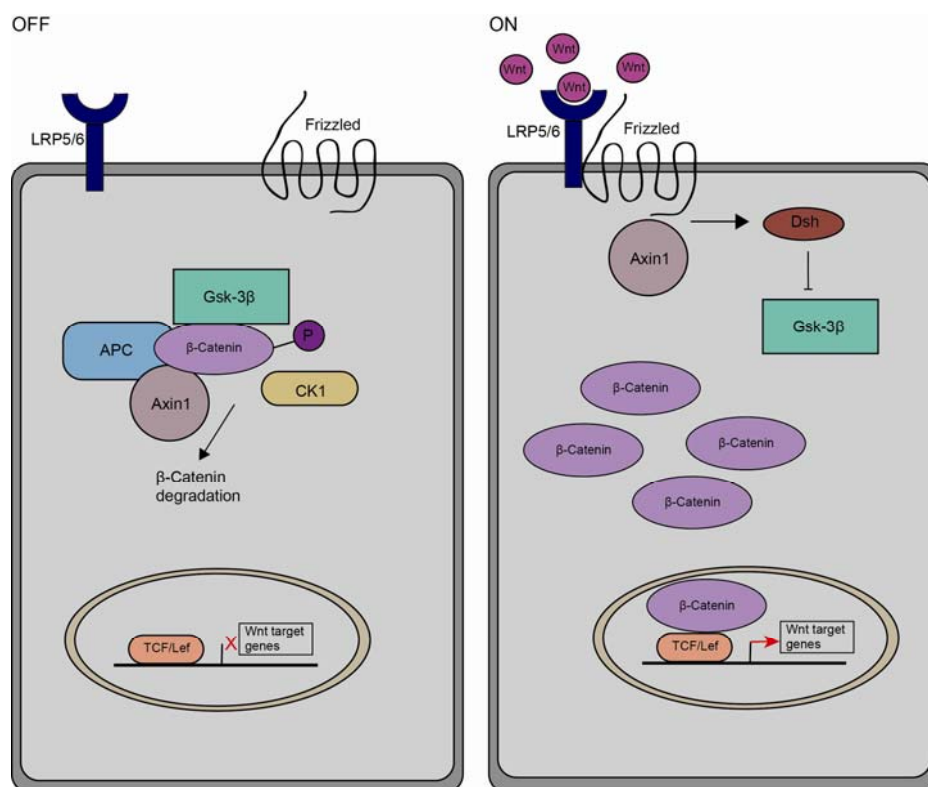


Fig. 9) The canonical Wnt-signalling pathway. Upon binding of Wnt-ligand to the receptor complex formed by frizzled and LRP, cytoplasmic β -Catenin is stabilized, translocates to the nucleus and can activate target gene transcription (ON). In absence of Wnt, β -Catenin is phosphorylated and targeted for degradation (OFF).

1.5.2) Impact of Wnt / β -Catenin signalling in skin

Wnt / β -Catenin signalling in the skin has been shown to have crucial functions in morphogenesis of the HF (Andl et al., 2002). In absence of canonical Wnt signalling, placode formation is blocked (Huelsenken et al., 2001). In contrast, forced expression of stabilized β -Catenin, resulting in enhanced Wnt signalling, leads to precocious and increased HF placode formation (Narhi et al., 2008; Zhang et al., 2008).

In adult skin, Wnt / β -Catenin signalling is needed to activate stem cells of the HF bulge region to start a new anagen phase after telogen (Lowry et al., 2005; Stenn and Paus, 2001). Moreover, forced expression of β -Catenin in the epidermis resulted in *de novo* HF formation (Gat et al., 1998; Lo Celso et al., 2004). Also, canonical Wnt signalling is required for proper hair cycling. Inactivation of β -Catenin in the DP resulted in premature catagen and disturbed HF regeneration (Enshell-Seijffers et al., 2010). Expression of stabilised β -Catenin in the epidermis leads to precocious induction of anagen (Lo Celso et al., 2004; Lowry et al., 2005; Van Mater et al., 2003).

Furthermore, aberrant Wnt signalling is associated with skin cancer development. Activating mutations of β -Catenin lead to formation of HF tumours (Gat et al., 1998; Lo Celso et al., 2004). Blocking of Wnt / β -Catenin signalling in epidermal cells promotes sebaceous cell fate and squamous differentiation (Merrill et al., 2001; Niemann et al., 2002). Moreover, activating mutations in the β -Catenin gene and inactivating mutations of the transcription factor Lef1 (lymphoid enhancer factor1) are present in human skin tumours (Chan et al., 1999; Takeda et al., 2006)

1.5.3) K14 Δ NLef1 mouse model

To analyse the function of Wnt / β -Catenin signalling in the skin in more detail, a transgenic mouse model displaying inhibited Lef1 mediated β -Catenin signalling in the epidermis was generated (K14 Δ NLef1 mice) (Niemann et al., 2002). In these mice, an N-terminally truncated version of the transcription factor Lef1 is expressed in the epidermis. The N-terminus of the Lef1 transcription factor

contains the binding site for β -Catenin. As the binding domain is lacking in K14 Δ NLef1 mice, β -Catenin can no longer bind to Lef1 and fails to form a transcriptional activator. Target gene expression is therefore repressed. The mutated transcription factor Lef1 is expressed under the control of the K14 promoter. Thus, all basal cells of the IFE, HF and SG express mutant Lef1 and display inhibited Wnt signalling.

K14 Δ NLef1 mice show severe hair loss starting by the age of six weeks. Moreover, epithelial cysts derived from HFs are formed and ectopic SG formation along the HF is detected. At about three months of age, K14 Δ NLef1 mice developed spontaneous benign sebaceous adenomas and sebomas (Niemann et al., 2002). Sebaceous tumour formation can also be induced by performing a chemical carcinogenesis experiment with K14 Δ NLef1 mice. It was demonstrated that mutated Lef1 acted as a tumour promoter and specified the type of the developing tumours (Niemann et al., 2007).

1.5.4) K14 Δ NLef1/L61Rac1 double transgenic mice

Previously, it had been reported that the small GTPase Rac1 plays an important role in maintaining stem cells properties in epidermal cells. Upon deletion of Rac1, epidermal stem cells divided more frequently and underwent terminal differentiation. Activation of Rac1 lead to an expansion of the cell population capable of clonal growth (Benitah et al., 2005).

By crossing L61Rac1 into the background of K14 Δ NLef1-mice, the effect of active Rac1 on tumour growth, histology and invasiveness in benign tumours should be addressed. Another important aspect to analyse was the potential expansion of progenitor compartments as described by Benitah and colleagues (Benitah et al, 2005).

K14 Δ NLef1 mice were crossed to mice expressing constitutively active Rac1 (L61Rac1 transgenic mice (Behrendt et al., 2012; Stachelscheid et al., 2008; Tschardtke, 2006). Double transgenic mice (K14 Δ NLef1/L61Rac1-mice) did not show obvious histological differences to K14 Δ NLef1 mice regarding normal skin. Mice that were subjected to a one-step carcinogenesis experiment developed a comparable number of tumours as K14 Δ NLef1 control mice (Tschardtke, 2006).

1.6) Aims

HF and SG are two integral parts of the pilosebaceous unit of mammalian epidermis and contribute to formation of an intact epidermal barrier. Progress has been made in our understanding of HF morphogenesis and regeneration. In addition to the stem cells of the HF bulge region, other stem and progenitor compartments have been identified within the HF. However, it is not known when these stem and progenitor cell compartments are established and when they first become activated for tissue formation and regeneration.

Recently, it has been demonstrated that stem cells of the HF bulge region play a role in the process of SG regeneration in adult skin. In contrast, hardly anything is known about the cellular mechanisms involved in SG development.

Therefore, one aim of this thesis is to identify spatio-temporal distribution of HF stem and progenitor cell compartments during SG morphogenesis in neonatal mouse skin. We want to determine the cellular mechanisms of SG morphogenesis in more detail and to identify the stem cell population giving rise to sebocytes. Furthermore, to investigate the origin of cells forming the SG, lineage tracing experiments are performed during morphogenesis.

In addition, during adult skin homeostasis, the small GTPase Rac1 is important for maintenance of the HF stem cell compartment. Activation of Rac1 leads to an expansion of cells capable of clonal growth. To address the role of active Rac1 in SG cell differentiation and skin tumour formation, constitutively active Rac1 was expressed in benign sebaceous skin tumours. From these experiments, we want to get insight into the role of Rac1 in skin tumour formation, differentiation and progression. Therefore, histology and expression of skin stem cell and differentiation markers will be analysed in skin tumours. To understand the potential role of Rac1 in regulating important aspects of progenitor commitment, proliferation and differentiation, gene expression profiles of distinct tumour cell populations will be analysed.

2) Material and Methods

2.1) Chemicals and reagents

2.1.1) Chemicals

Table 1) Chemicals

Reagent	Company
Adenine	Sigma, Germany
Agarose	
Bovine Serum Albumine (BSA)	
BrdU	
Cholera enterotoxin	
Crystal violet	
DAPI	
DEPC	
Dithiothreitol (DTT)	
EGF	
Fish skin gelatine (FSG)	
Formamid	
Glutaraldehyde	
Hydrocortisone	
Igepal	
Insulin	
K ₂ HPO ₄	
MgCl ₂	
Mineral oil	
Mitomycin C	
Normal donkey serum (NDS)	
Nuclear fast red	
Normal goat serum (NGS)	
Propidium iodide (PI)	
Proteinase K	
Rabbit serum (RS)	
Sunflower oil	
Tamoxifen	
Thermolysin	
Triton X 100	
Acetone	Roth, Germany
EDTA	
Ethanol (EtOH)	
Formaldehyde	
HEPES	
Methanol (MeOH)	
NaCl	
Tris	
Xylol	
2-propanol	
DMEM/HAMsF12-medium	Biochrom, Germany
PBS (10x)	
Penicillin/Streptomycin	
Glutamine	Roche, Germany
dNTPs	
NBT/BCIP	
tRNA	

Mayer's Heamatoxylin	Merck, Germany
Kayser glycerol gelatine	
Paraformaldehyde	
Eosin	AppliChem, Germany
Tween-20	
FCS	PAA, Germany
FCS Gold	
mTRAP buffer	Active Motif, Belgium
protease	
Streptavidin beads	
PNA	
Citrate buffer	BioGenex, Germany
OilRedO	Amresco
OCT	Sakura, Germany
Pertex	Leica, Germany
low range marker	Fermentas, Germany
EdU	Invitrogen, Germany
"Ready to load" enzyme mix	BioBudget, Germany
chelex	Biorad, Germany
DMEM	GIBCO, Germany
Milk powder	Heirler
TdT	USB
Betaisodona	Mundipharma, Germany

2.1.2) Solutions and buffers

Table 2) Solutions and buffers

Solution	Composition
10x TAE buffer	0.9 M Tris Ultra
	0.89 M Boric acid
	20 mM EDTA
1x TAE buffer	100 ml 10x TAE buffer
	900 ml dH ₂ O
DMEM / HAMs F12 medium supplemented with	100 IU/ml penicillin
	100 µg/ml streptomycin
	1.8 x 10 ⁻⁴ M adenine
	0.5 g/ml hydrocortison
	10 ng/ml EGF
	10 ⁻⁵ M cholera toxin
	5 µg/ml insulin
10 % FCS (chelex-100 resin treated)	
Lysis buffer	0.2 M NaCl
	0.1 M Tris HCl pH 8,5
	5 µM EDTA
	0.2% SDS
	8.4 ml dH ₂ O
	add 5 UI Proteinase K (20mg/ml) before use
Mowiol/DABKO	4.8 g Mowiol
	12 g Glycerin
	12 ml H ₂ O
	stirr 3 - 4 h
	add 24 ml 0.2 M Tris pH 8
	heat to 50 °C and stir overnight
	add 1.2 g DABKO (2,5%)

2.1.3) Antibodies

The primary antibodies used in this study are listed in Table 3; secondary antibodies are listed in Table 4.

Table 3) Primary antibodies

antigen	host	dilution	reference / company
Adipophilin	guinipig	1:3000	Fitzgerald Industries
BrdU	mouse	1:10 (sections)	BD
BrdU	rat	1:500	Oxford Biotech
CD49f-PE (Itga6)	rat	1:25	BD
GFP	chicken	1:3000 / 1:5000 (K14NuMA-GFP sections)	Abcam
GFP-488	goat	1:500	Rockland
K14	rabbit	1:3000	Covance
Laminin	rabbit	1:100	Sigma
Lrig1	goat	1:100 / 1:50 (K14NuMA-GFP sections)	R&D Systems
MTS24	rat	1:50	(Gill et al., 2002)
P-Cadherin	goat	1:250	R&D Systems
Plet1	rat	1:3	(Raymond et al., 2010)
Scd1	goat	1:150	Santa Cruz
Scd1	rat	1:150	R&D Systems
Sox9	rabbit	1:3000	(Stolt et al., 2003)

Table 4) Secondary antibodies

species	conjugate	dilution	reference / company
Anti-chicken	Alexa488	1:500	Molecular Probes
Anti-goat	Alexa488, Alexa594, Cy5	1:500	Molecular Probes
Anti-guinipig	Alexa488	1:500	Molecular Probes
Anti-mouse (IgG1)	Alexa488	1:1000	Molecular Probes
Anti-rat	Alexa594, Cy5	1:400	Molecular Probes
Anti-rabbit	Alexa488, Alexa594, Cy5	1:500	Molecular Probes
Anti-rabbit	HRP	1:500	DAKO

HRP = horseradish peroxidase

2.1.4) Kits

Table 5) Kits

Kit	Company
Click-It EdU Kit	Invitrogen, Germany
Expand Long Template	Roche, Germany
Quanti Tect Reverse Transcriptase	Qiagen, Germany
RT ₂ RT SYBR Green qPCR Master Mix	Super Array
Super Script II First Strand Synthesis	Invitrogen, Germany
Super Script III First Strand Synthesis	
TaqMan gene expression assay	Applied Biosystems

2.2) Mouse experiments

All experiments conducted with mice have been performed according to institutional guidelines and animal license given by the State Office of North Rhine-Westphalia, Germany.

The used mouse strains were kept on a C57Bl/6 background.

2.2.1) Mouse models

Table 6 summarises the transgenic mouse models used in this study. In addition, C57Bl/6-mice were applied for most of the experiments.

Table 6) Mouse models applied in this study

Mouse model	reference
K15CreER(T2)/R26REYFP	(Petersson et al., 2011; Srinivas et al., 2001)
K14 Δ NLef1	(Niemann et al., 2002)
K14L61Rac1	(Behrendt et al., 2012; Stachelscheid et al., 2008; Tschardtke, 2006)
K14NuMAGFP	(Poulson and Lechler, 2010)

2.2.2) Activation of Cre recombinase

A single dose of Tamoxifen was injected intraperitoneally (i.p.) into the mice. Therefore, 1 mg or 2 mg Tamoxifen (Sigma Aldrich) powder was dissolved in 200 μ l sun flower oil (Sigma Aldrich) by robust shaking for 1 h at room temperature (Indra et al., 1999). AK15CreER(T2)/R26REYFP-mice received 2 mg of Tamoxifen and mice from the higher expressing CK15CreER(T2)/R26REYFP line were treated with 1 mg Tamoxifen. Tamoxifen is an oestrogen analogue. It is used to activate Cre recombinase fused to a modified oestrogen receptor. Cre normally located in the cytoplasm can translocate into the nucleus and becomes activated. In both mouse lines, activated Cre recombinase leads to the excision of a stop-cassette in front of the EYFP-gene (Fig. 8). Therefore, EYFP can be expressed in all cells with activated

Cre recombinase. As the excision of the stop-cassette is irreversible, all daughter cells also express the EYFP-gene.

2.2.3) BrdU / EdU injections

To mark proliferating cells within the tissue, mice were injected i.p. with 5-bromo-2'-deoxyuridine (BrdU, Sigma Aldrich, Germany) or 5-ethynyl-2'-deoxyuridine (EdU, Invitrogen, Germany) 1 – 48 h before sacrificing them. BrdU and EdU are base analogues that are incorporated in DNA of dividing cells.

BrdU was used at a concentration of 100 mg/kg bodyweight; EdU was used at a concentration of 40 mg/kg bodyweight.

EdU-incorporation was monitored using the Click-it EdU kit following the manufacturer's instructions (Invitrogen, Germany). BrdU-incorporation was analysed by antibody staining (see 2.3.3).

2.2.4) Tissue preparation

To analyse HF and SG morphogenesis, skin tissue was prepared from mice between E15.5 and P30. In general, back and tail skin was prepared following the protocols described below.

2.2.4.1) Tissue preparation for paraffin and cryo embedding

Mice were sacrificed and the skin was prepared as described before (Paus et al., 1999). Briefly, back skin was isolated and stretched out on thick paper. Small pieces (about 0.5 cm²) of skin were cut along the longitudinal axis of the HFs. For tail skin preparation, the tail was cut off the mouse. The tail was sliced open on the ventral side; skin was peeled of the bone and stretched out on thick paper.

Before paraffin embedding, the tissue was fixed for 2h with 4% Formalin/PBS and removed from the paper.

For cryo embedding of skin pieces, the tissue was prepared as described above. Unfixed tissue was embedded in OCT (Sakura), allowed to freeze slowly in cold isopentane and stored at -80°C .

2.2.4.2) Preparation of epidermal whole mounts

For three-dimensional analysis of the epidermis, whole mounts of mouse epidermis were generated as described before (Braun et al., 2003). Briefly, tail skin was prepared (2.2.4.1) and incubated in 5 mM EDTA at 37°C to allow separation of the epidermis from the underlying dermis. Skin of newborn mice was incubated for 1.5 h whereas skin of adult mice was incubated for up to 3 h. To prepare epidermal whole mount samples from back skin, the tissue was incubated for 2 h in 20 mM EDTA and separated from the dermis. Epidermal whole mounts were fixed for 1 h in 3.4 % Formaldehyde or 0.2 % glutaraldehyde/ 2 % formaldehyde and kept in PBS at 4°C .

2.3) Tissue analysis and histology

2.3.1) Deparaffinisation

Sections of paraffin embedded tissue were deparaffinised before proceeding with stainings. Therefore, sections were incubated two times for 10 min in 100 % Xylol (Roth, Germany). Next, sections were kept two times for 5 min in 100% EtOH (Roth, Germany) followed by incubation in 95 %, 70 % and 50 % EtOH for 5 min respectively. Before proceeding with the staining protocols, the sections were incubated for 5 min in tap water followed by 5 min in distilled water to wash out residues of EtOH.

2.3.2) Haematoxylin and eosin staining

To visualize the histology of skin sections, deparaffinised sections were stained with haematoxylin and eosin. For nuclear staining, sections were incubated for 1-3 min in haematoxylin (Merck, Germany) followed by tap water to develop the

staining. After brief washing in distilled water, sections were briefly counter stained with eosin (AppliChem, Germany) to visualise the cytoplasm of the cells. Next, the sections were incubated shortly in 70 % and 95 % EtOH followed by incubation in 100 % 2-propanol and 100 % xylol. The sections were finally mounted with Pertex (Leica, Germany). Analysis and imaging of the staining was performed with a Leica DM4000B microscope (Leica Mikrosysteme GmbH, Wetzlar) supplied with a KY-F75U digital-camera (JVC Professional Europe Ltd., Frankfurt).

2.3.3) Immunofluorescence stainings

Immunofluorescence stainings were performed on paraffin or cryo sections of mouse skin or on epidermal whole mounts. Nuclear staining was performed for 30 min at room temperature with DAPI (Sigma, Germany) at a concentration of 1 µg/ml. Imaging of all immunofluorescence stainings was performed by confocal microscopy (Olympus IX80) supplied with an Olympus LG ESF200 camera unless specified differently.

2.3.3.1) Immunofluorescence stainings of epidermal whole mounts

Epidermal whole mounts were blocked in TB buffer containing 0.5 % milk powder, 0.25 % FSG and 0.5 % TritonX-100 in TBS (20 mM HEPES, pH7.2, 0.9 % NaCl) (Braun et al., 2003). Primary antibodies were diluted in TB buffer and incubated over night at room temperature. Washing steps to remove antibody residues were carried out with 0.02 % Tween (AppliChem, Germany) in PBS. Secondary antibodies diluted in TB buffer were incubated for 3 h up to overnight. The dilutions of the antibodies applied are listed in Table 3 and 4.

2.3.3.2) Immunofluorescence stainings of paraffin sections

Paraffin sections were deparaffinised and rehydrated before proceeding with antibody staining (2.3.1). The antibodies used are listed in Table 3 and 4. For staining of tumour tissue, the sections were incubated in citrate buffer

(BioGenex, USA) for 20 min at $< 120^{\circ}\text{C}$ under pressure in the 2100 Retriever (Proteogenix, France) to unmask the antigens. After washing with PBS, sections were incubated in blocking solution (10% RS (Sigma, Germany) in PBS) for 1 h at room temperature. Primary antibodies were incubated over night at 4°C . Secondary antibodies were incubated for 30 min at room temperature. After each antibody incubation step, washing was performed 3 times for 5 min with PBS. Sections were mounted with Mowiol/DABKO.

2.3.3.3) Immunofluorescence stainings of cryo sections

Sections of frozen tissue from K14NuMA-GFP mice (7-10 μm) were fixed in 4 % PFA or acetone before proceeding with antibody stainings except for staining with Scd1. Here, fixation was carried out after Scd1 staining was done. Dilutions of the used antibodies are listed in Table 3 and 4; blocking solutions are specified in Table 7. Primary antibodies were incubated over night at 4°C . The primary antibody against GFP was incubated for 15 min at room temperature. Secondary antibodies were incubated for 30 min at room temperature. Washing was carried out with PBS thrice for 5 min after each antibody incubation step. Sections were mounted with Mowiol/DABKO.

Table 7) Blocking solutions for immunofluorescence stainings on cryo sections

Antibody	Blocking solution (in PBS)
GFP (chicken)	3% BSA, 5 % RS, 5 % NDS
Laminin	10 % NGS
Lrig1	2.5 % BSA, 0.25 % FSG, 0.1 % TritonX100
Scd1 (goat)	10 % RS

All used ingredients of the blocking solutions were purchased from Sigma, Germany.

2.3.3.4) Immunofluorescence staining of cells

Keratinocytes from K15CreER(T2)/R26EYFP mice were used for colony forming assays (2.6.5). To verify YFP expression after formation of colonies, immunofluorescence staining was performed. PFA-fixed cells (2.6.4) were permeabilised for 10 min with 0.5 TritonX100 in PBS (Sigma, Germany) and

blocked for 1h in 10 % NGS (Sigma, Germany). Antibody against GFP coupled to Alexa488 (1:500, Rockland) was incubated over night and washed off with PBS. Nuclei were stained with DAPI for 10 min at room temperature. After washing with PBS and distilled water, YFP expression was monitored using an Olympus IX80 fluorescence microscope equipped with an IX2-KCB camera.

2.3.4) Immunohistochemistry (IHC)

To visualise the basal layer of the epidermis, K14-IHC was performed on paraffin sections of mouse skin. Sections were deparaffinised and rehydrated. To unmask the antigens, sections were incubated in citrate buffer (Biogenex, USA) at 100°C for 20 min. To inhibit peroxidases within the tissue, the sections were treated for 20 min with 3% H₂O₂ in MeOH. After blocking with 10 % NGS for 1 h at room temperature, sections were incubated with primary antibody against K14 (1:10000) over night at 4°C. After washing, secondary antibody coupled to horseradish peroxidase (HRP, DAKO Envision) was incubated for 30 min at room temperature followed by detection with AEC substrate (DAKO) for 2-3 min. To better visualise the histology of the skin sections, brief counter staining with diluted haematoxylin (1:4) was done. Sections were mounted with Kaisers glycerol gelatine. Analyses of the stainings were performed with a Leica DM4000B microscope (Leica Mikrosysteme GmbH, Wetzlar) and pictures were taken with a KY-F75U digital-camera (JVC Professional Europe Ltd., Frankfurt).

2.3.5) Alkaline Phosphatase reaction (AP)

Cells of the dermal papillae and the dermal condensate produce alkaline phosphatase (Handjiski et al., 1994). This enzyme dephosphorylates organic molecules. By adding a substrate for alkaline phosphatase on skin sections, the localisation of the DP or the dermal condensate can be visualised.

Cryo sections (7-10 µm) of mouse tail skin were allowed to dry at room temperature and were fixed in ice cold acetone (-20°C) for 10 min. After washing in 1 x PBS, 20 µl of NBT/BCIP-solution (Roche, Germany) were mixed with 1 ml buffer reaction buffer (0.1 M Tris HCl, pH 9.5, 0.1 M NaCl). Alkaline phosphatase

dephosphorylates BCIP. The resulting product reacts with NBT and forms an insoluble blue dye. After 2-3 min of incubation at room temperature, enzyme activity could be detected as blue precipitation and the reaction was stopped by washing with dH₂O. The sections were counter stained with Nuclear Fast Red (Sigma, Germany) and mounted with Kaiser's glycerol gelatine (Merck, Germany). Images were taken using a Leica DM4000B microscope (Leica Mikrosysteme GmbH, Wetzlar) supplied with a KY-F75U digital-camera (JVC Professional Europe Ltd., Frankfurt).

2.3.6) OilRedO staining

OilRedO staining was used to visualise the lipids produced by mature sebocytes of the SG within the skin. OilRedO (Amresco, Ohio, US) was dissolved in 60 % 2-propanol by stirring for 1 h at RT to a concentration of 1 %. Before usage, the solution was filtrated. Epidermal whole mounts were equilibrated for 5 min in 60 % 2-propanol and then incubated for 30 min up to 1 h in the OilRedO solution. After washing in PBS epidermal whole mounts were shortly counterstained with 1:4 diluted haematoxylin (Merck, Germany) and mounted with Mowiol/DABKO. The stainings were visualised with a Leica DM4000B microscope (Leica Mikrosysteme GmbH, Wetzlar) supplied with a KY-F75U digital-camera (JVC Professional Europe Ltd., Frankfurt).

2.4) Micro dissection

For transcriptional analyses of different tumour cell populations, small pieces of tumour tissue were isolated using laser capture micro dissection. To prepare samples for laser micro dissection, 8 µm cryo sections of tumour tissue were cut with a cryostat (Leica, Germany) and mounted on special slides covered with a membrane facilitating micro dissection (ZEISS, Germany). The sections were kept in 70 % EtOH at -20°C until further usage. To visualise the structure of the tissue, a brief haematoxylin staining was performed. Sections were shortly washed in PBS, followed by distilled water and kept 10 sec in haematoxylin solution. Brief incubation in tap water was performed to develop the staining,

followed by incubation for 1 min in 70 %, 90 % and 100 % EtOH respectively. To avoid RNase activity, all solutions were prepared with 0.1% DEPC treated water. Laser micro dissection was performed with a ZEISS Observer.Z1 microscope and a ZEISS PALM MicroBeam laser. Pictures were taken using a Hitachi HV D30 camera. Isolated samples were captured in the cap of 0.5 ml micro tube (ZEISS, Germany). The tube cap was coated with 4 μ l of mTRAP buffer (Active Motif, Belgium) supplied with 10 ng/ μ l tRNA (Roche, Germany). The collected tissue samples were directly frozen on dry ice and kept at -80°C until further usage.

First, the accuracy of the method was tested (Fig. 10). SGs were isolated from cryo sections of mouse back skin. To assure that only SG tissue and no cells of the surrounding HF or dermis were cut out, presence of markers specific for the respective cell population was analysed by PCR (see 2.5.2). As shown in Figure 10, all isolated SG-samples showed strong expression of the sebocyte differentiation marker *Scd1*. In contrast, the samples were negative for expression of the HF marker *K19* and the dermal marker *Vimentin*. This demonstrates convincingly that laser micro dissection was precise enough to isolate distinct cell populations from skin.

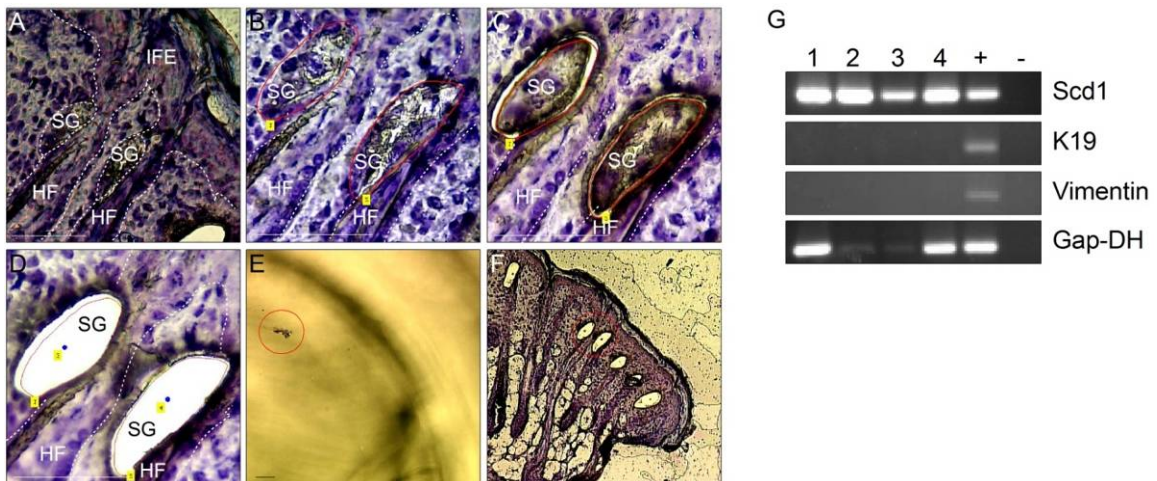


Fig. 10) Isolation of small tissue pieces and RT-PCR. A-F) Microdissection of SG tissue from wt skin. Area of interest is marked with software (red line in B). Laser cuts along the marked line (C). Area of interest is catapulted away (wholes in D). Piece of tissue is collected in sample tube (red circle in E). Overview of section with area of interest (red circle in F). G) PCR-analysis of four different isolated SGs. IFE = Interfollicular epidermis, HF = hair follicle, SG = sebaceous gland, + = wt-skin, - = water control. Scale bars: 50 μ m.

2.5) Molecular Biology

2.5.1) Genotyping of experimental mice

In order to identify the genotype of mice, tail biopsies were taken from 3 week old animals and proceeded as described below.

2.5.1.1) Isolation of genomic DNA (gDNA)

Tail biopsies were incubated in lysis buffer containing 0.2 M NaCl, 0.1 M Tris / HCl, pH 8.5, 5 μ M EDTA, 0.2 % SDS and 100 μ g/ml proteinase K (Sigma Aldrich, [39 U/mg]) for 3 h at 55°C and centrifuged for 30 min at 12000 rpm to pellet cellular debris. Supernatant was transferred to a new tube and 2 volumes of 2-propanol were added to precipitate gDNA. After centrifugation at 12000 rpm the gDNA pellet was resuspended in distilled water at 37°C over night and gDNA samples were kept at 4°C.

2.5.2) Polymerase Chain Reaction (PCR)

PCR was used to identify the genotype of mice. Generally, 500 ng gDNA were incubated with 10 pmol of primer pairs (see Table 8), 1U “ready to load enzyme mix” (Bio Budget, Germany) and 1x reaction buffer containing dNTPs (Bio Budget, Germany) in a total volume 25 μ l. The PCR program used consisted of an initial denaturation step at 95°C for 5 min, followed by 30-35 cycles of denaturation for 30 sec at 95°C, primer annealing for 60 sec at the appropriate temperature and elongation of the PCR product for 45 sec at 72°C. After a final elongation step for 5 min at 72°C, the samples were kept at 4°C until gel electrophoresis was done to separate the DNA fragments.

Table 8) Genotyping primers

Mouse strain	Primer	Oligonucleotide 5'-3'
R26EYFP (Srinivas et al., 2001)	YFP 1neu	CCA AAG TCG CTC TGA GTT GTT ATC
	YFP 2	GCG AAG AGT TTG TCC TCA ACC
	YFP 3wt	GGA GCG GGA GAA ATG GAT ATG
K15CreER(G)T2 (Petersson et al., 2011)	K15 for	AGG TGT GCG GGC AGC TGT GTT TGT
	K15 rev	GGA CAT CTT CCC ATT CTA AAC AAC ACC CTG
K14 Δ NLef1 (Niemann et al., 2002)	dNLef_for_neu	TGT CCC TTG TAT CAC CAT GGA CC
	dNLef_rev	CCA AAG ATG ACT TGA TGT CGG CT
K14L61Rac1 (Tschamntke, 2006)	SF3	TTG GTT GTG TAA CTG ATC AGT AGG C
	SF5	TGG AGA GCT AGC AGG AAA CTA GG

All primers were purchased from MWG, Germany

Moreover, PCR was used to verify gene expression in cDNA samples from isolated tissue (2.5.5 and 2.5.6). In general, 1 μ l of cDNA was used as template and incubated with the same reaction mix as described above. Primers used for detections of cDNA are listed in Table 9. The PCR was carried out applying the program described above.

All PCR reactions were done in TGradient Thermocycler or Personal Thermocycler (Biometra).

Table 9) PCR primers for cDNA samples (conventional and real time PCR)

Gene	Primer	Oligonucleotide 5'-3'
GAPDH	GAPDH for	AAC TTT GGC ATT GTG GAA GG
	GAPDH rev	ACA CAT TGG GGG TAG GAA CA
K19	K19 for	TGC TGG ATG AGC TGA CTC TG
	K19 rev	AAT CCA CCT CCA CAC TGA CC
Scd1	Scd1 for	ACA ACT ACC ACA CCT TCC CCT TC
	Scd1 rev	AGC CCA AAG CTC AGC TAC TCT TGT GAC
Vimentin	Vimentin for	CAG CTC ACC AAC GAC AAG G
	Vimentin rev	TTC CAC TTT CCG TTC AAG GT
Elovl3	Elovl3 for	CTG TTG CTC ATC GTT GTT GG
	Elovl3 rev	GCT TGA GGC CCA CTG TAA AC
Elovl4	Elovl4 for	GGGATCATACAACGCAGGATA
	Elovl4 rev	CCA CCA CAG AGT GAA CAT GG
18S rRNA	18S for	CCT GCC CTT TGT ACAC
	18S rev	CGA TCC GAG GGC CTC AC

All primers were purchased from MWG, Germany

2.5.3) Agarose gel electrophoresis

To determine the size of PCR amplified DNA fragments, PCR samples were separated on 2 % Agarose (w/v) gels in 1 x TAE electrophoresis buffer at 100 V. The correct size of the PCR products was identified with the help of a DNA low range marker (Fermentas, Germany).

2.5.4) Quantitative real-time-PCR

Harvested tissue was snap frozen in Trizol (Ambion, Life Technologies, Germany). To isolate RNA, samples were thawed at RT and tissue in Trizol was shred into small pieces using a tissue disintegrator (Janke & Kunkel, Germany). To purify RNA, the general protocol provided with the Trizol reagent (Ambion, Life Technologies, Germany) was applied according to the manufacturer's indications. Isolated RNA was dissolved in RNase free water and kept at -80°C. To synthesize cDNA, the QuantiTect Reverse Transcriptase Kit (Qiagen, Germany) was used according to the manufacturer's protocol. CDNA samples were kept at 4°C.

To evaluate the expression levels of various genes, qRT-PCR was performed using RT₂ RT SYBR Green qPCR Master Mix (SuperArray Bioscience Cooperation, USA) or TaqMan gene expression assays (Applied Biosystems). For qRT-PCR with SYBR green, 5 pmol primer pair was mixed with SYBR green master mix and 1 µl template DNA (cDNA libraries were diluted 1:10) in a total volume of 10 µl (SuperARRAY Biosciences Cooperation, USA). TaqMan gene expression assays were carried out in a total volume of 10 µl per well according to the manufacturer's instructions (Applied Biosystems).

The real time PCRs were done in 96 well plates and run in a StepOnePlus real time PCR system (Applied Biosystems). The used primers and probes are listed in Table 9 and 10.

The expression levels were calculated relative to expression of 18S rRNA (SYBR green) or GAPDH (TaqMan) using the delta ct method.

Table 10) TaqMan probes

Gene	TaqMan probe (assay ID, Applied Biosystems)
Dhcr24	Mm00519071_m1
Nupr1	Mm00498104_m1
Scd1	Mm00772290_m1
GAPDH	Mm99999915_g1

2.5.5) mRNA isolation and cDNA synthesis

To test whether micro dissection was precise (2.4) a “quick protocol” combining mRNA isolation and cDNA synthesis was used. Tissue samples (in mTRAP lysis buffer), isolated by micro dissection, were allowed to thaw on ice. To collect tissue and mTRAP buffer at the bottom of the tube, samples were shortly centrifuged. 10 mM of dNTPs and 50 ng of Random Hexamers (both SuperScript® III First-Strand Synthesis Kit, Invitrogen, Germany) were added. To lyse the isolated cells, samples were put for 5 min at 65°C on a thermo shaker (Eppendorf, Germany) and directly transferred on ice. Next, each sample was supplied with 1 µl of 10 x RT buffer, 0.5 µl “RNaseOUT”, 0.5 µl 10 mM DTT and 1 µl Superscript III enzyme (all components SuperScript® III First-Strand Synthesis Kit, Invitrogen, Germany). To allow annealing of the random hexamers to the mRNA, samples were incubated for 5 min at 25°C in a thermocycler (Biometra). For reverse transcription of the mRNA into cDNA, samples were incubated at 50°C for 60 min. Finally, the reaction was stopped by keeping the samples for 15 min at 70°C. Samples were stored at 4°C until further usage.

2.5.6) cDNA-library-generation

To analyse and compare gene expression in different cell populations of the skin or in skin tumours, cDNA libraries were generated as described by Hartmann and Klein (Fig. 11). In principle, this method allows analysing the transcription profile of one single cell and can be applied for small pieces of tissue as well. RNA is isolated and reversely transcribed into cDNA. Amplification of the cDNA of the whole transcriptome of the cell is performed to yield enough cDNA for micro array analysis (Hartmann and Klein, 2006).

In this study, the method was used to compare transcription profiles of different cell populations within skin tumours. Therefore, small tissue pieces (10-100 cells) were collected in mTRAP lysis buffer (2.4). 1 µg of Protease (Active Motif, Belgium) and biotinylated oligo-dT peptide nucleic acids (PNAs, Active Motif, Belgium) were added to the sample (Fig. 11 A). Proteolytical digestion of the cells was carried out at 45°C for 10 min. An incubation step at 70°C for 1 min and at 22°C for 15 min followed, allowing the PNAs to bind to the released mRNA (Fig. 11 B). Streptavidin conjugated magnetic beads (4 µl, Active Motif, Belgium) were added and the tubes were kept for 45 min at room temperature on a rotator (Stuart) (Fig. 11 C). As the affinity between streptavidin and biotin is very high, biotinylated PNAs attached to the mRNA bound to the magnetic beads. To wash off lysis buffer, cellular debris and gDNA, 10 µl of wash buffer 1 (Table 12) were added to the tubes. To separate the gDNA and the cellular debris from the mRNA, the tubes were placed on a magnetic rack (Invitrogen, Germany). Magnetic streptavidin-conjugated beads bound to mRNA are pelleted, whereas gDNA and cellular debris remain dissolved in the supernatant. The supernatant was transferred to a fresh tube and 20 µl of wash buffer 2 (Table 12) were added to the beads. After having placed the tubes on the magnetic rack, the supernatant was transferred to the fresh tube and 20 µl of wash buffer 1 were added. Tubes were placed on magnetic rack and supernatant was removed for the third time. Next, 20 µl of reaction mix for reverse transcription were mixed with the beads (Fig. 11 D). Primers were allowed to anneal for 15 min at room temperature. Reverse transcription was carried out at 44°C for 45 min. Then, 20 µl of tail wash buffer (Table 12) were added and the tubes were placed on the magnetic rack. Supernatant was discarded and 10 µl of tailing buffer (Table 12) were added. To release the mRNA-cDNA hybrids from the magnetic beads, denaturation was carried out at 94°C for 4 min (Fig. 11 E). Terminal deoxynucleotide transferase (10 U, Amersham, Freiburg, Germany), catalysing the addition of a G-tail to the cDNA, was added (Fig. 11 F). The samples were first incubated for 60 min at 37°C for the tailing reaction. Afterwards, the enzyme was inactivated by incubation at 70°C for 5 min. To amplify the synthesised cDNAs, PCR was performed. 5.5 µl of the following mix were added to each sample: 350 mM dNTPs, 1.2 µM CP2-primer (Table 11) and 5 U Pol Mix (DNA Polymerase, Expand Long Template Kit, Roche, Germany) (Fig. 11 G). The PCR

programme comprised 20 cycles of 15 s denaturation at 94°C, 30 s of primer annealing at 65°C and 2 min of primer extension at 68°C followed by 20 cycles with a 10 s elongation of the extension time and a final elongation step at 68°C for 7 min.

After PCR-amplification, the cDNA libraries were stored at -20°C. To assure that mRNA was successfully transcribed into cDNA, PCR for 18S or GAPDH was performed (2.5.1.2). If positive results were obtained by PCR, gene expression profiles of cDNA libraries were determined by oligo nucleotide arrays (2.5.7).

Table 11) Primers used for cDNA library generation

Primer	Oligonucleotide sequence
CFL15CN8	C ₁₅ GTCTAGAN ₈
CFL15CT24	C ₁₅ GTCTAGAT ₂₄ VN
CP2-primer	TCAGAATTCATGC ₁₅

N = any base, V = A, C or G; Primers were purchased from Metabion, Germany.

Table 12) Solutions for library generation

solution	components
Wash buffer 1	50 mM Tris-HCl, pH 8.3
	75 mM KCl
	3 mM MgCl ₂
	10 mM DTT
	0,25 % Igepal
Wash buffer 2	50 mM Tris-HCl, pH 8.3
	75 mM KCl
	3 mM MgCl ₂
	10 mM DTT
	0.5% Tween-20
Reverse transcription reaction mix	0.5 mM dNTPs
	200 U SuperScript II
	30 µM CFL15CN8 primer
	15 µM CFL15CT24
	0,25 % Igepal
	10 mM DTT
Tail wash buffer	SuperScript-buffer (Invitrogen)
	50 mM KH ₂ PO ₄ , pH 7
	1 mM DTT
	0,25 % Igepal
Tailing buffer	10 mM KH ₂ PO ₄ , pH 7
	4 mM MgCl ₂
	0.1 mM DTT
	200 µM dGTP

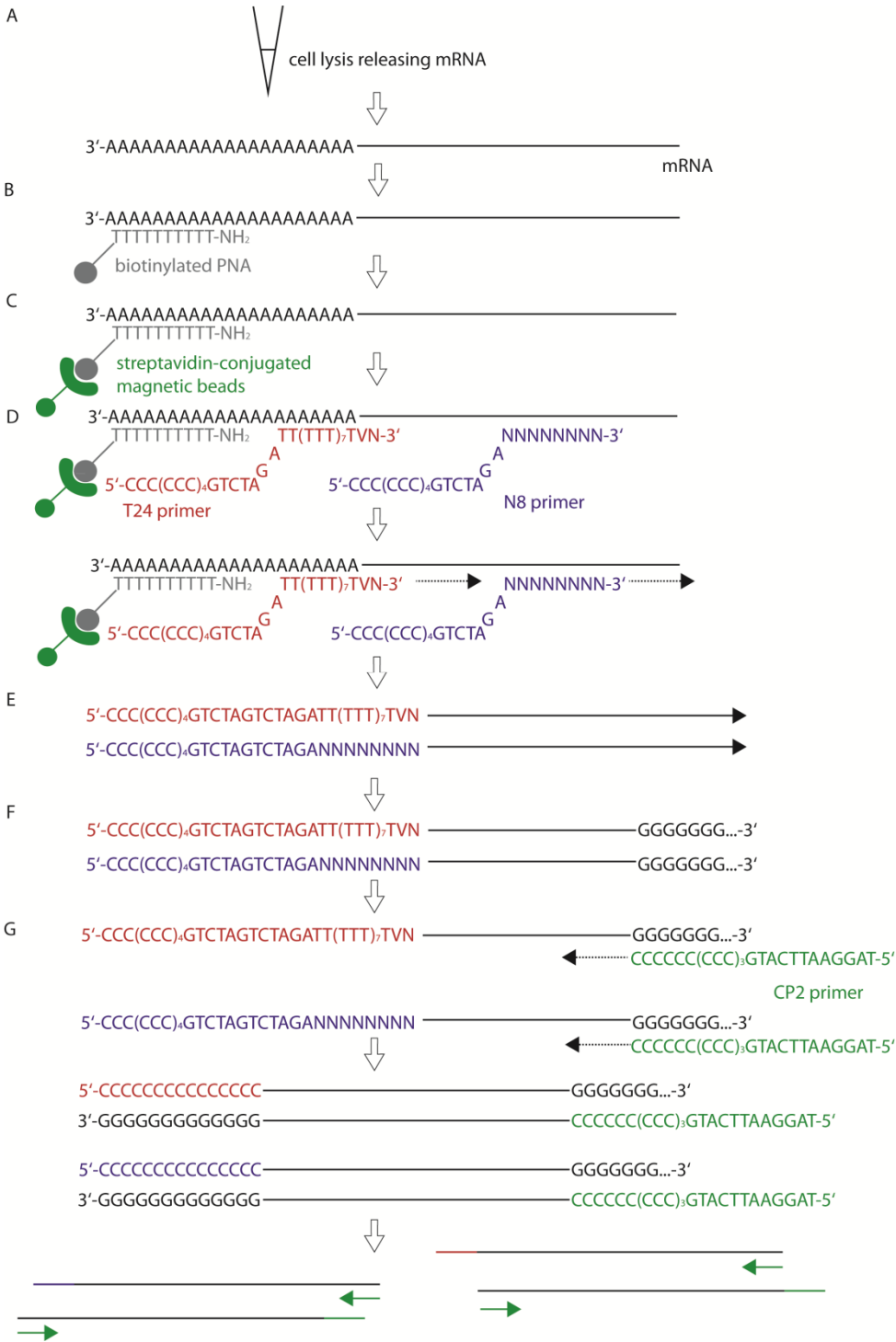


Fig. 11) Generation of cDNA libraries. Scheme depicting the main steps during synthesis of cDNA libraries. Modified from Hartmann and Klein, 2006.

2.5.7) Oligonucleotide array analysis

In order to analyse the gene expression profile of the cDNA libraries, oligonucleotide array analysis was performed (Hartmann and Klein, 2006). Therefore, the cDNA libraries were labelled with digoxigenin-conjugated nucleotides. The reaction was performed in a PCR cycler (MJ research) in the presence of 3 % formamide, 2.4 μ M CP2-BGL-primer (Table 11), dNTPs (0.35 mM dATP and dGTP, 0.3 mM dTTP and dCTP), 0.05 mM digoxigenin-labelled nucleotides (Roche and Perkin Elmer), TAQ-polymerase and the appropriate reaction buffer (Roche, Germany). A reference sample containing cDNA from different mouse tissues was labelled with biotin-conjugated nucleotides. The labelled cDNA libraries were purified using QIAGEN purification columns (QIAGEN Germany).

Murine large-scale oligonucleotide micro arrays containing 17000 oligonucleotides of 70 nt length (Operon, Netherlands) were prehybridised for 45 min at 42°C in prehybridisation buffer (Table 13). Hybridisation of the labelled cDNA libraries onto the micro array slide was carried out in an Arraybooster hybstation (Implen, Munich) at 42°C over night. The micro arrays were washed twice in wash buffer 1, followed by wash buffer 2 and wash buffer 3 (Table 13) for 10 min at 50°C. To detect differences in gene expression between the sample and the reference, the labelled cDNA fragments hybridised onto the array were stained with antibodies against digoxigenin and biotin (anti-Dig-Cy5 and streptavidin-Cy3, Jackson laboratories). After washing with wash buffer 4 (Table 13), the micro array slides were scanned in a Genepix 4000A scanner (Axon Instruments, Union City).

Table 13) Solutions for Oligonucleotide array hybridisation

solution	components
Prehybridisation buffer	5 x SSC
	0.1 % SDS
	0.1 % BSA
Wash buffer 1	1 x SSC
	0.1 % SDS
Wash buffer 2	0.5 x SSC
	0.1 % SDS
Wash buffer 3	0.1 x SSC
Wash buffer 4	4 x SSC
	0.2 % Tween-20

Micro array data were analysed using GeneSpring and normalized by Lowess in the group of Christoph Klein in Regensburg. Gene expression profiles of basal cells from K14 Δ NLef1/L61Rac1 adenoma were compared to sebocytes from K14 Δ NLef1/L61Rac1 adenoma and undifferentiated cells from K14 Δ NLef1/L61Rac1 carcinoma. Also, profiles of sebocytes from K14 Δ NLef1/L61Rac1 adenoma were compared to undifferentiated cells isolated from K14 Δ NLef1/L61Rac1 carcinoma.

2.6) Cell biology

2.6.1) Isolation of primary keratinocytes

Primary keratinocytes were isolated from mice at P 1-3. Mice were sacrificed, and disinfected with Betaisodona (Mundipharma, Germany) and 70 % EtOH. Back and tail skin was harvested and floated (dermal side down) on 0.5 % (v/v) Thermolysin (Sigma, Germany) diluted in DMEM-Hams/F12-medium (Biochrom, Germany) (without additives) for 30 min up to 1 h. The epidermis was isolated from the dermis using forceps, minced in DMEM-Hams/F12 medium (without additives) and incubated for 15 min on a rotator (ELMI RM-2L) in DMEM-Hams/F12 medium. Isolated keratinocytes were filtered (70 μ m, BD, Germany). In order to obtain a defined input of cells for FACS analyses cell number was determined with a CASY cell counter. For FACS analyses, cells were stained as described below.

2.6.2) Cultivation of J2-3T3 fibroblasts and primary keratinocytes

J2-3T3-fibroblasts were cultured in DMEM-medium (GIBCO, Germany) supplemented with 10 % FCS (PAA, Germany), penicillin (100 U/ml) and streptomycin (100 μ g/ml) (Biochrom, Germany) at 37°C and 5 % CO₂. For keratinocyte co culture, fibroblasts were treated for 2 h with 4 μ g/ml Mitomycin C (Sigma, Germany) to inhibit proliferation of the fibroblasts.

FAC-sorted (see 2.6.3) primary keratinocytes were co cultured with Mitomycin C pre-treated J2-3T3-fibroblasts. Co culture was necessary as fibroblasts produce matrix components required for keratinocyte attachment and growth. Cell culture

was performed on collagen-coated culture dishes (Beckton Dickinson, UK) in DMEM-Hams/F12 medium (Biochrom, Germany) supplemented with penicillin (100 IU/ml), streptomycin (100 µg/ml) (Biochrom, Germany), adenine (1.8×10^{-4} M) (Sigma, Germany), glutamine (2 mM) (Biochrom, Germany), hydrocortisone (0.5 µg/ml), epidermal growth factor (Shubbar et al.) (10 ng/ml), cholera enterotoxin (10^{-5} M), insulin (5 µg/ml) (Sigma, Germany) and 10 % fetal calf serum (FCS Gold) (PAA, Germany). To avoid differentiation of keratinocytes, stimulated by Ca^{2+} , FCS was treated with Chelex-100 resin (BioRad, Germany) over night at room temperature, pH 7. The treated FCS was sterile filtered before being added to the medium.

Cells were kept at 32°C in an atmosphere of 5 % CO_2 in a humidified incubator (Carroll et al., 1995; Morris et al., 1987; Rheinwald, 1989; Rheinwald and Green, 1975).

2.6.3) Fluorescence activated cell sorting

To purify YFP positive cells from isolated primary keratinocytes, Fluorescence activated cell sorting (FACS) was performed. For characterisation of YFP positive cell populations within the skin of newborn K15CreER(T2)/R26EYFP-mice, primary keratinocytes were isolated as described in 2.6.1. In these mice, Tamoxifen-inducible Cre recombinase is expressed in K15-expressing cells. The mice had been treated with Tamoxifen intra uterally during embryogenesis to induce YFP expression in cells expressing the Keratin15 promoter. In newborn mice, K15 expression is detected in cells of the IFE (Liu et al., 2003; Nöbel, 2009).

To purify YFP positive cells from isolated primary keratinocytes, a defined number of primary keratinocytes was subjected to FACS-analysis.

Isolated primary keratinocytes were co stained with an antibody against Itgα6 (PE-coupled, BD, Germany) for 45 min at 4°C to mark basal epithelial cells (Nowak and Fuchs, 2009; Watt, 2002). Cell viability was detected by staining with PI (Sigma, Germany). FAC-sorting of the cells was done with a FACS-Aria III (Beckton-Dickinson). YFP positive/Itgα6^{high} and YFPnegative/Itgα6^{high} cells were sorted to compare clonogenic potential of YFP positive versus YFP

negative basal epidermal cells. Cells were collected in tubes with DMEM-Hams/F12 medium and directly plated out on collagen coated dishes (Beckton Dickinson, UK) with growth inhibited fibroblasts (see 2.6.2).

2.6.4) Colony forming assay

Colony forming assays were performed to evaluate the clonogenic and growth potential of FAC sorted keratinocytes isolated from K15CreER(T2)/REYFP mice. YFP positive and YFP negative epidermal cells (3000, 6000 and 10000) were plated in triplicates on collagen coated 6-well plates with growth arrested fibroblasts (see 2.6.2). Keratinocytes were allowed to grow at 32°C and 5 % CO₂ in DMEM-Hams/F12 medium for three weeks to form colonies. Fibroblasts were washed off with 0.02% EDTA in PBS and the keratinocytes were fixed for 10 min with 4 % PFA. To verify YFP expression in the cells, immunofluorescence staining was performed (see 2.3.3.4). For evaluating the colony forming efficiency, colonies were stained with 0.05 % crystal violet (Sigma, Germany) for 1h and washed with PBS for 15 min. Colonies were classified according to their size. Large colonies (>2 mm²) are derived from holoclones having a high reproductive capacity. Colonies smaller than 1 mm² originate from a paraclone with short replicative lifespan. Meroclones form colonies of 1-2 mm² size with intermediate characteristics (Barrandon and Green, 1987). Area of the colonies was measured with ImageJ (version 1.41 b, National Institutes of Health, USA). The clonogenic potential was calculated for YFP positive and YFP negative cells by dividing the number of colonies by the number of plated cells and multiplying by 100%.

3) Results

3.1) Analysis of SG and HF morphogenesis in mouse tail skin

HF morphogenesis in mouse back skin has been extensively studied over the past decades. Progress has been made understanding the underlying cellular and molecular mechanisms of HF formation (Fuchs, 2007; Millar, 2002; Paus et al., 1999; Schmidt-Ullrich and Paus, 2005; Schneider et al., 2009).

In contrast to back skin HF development, less is known about the formation of tail skin HFs. Nevertheless, mouse tail skin is often used as a tool to study cellular and molecular processes within HFs (Braun et al., 2003; Janich et al., 2011; Jensen et al., 2009; Jensen et al., 2008b; Petersson et al., 2011).

It has been described that tail skin HFs are arranged in triplets (Schweizer and Marks, 1977). However, it remains unknown how tail follicle morphogenesis is regulated, if the required signals differ from back skin and how HF triplets are formed. Here, we investigate the processes of HF triplet formation during early morphogenesis in more detail.

3.1.1) HFs in mouse tail skin develop in two waves

To investigate the timing of the formation of HF triplets during morphogenesis, tail skin sections and epidermal whole mounts were analysed from P0 to P8 (Fig. 12). Development of HFs was evaluated according to defined morphological stages (Paus et al., 1999).

Formation of HFs is initiated by a molecular crosstalk of the epidermis with the underlying mesenchyme. First, mesenchymal signals define where HFs will be formed. Subsequently, epidermal signals lead to the formation of epidermal thickenings (placodes) (Fuchs, 2007). A signal from the placode to the mesenchyme induces the formation of a dermal condensate beneath the placode. The epithelial placode stretches towards the dermal condensate forming the hair germ (HG). Further elongation of the HG leads to enclosure of the dermal condensate forming the dermal papillae (DP) (Botchkarev and Paus, 2003; Duverger and Morasso, 2009; Paus et al., 1999).

In tail skin sections, HGs (stage 2) were seen regularly distributed over the skin sample and grew deeper into the dermis with further development (Fig. 12 A, B, K and L). Once HFs had reached stage 3 or 4 of HF morphogenesis (Paus et al., 1999), new placodes formed adjacent (left and right) to the first central HF (Fig. 12 C, H, Q and V).

Alkaline phosphatase (AP) staining was used to detect dermal condensates and DP (Handjiski et al., 1994). Dermal condensates underneath the placode and HG of the central follicle could be detected at stage 2, 3 and 4 of HF morphogenesis (Fig. 12 F-H). At stage 4 of HF development, the bulb of the central follicle had enclosed the dermal condensate thereby forming the DP. New dermal condensates could be detected below the placodes of the left and right side follicle (Fig. 12 H, I, J).

Taken together, analysis of tail HF development between P0 and P8 demonstrates that HFs of triplets are generated in two waves. First, the central follicle was formed and the two side follicles developed with a delay of 2-3 stages of HF morphogenesis (Fig. 12).

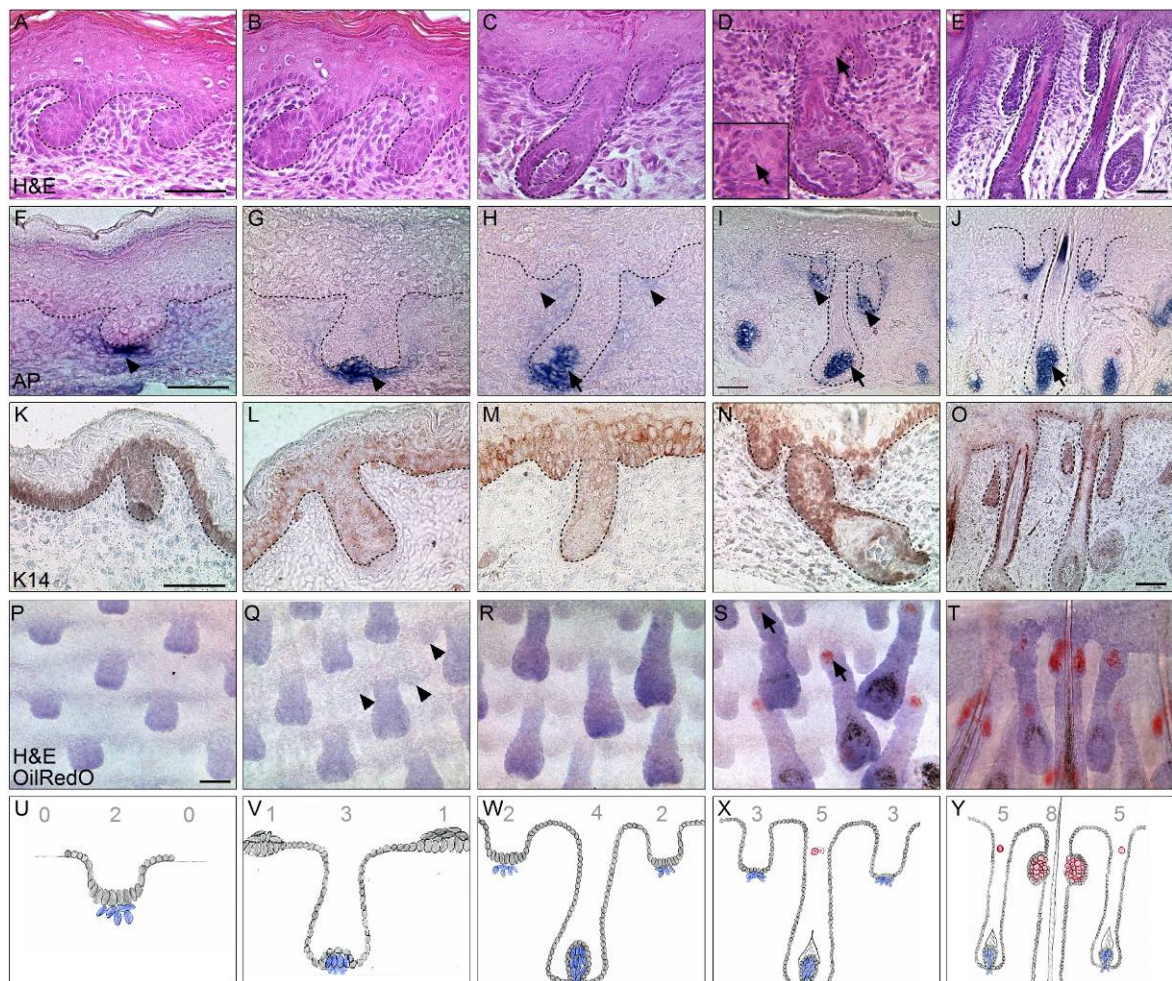


Fig. 12) HF morphogenesis in tail skin proceeds in two distinct waves. A-E) Hematoxylin and Eosin (H&E) stained skin sections of early postnatal development. Note emergence of sebocytes (arrow in D and in inset). F-J) Alkaline phosphatase (AP) staining to detect the dermal condensate (arrowhead) and dermal papillae (DP) (arrow). Note arising dermal condensates (arrowheads in F-I). K-O) K14-immunohistochemistry to mark the basal layer of the IFE. P-T) Epidermal whole-mounts stained with Hematoxylin and OilRedO. Note appearance of outer follicles (arrowheads in Q) and first visible sebocytes (arrowheads in S). U-Y) Scheme depicting the different stages of tail HF morphogenesis (DP-cells in blue, sebocytes in red). Scale bars: 50 μ m.

3.1.2) HF morphogenesis in tail skin is delayed compared to back skin

Next, we compared the time point of HF initiation in back and tail skin.

It is known, that HF morphogenesis in mouse back skin starts with the formation of primary guard hairs at E14.5 (Schmidt-Ullrich and Paus, 2005). We have compared back and tail skin samples of the same animals at different time points during morphogenesis (n=3 embryos per time point). At E15.5 when placodes have already formed in back skin (Fig. 13, upper row); tail skin does not show

epidermal thickenings or placodes (Fig. 13, lower row). Epidermal thickenings could first be detected at E16.5 in mouse tail skin (Fig. 13, lower row). This demonstrates that HF formation in tail skin was initiated with a delay of approximately one day compared to back skin.

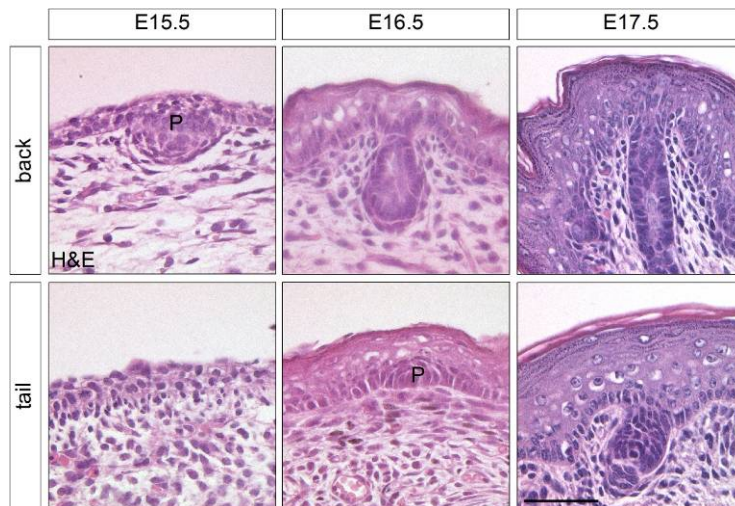


Fig. 13) Timeline of HF morphogenesis in mouse back and tail skin. Comparison of Hematoxylin and Eosin stained sections of mouse back and tail skin (E15.5 - E17.5). Note that HFs develop later in tail skin. P = placode. Scale bar: 50 μ m.

3.1.3) Different HF patterning in back and tail skin

Another striking difference between tail and back skin samples is the spatial organisation of HFs within the skin.

In back skin, different types of HFs are known. Guard HFs make up 1-3 % of the coat HFs. They produce long tylotrich hair that has also sensory function. Awl/Auchene hair makes up 30 % of the mouse coat. They are shorter than guard hairs. A third type of HFs produces zig zag hair, also known as undercoat hair. The different types of HFs develop in three distinct waves starting with the development of guard hairs at E14.5. In the second wave, awl/auchene HFs are formed around E16.5. The third wave of HF formation occurs at E18.5 forming the zigzag HFs (Duverger and Morasso, 2009; Schmidt-Ullrich and Paus, 2005). Mouse back skin HFs are arranged in a specific pattern. Guard HFs are first interspersed by awl/auchene HFs and finally, zigzag HFs fill the remaining spaces (Duverger and Morasso, 2009) (Fig. 14 A, C). In mouse tail skin, HFs develop in two waves (Fig. 12 P-Y). So far it is unknown if two types of HFs

distinguished by differences in structure and size are formed during these two waves. Furthermore, tail skin HFs are arranged in a distinct pattern different from the one observed in back skin (Fig. 14 B, D). Groups of three HF constitute a triplet. The triplets are arranged in rows from the anterior to the posterior end of the tail. Interestingly, we could detect triplets of HFs at different stages of development within one row of HF triplets. At P1.5, HFs on the dorsal side of the tail had reached stage 6 of morphogenesis (Fig. 14 B). In contrast, at the ventral side, HF morphogenesis had only proceeded to stage 4 (Fig. 14 B).

Taken together, these data show that tail skin HFs are arranged in a different pattern than HFs in back skin. Moreover, development of HFs in tail skin follows a gradient from the dorsal to the ventral side of the tail.

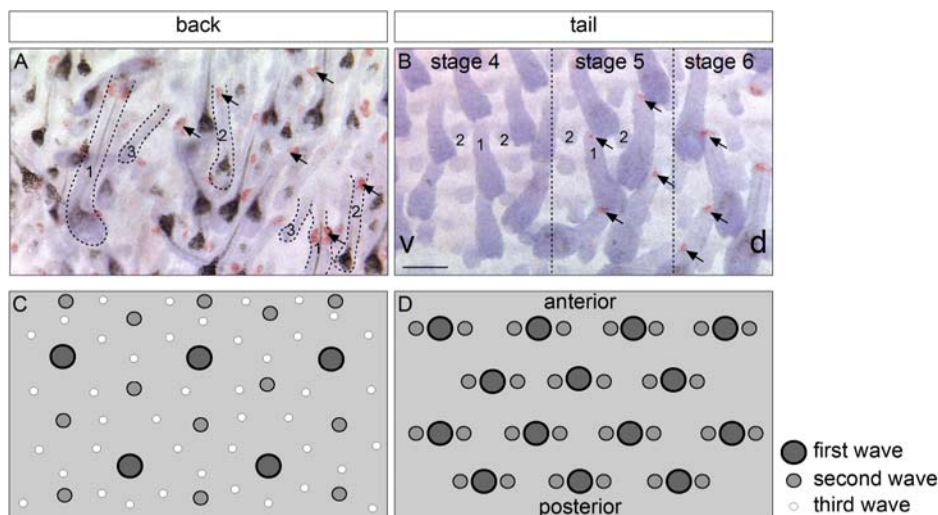


Fig. 14) Comparison of HF patterning in back and tail skin. A,B) Hematoxylin and OilRedO stained epidermal whole mounts of back (A) and tail skin (B) at P 1.5. Note different types of HFs in back skin in A (1= guard hairs, first wave; 2= awl/auchene hairs, second wave; 3= zigzag hairs, third wave). In tail skin two types of HFs are formed (1=central HF, first wave; 2=side follicles, second wave). Arrows point to SGs. C, D) Scheme depicting patterning of HF in back (C, modified from Duverger and Morasso , 2009) and tail (D) skin. Note different waves of HF formation (first wave: dark grey; second wave: light grey; third wave; white). Scale bar 50 μ m.

3.1.4) Two SGs emerge from one cluster of sebocytes

One crucial event during HF morphogenesis is the formation of the SG. The SG is a holocrine gland attached to the HF. It provides lipids (sebum) thereby contributing to maintaining an intact epidermal barrier (Niemann, 2009; Schneider and Paus, 2009). Until now, the development of the SG is not well characterised. To understand cellular processes during SG development, we have analysed SG formation in more detail.

The SG is formed at stage 5 of HF morphogenesis at the upper part of mouse back skin pelage HFs (Paus et al., 1999). Mature sebocytes were identified by staining with the lipid dye OilRedO. In tail skin, first sebocytes were detected at the upper part of HFs that had reached stage 5 of HF morphogenesis (Fig. 12 S, 15 A). As the HF developed further, the number of sebocytes increases forming a cluster (Fig. 15 B, C). Once the HF had reached stage 7 of development, the agglomeration of sebocytes splits up, thereby generating two small clusters of cells (Fig. 15 C). Each of these clusters progresses into one glandular structure with a sebaceous duct (Fig. 15 C, D, E). Surprisingly, the two SGs attached to adult HFs are formed from one single group of cells.

To study the process of SG formation in more detail, we have analysed the expression of *Scd1* (stearoyl CoA desaturase 1) and adipophilin. *Scd1* is an enzyme of the fatty acid metabolism, converting saturated into monounsaturated fatty acids (Enoch et al., 1976). It has been shown that *Scd1* is essential for proper SG maintenance and skin barrier function (Binczek et al., 2007; Miyazaki et al., 2001). Adipophilin is expressed by lipid producing cells and localises to the lipid droplets in the cytoplasm (Heid et al., 1998). We detected *Scd1* expression at stage 5 of HF morphogenesis when first sebocytes are formed (Fig. 15 F). At this stage, sebocytes could also be visualised by OilRedO staining (Fig. 15 A). Remarkably, adipophilin expression was found slightly delayed to *Scd1* (Fig. 15 F, G) and not all cells of the growing SG were positive for both markers (Fig. 15 G-I). This indicates that adipophilin marks a subpopulation of sebocytes. Another possibility could be that adipophilin is expressed by more mature sebocytes than *Scd1*.

Taken together, these data show that two SGs of mouse tail skin HF are formed from one single cluster of sebocytes.

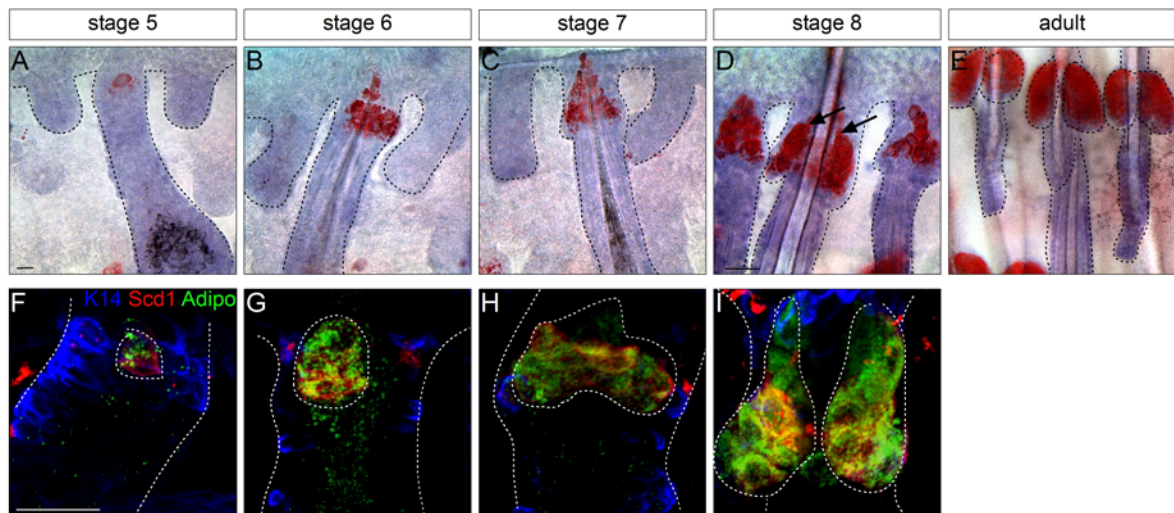


Fig. 15) Development of the SG in mouse tail skin. A-E) Hematoxylin and OilRedO stained epidermal whole mounts at stage 5, 6, 7, 8 of HF morphogenesis and adult age. Note appearance of sebaceous ducts at stage 8 (arrows in D). F-I) Adipophilin (Adipo, green), Scd1 (red) and K14 (blue) stained epidermal whole mounts visualizing the developing SG at stage 5, 6, 7 and 8. Note that two SGs develop from one cluster of cells. Scale bar: 25 μ m.

3.1.5) Proliferation during HF morphogenesis is not confined to a distinct region of the HF

During HF morphogenesis, massive proliferation is required to provide cells for the growing HF. To analyse where proliferation takes place and if it is confined to particular regions of the HF during morphogenesis, a short pulse (1 h) BrdU-incorporation assay was performed (Fig. 16). Proliferation analysis revealed that dividing cells are not accumulated in a particular area of the HF (Fig. 16 A, B, C, D). BrdU positive cells were scattered all along the HF between stage 2 and stage 6 of HF morphogenesis indicating that all cell compartments of the HF expand to a similar extent.

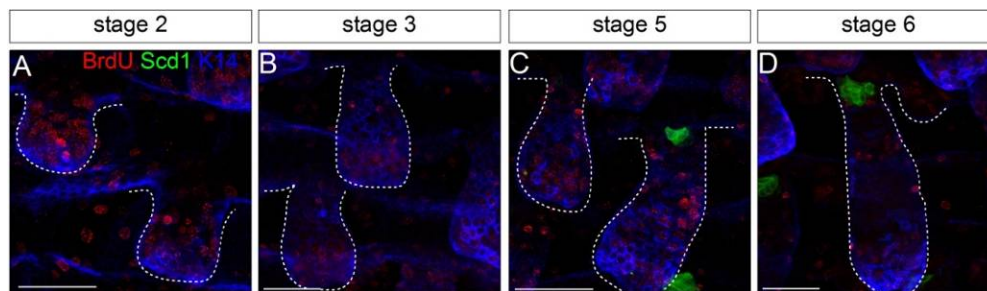


Fig. 16) Localisation of proliferating cells during HF morphogenesis. A-B) Epidermal whole mounts stained with antibodies against BrdU (red), Scd1 (green) and keratin14 (K14, blue) at stage 2 (A), stage 3 (B), stage 5 (C) and stage 6 (D) of HF morphogenesis. Scale bar : 50 μ m

3.1.6) Spatio-temporal analysis of stem and progenitor cell populations during HF morphogenesis

Various stem cell populations contributing to regeneration of the HF and SG have been identified (Blanpain and Fuchs, 2009; Jaks et al., 2010; Petersson et al., 2011). In particular, the bulge region, the junctional zone and the isthmus of the adult HF have been shown to contain stem and progenitor cells able to reconstitute HFs and SGs (Jensen et al., 2009; Jensen et al., 2008b; Nijhof et al., 2006). To analyse when stem cell compartments are established, expression of molecules marking the above mentioned cell compartments, was analysed during early postnatal tail skin development.

Sox9 has been shown to be a robust marker for HF stem cells residing in the bulge region (Vidal et al., 2005). Furthermore, it has been shown that the stem cell population expressing Sox9 is already established in placodes of pelage HF from E15.5 onwards (Nowak et al., 2008). To investigate if the Sox9 positive cell population is also established during early tail HF morphogenesis, we have performed immunofluorescence stainings for Sox9 together with P-Cadherin (PCad). PCad marks the lower portion of the developing HF (Nowak et al., 2008). Our analyses showed that Sox9 also marks a distinct cell population above the PCad positive compartment at stage 2 of HF morphogenesis in tail skin (Fig. 17 A). As the HF elongated, the Sox9 expressing compartment expanded further (Fig. 17 B, C). At stage 5 of HF morphogenesis, Scd1 expressing sebocytes were detected (Fig. 17 D, E). Of note, these arose above the Sox9 expressing zone which localised to the presumable future bulge region at this stage of HF morphogenesis.

Recently, Lrig1 has been shown to be expressed by stem and progenitor cells of the junctional zone of the HF able to give rise to cells of the SG and IFE in adult skin (Jensen et al., 2009). Cells in the isthmus region of the HF express the MTS24-antigen Plet1 (MTS24/Plet1). These cells showed a high clonogenic potential *in vitro* (Nijhof et al., 2006). Moreover, cells of the upper isthmus were able to give rise to HF, SG and IFE in reconstitution assay (Jensen et al., 2008a). To investigate if Lrig1 or MTS24/Plet1 positive cells potentially participate in morphogenesis of the SG, expression of these markers was analysed during early HF development. Lrig1 expression was already detected at stage 2 of HF morphogenesis (Fig. 17 F). Similar to the Sox9 positive keratinocytes, the cluster of Lrig1 expressing cells expanded as the HF elongated, but remained at the upper part of the HF (Fig. 17 G, H). Interestingly, Scd1 positive cells could be detected in the Lrig1 positive compartment indicating that sebocytes were formed surrounded by Lrig1 positive cells (Fig. 17 I, J). In contrast, MTS24/Plet1 expression was not detected before stage 6-7 of HF morphogenesis (Fig. 17 K-M), once first sebocytes had been formed at the upper part of the HF (Fig. 17 M).

Taken together, these data show that Sox9 and Lrig1 are expressed prior SG formation and could potentially play a role in its formation. MTS24/Plet1 positive cells however are unlikely to contribute to SG formation as expression of this marker could only be detected at stage 7 when first sebocytes were already visible.

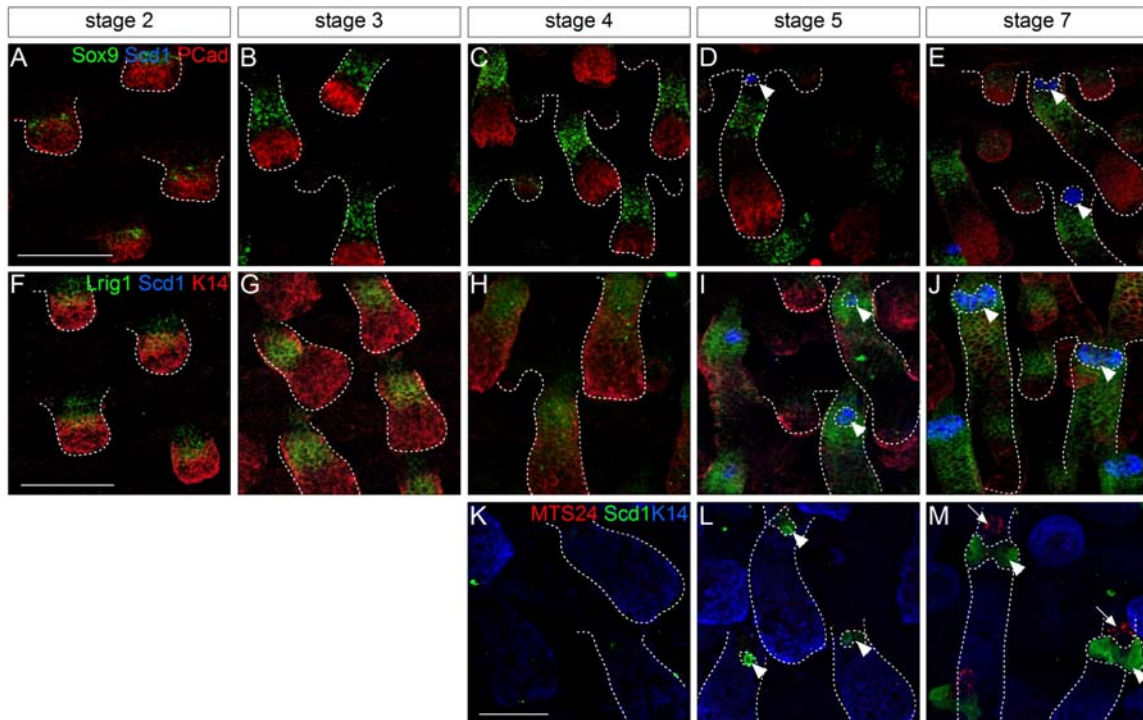


Fig. 17) Expression of stem and progenitor markers during HF morphogenesis. A-E) Immunofluorescence staining of Sox9 (green), Scd1 (blue) and P-Cadherin (PCad, red) of epidermal whole mounts during HF development. Note appearance of first sebocytes at stage 5 of HF morphogenesis (arrowheads in D and E). F-J) Expression analysis of Lrig1 (green), Scd1 (blue) and Keratin 14 (K14, red) shows that sebocytes (arrowheads in I and J) arise within the Lrig1 positive zone of the developing HF. K-M) Staining for MTS24/Plet1 (red) Scd1 (green) and K14 (blue) reveals that sebocytes (arrowheads in L) arise before progenitor marker MTS24/Plet1 (arrows in M) is detected. Scale bars: 100 μ m

3.1.7) Dynamic expression of stem cell markers Lrig1 and Sox9 during HF and SG morphogenesis

Analysis of Lrig1 and Sox9 expression demonstrated that both markers are expressed from early HF morphogenesis onwards. Immunofluorescence stainings revealed expression of Lrig1 and Sox9 in the same region of the developing HF (Fig. 17 A-E and F-J). To investigate if both markers are expressed by the same cells, co immunofluorescence stainings were performed (Fig. 18). Lrig1 and Sox9 are indeed co expressed by cells of the HF at stage 3 and 4 (Fig. 18 A, B, E). Interestingly, at stage 5 of HF morphogenesis when sebocytes first arise (Fig. 17 D, I, L), either marker is expressed by distinct compartments within the HF and this pattern remains throughout further development (Fig. 18 C, D, F). In particular, Lrig1 expressing cells localize to the

upper part of the HF, close to the IFE, where the SG will be formed. In contrast, Sox9 expressing cells localise further down the HF at the future bulge region. These data suggest a dynamic expression of Lrig1 and Sox9 during HF morphogenesis. Co expression of both markers at earlier stages of HF morphogenesis suggests that both stem cell compartments share characteristics of simple progenitors during development. By mechanisms that are not known so far, the cell populations separate during HF morphogenesis. Localisation of Lrig1 expression at the upper part of the HF once the SG starts to form indicates that Lrig1 positive stem cells are likely to play a role in formation of the SG.

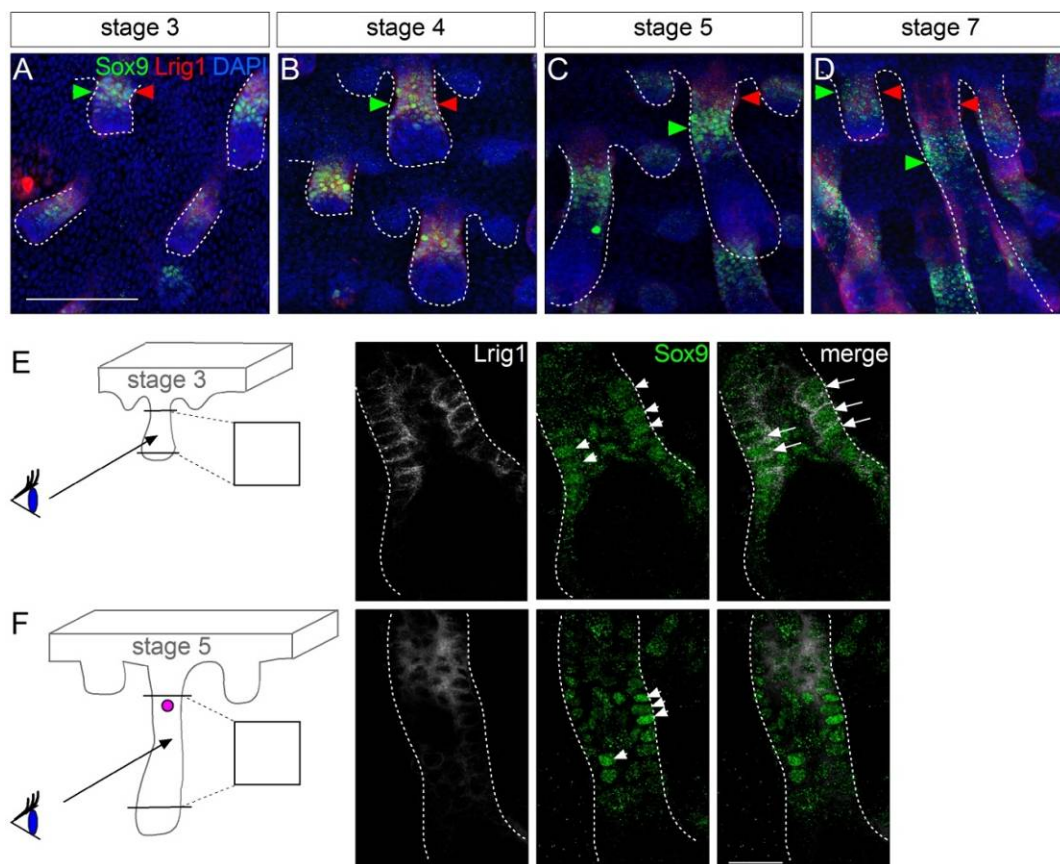


Fig. 18) Dynamic expression of progenitor markers Lrig1 and Sox9 during HF morphogenesis. A-F) Epidermal whole mounts analysed for expression of stem cell marker Sox9 (green) and Lrig1 (red). Co expressing cells are marked with white arrows in E and F. Red arrowheads (A-D) mark the Lrig1 stem cell compartment, green arrowheads (A-D) and white arrowheads (E, F) point to Sox9 expressing cells. A-D) Z-projections of epidermal whole mounts, E, F) sections through epidermal whole mounts. Scale bars: A-D) 100µm, E,F) 20µm.

3.2) Cellular mechanisms of SG morphogenesis

3.2.1) Sebocytes emerge adjacent to Lrig1 expressing cells

Our initial results suggested that Lrig1 positive stem cells could give rise to sebocytes. To investigate this in more detail, co immunofluorescence stainings of Lrig1 and Scd1 at different steps of HF formation were performed. The first sebocyte visible at stage 5 of HF morphogenesis arose adjacent to Lrig1 expressing cells (Fig. 19 A). Furthermore, an increasing number of sebocytes was surrounded by Lrig1 positive cells. However, the sebocytes were Lrig1 negative (Fig. 19 A, B). At stage 7 of HF morphogenesis, when the cluster of sebocytes splits up forming two individual glands, each cluster of Scd1 expressing cells was enclosed by Lrig1 positive stem cells (Fig. 19 C, D).

These data showed that sebocytes arise within the Lrig1 positive stem cell compartment.

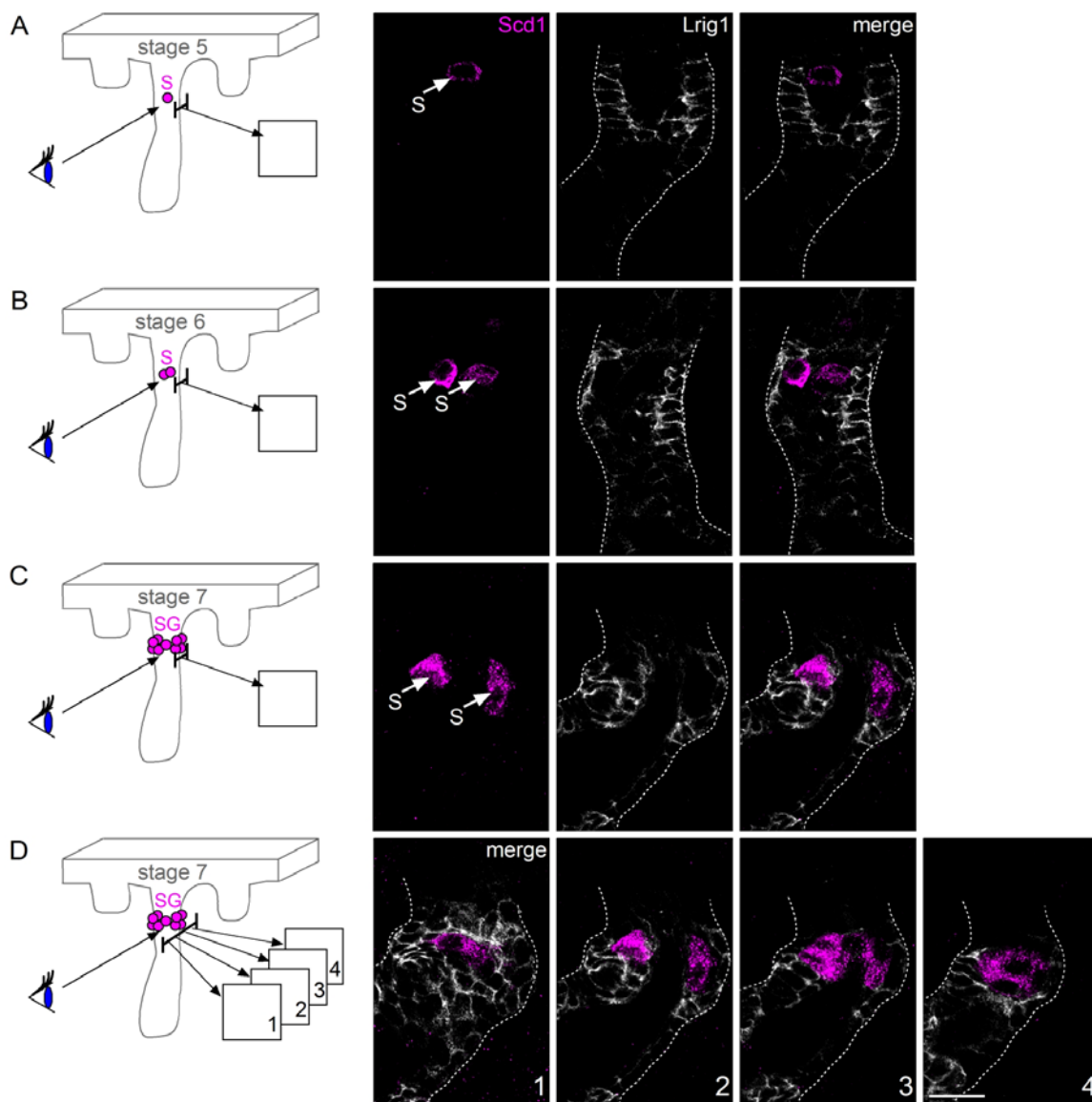


Fig. 19) Sebocytes arise next to Lrig1 positive stem cells. A-D) Sections through epidermal whole mounts stained with Lrig1 (white) and Scd1 (magenta) shows that sebocytes (S) arise adjacent to Lrig1 expressing cells. SG = sebaceous gland. Scale bar: 20µm.

3.2.2) Lrig1 positive stem cells generate sebocytes by asymmetric cell fate decision

The data suggested that Lrig1 positive stem cells give rise to sebocytes (Fig. 19). We hypothesised that Lrig1 positive cells underwent asymmetric cell fate decision to generate sebocytes. To test this, we have determined the orientation of mitotic spindles within this progenitor compartment.

To visualise spindle orientation in cells of the HF, skin sections of K14NuMA-GFP mice (Poulson and Lechler, 2010) were analysed for expression of NuMA, a marker of spindle poles. In this mouse model, NuMA-GFP is expressed under control of the K14 promoter. Therefore, it is present in all basal cells of the IFE, HF and SG, localising to the nucleus. In non-dividing cells, NuMA-GFP is localised diffusely within the nucleus. Once cells undergo division, NuMA-GFP expression is detected at the spindle poles of the dividing cell (Poulson and Lechler, 2010). We have analysed spindle orientation of mitotic cells at the upper part of the developing HF between P0 and P5 (Fig. 20).

At least two scenarios of cell division can occur within the Lrig1 positive compartment. Orientation of the cell division axis in parallel to the basement membrane would lead to two Lrig1 positive stem cells and increase the cell compartment. If Lrig1 stem cells would divide perpendicularly to the basement membrane, one daughter cell could leave the basement membrane and differentiate towards the sebocyte lineage.

Skin sections (n = 171) of K14NuMA-GFP mice were stained for GFP together with Scd1, Lrig1 or Laminin1 (Fig. 20) to analyse the orientation of the spindle poles. Laminin1 was used to determine spindle orientation in relation to the basement membrane. Spindle poles detected at the upper part of stage 5 to stage 7 HFs were quantified. The majority of cell divisions (84%) observed in Lrig1 positive cells occurred perpendicularly to the basement membrane. One spindle pole was oriented towards the basement membrane, the other pole pointed towards the Scd1 expressing sebocytes. Only 16% of the counted spindles were orientated in parallel to the basement membrane (Fig. 20 A, C).

These data indicate that Lrig1 positive stem cells can give rise to Scd1 positive sebocytes by asymmetric cell fate decision.

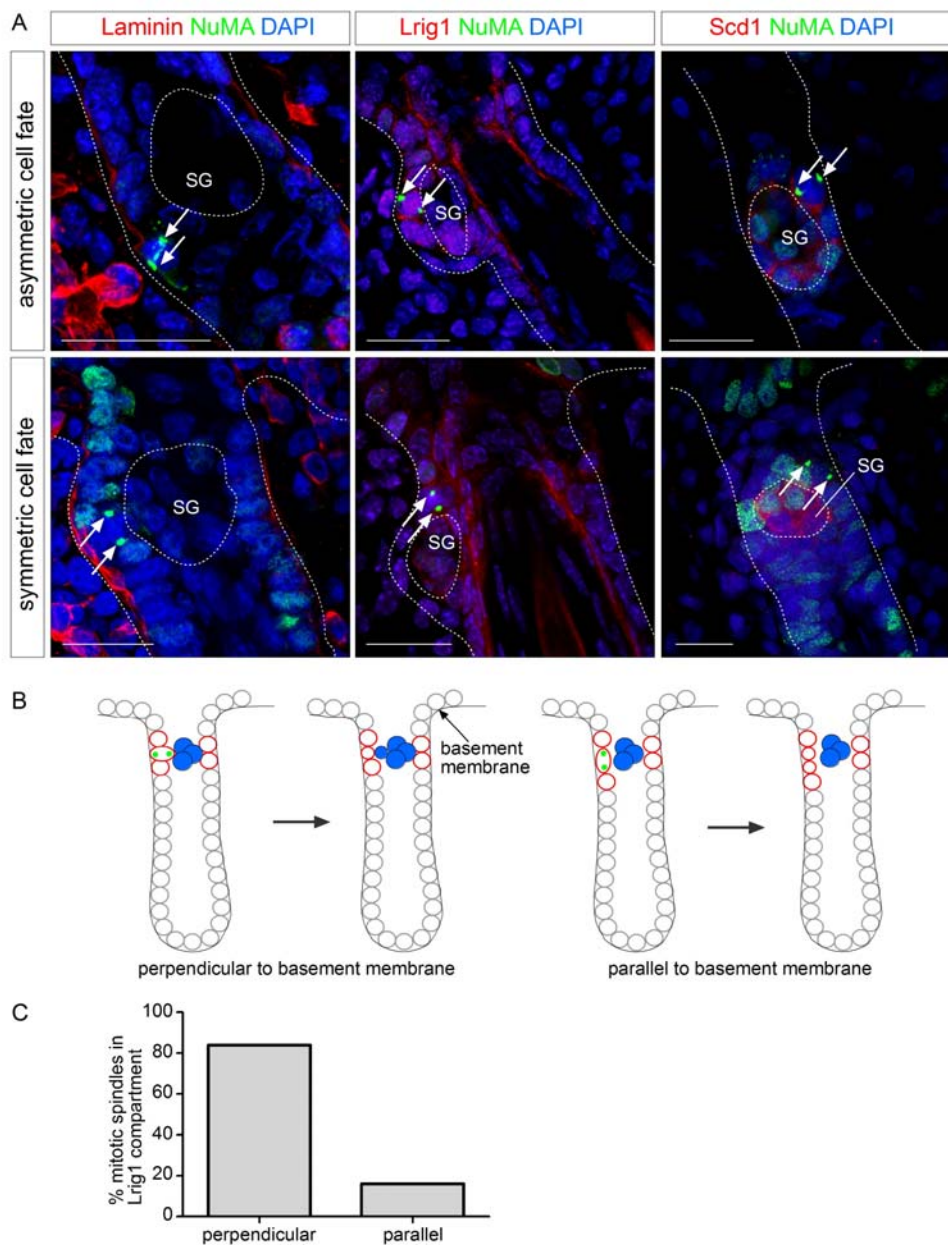


Fig. 20) Lrig1 positive cells generate sebocytes by asymmetric cell fate decision. A) Analysis of skin sections of K14NuMA-GFP mice for orientation of mitotic spindles during SG-development. NuMA-GFP (green, arrows) was costained with Laminin, Lrig1 or Scd1 (red) to visualize the cell type undergoing mitosis. Perpendicular spindle orientation (upper row, asymmetric cell fate) as well as parallel spindle orientation (lower row, symmetric cell fate) could be detected. B) Schematic drawing summarising symmetric and asymmetric cell fate within the Lrig1 progenitor compartment during SG morphogenesis. C) Quantification of perpendicular and parallel spindles detected within the Lrig1 compartment. $n = 171$ sections were counted. Scale bars: $20\mu\text{m}$.

3.2.3) Proliferating Lrig1 positive cells give rise to sebocytes

During development of the SG, expansion of the Scd1 positive compartment takes place. First, one Scd1 positive sebocyte is formed. Over time, a cluster of sebocytes develops that will finally split up forming two SGs. Proliferation via BrdU incorporation at the upper part of the HF was analysed to determine the cell compartment fuelling SG morphogenesis.

Determination of the spindle pole orientation demonstrated that Lrig1 positive stem cells gave rise to sebocytes by asymmetric cell fate decision (Fig. 20, 3.2.2). We wanted to analyse if the sebocytes themselves were able to proliferate and enlarge the cell cluster. Therefore, a 1h pulse of BrdU was given to mice (P 0 - P 2) and BrdU incorporation was analysed at different time points of development (Fig. 21).

Analyses of the upper part of the HF at stage 5 of HF morphogenesis revealed that BrdU positive cells were detected within the Lrig1 positive compartment. In contrast, Scd1 positive sebocytes were BrdU negative. As the sebocyte cluster increased in size (stage 7 of HF morphogenesis), Scd1 positive cells remained BrdU negative, whereas BrdU/Lrig1 double positive cells were detected around the sebocytes. These data indicate that proliferating Lrig1 positive cells could give rise to sebocytes.

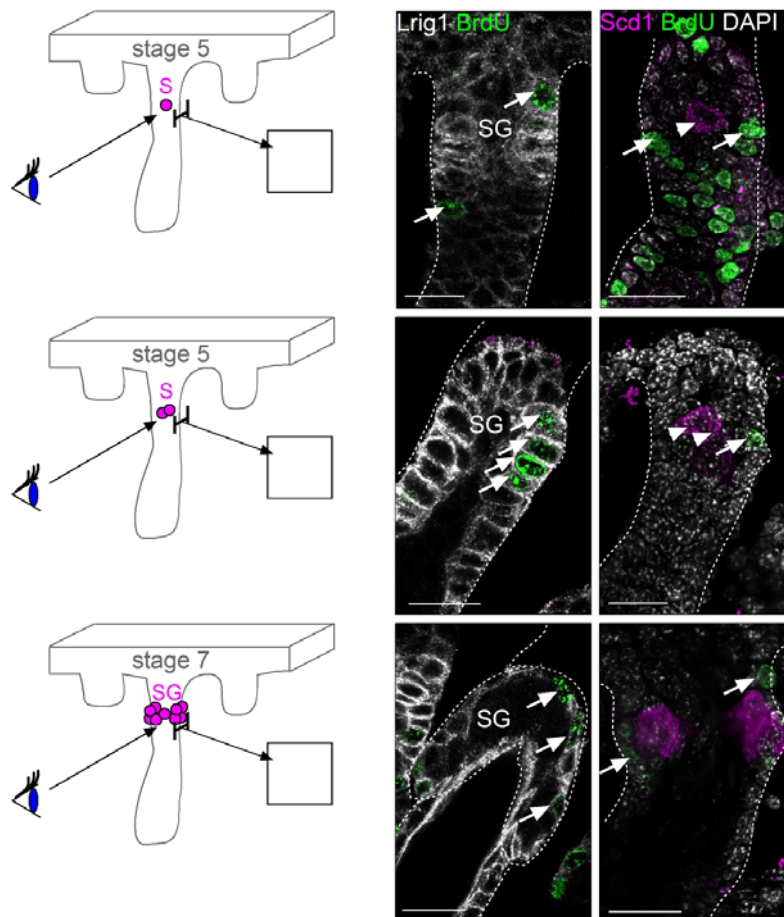


Fig. 21) Lrig1 positive cells proliferate to generate sebocytes. Colocalisation of Lrig1 (grey, left image) and BrdU (green) at stage 5 (upper and middle row) and 7 (lower row) of HF morphogenesis reveals that proliferation occurs in the Lrig1 positive compartment (arrows) and not in Scd1 positive cells (magenta, arrowheads). S, sebocytes; SG, sebaceous gland. Scale bars: 20 μ m.

To determine whether Lrig1 positive cells indeed gave rise to Scd1 positive sebocytes, short term EdU pulse-chase experiments were conducted. EdU incorporation was analysed at 1h and 48h of chase (Fig. 22). After 1h, EdU positive cells were seen within the Lrig1 positive compartment, whereas Scd1 positive cells remained EdU negative (Fig. 22 A, B). After 48 h, a weaker EdU label could also be detected in Scd1 positive sebocytes (Fig. 22 B, D). This indicates that Lrig1/EdU double positive cells proliferated thereby diluting the label out and giving rise to Scd1 positive sebocytes. Statistical analyses (Fig. 22 E) revealed that none of 233 counted HFs (n=3 mice) contained Scd1/EdU double positive cells after 1h EdU pulse. However, after 48h, 305 HFs comprising Scd1/EdU double positive cells (n=3 mice) could be detected. These data demonstrate that Lrig1 positive cells were initially labelled with EdU. The

EdU label was diluted out by proliferation of Lrig1 positive cells giving rise to sebocytes.

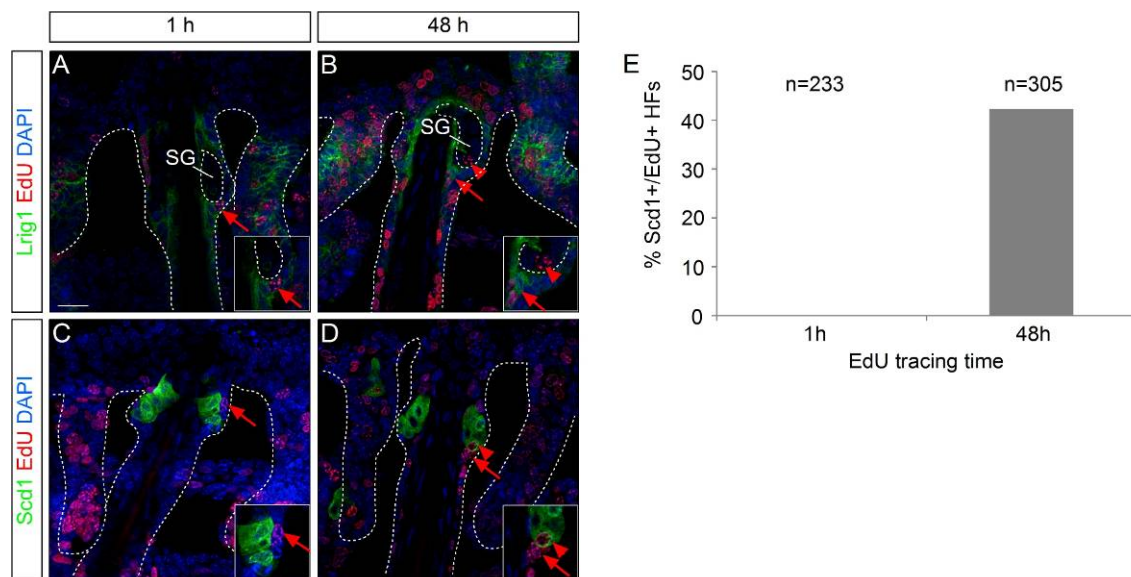


Fig. 22) Lrig1 positive cells proliferate and give rise to sebocytes. EdU labelling shows that initially, Scd1 positive cells (green in C) are negative for EdU-incorporation (red) (A, C). Note that Lrig1 positive cells (green in C and D) surrounding the SG incorporated EdU (red arrow). When chased for 48 h Scd1/EdU double positive cells (red arrowhead) and EdU positive cells (red arrow) were detected (B, D). E) Quantification of HFs with Scd1/EdU double positive cells at 1 h and 48 h after EdU pulse (n = 3 mice). Insets are enlargements of the SG. SG = sebaceous gland. Scale bars: 20 μ m.

3.3) Origin of cells forming HF and SG

One emerging issue in the field of skin biology is to identify the origin of cells generating the SG. Recently, it was demonstrated that early HF stem cells marked by the expression of Sox9 were required for the formation of the SG. In the absence of Sox9, neither HF stem cells nor SGs were formed (Nowak et al., 2008). The data presented in this thesis analysing Sox9 and Lrig1 expression suggested that HFs and SGs are formed by the same precursor cells during morphogenesis. To further investigate the origin of cells forming HFs and SGs, we have performed lineage tracing analysis during epidermal morphogenesis.

During adult homeostasis of HFs and SGs, stem cells of the bulge region regenerate the HF in a cyclic fashion (Schneider et al., 2009). Bulge stem cells have also been proposed to be the source for cellular renewal of the SG (Blanpain et al., 2004; Morris et al., 2004; Taylor et al., 2000). Recently, our group has provided strong evidence supporting this model (Petersson et al., 2011). Mice expressing inducible Cre recombinase under control of the K15 regulatory promoter sequence in bulge stem cells (AK15CreER(G)T2-mice) were crossed to R26REYFP reporter mice (Srinivas et al., 2001). Application of low doses of Tamoxifen leads to activation of Cre recombinase in 1-3 bulge stem cells. Excision of a stop cassette in front of the YFP gene leads to constitutive YFP expression in cells with active Cre and all descendents of these cells (Fig. 6). Therefore, the progeny of initially labelled bulge stem cells can be traced. It was demonstrated that bulge derived progeny reconstitute HF and SGs (Petersson et al., 2011). Interestingly, it was previously shown that the promoter fragment used for the generation of AK15CreER(G)T2- mice was already active during early postnatal morphogenesis (Liu et al., 2003). Moreover, expression of K15 protein was detectable as early as E15.5 in mouse epidermis (Nöbel, 2009). Therefore, we hypothesised that the K15 promoter fragment could already be active at E15.5 in the epidermis. The facts that K15 derived progeny contribute to SG regeneration and that the K15 promoter is active before the initiation of SG formation made our mouse model useful for lineage tracing approaches during early HF and SG morphogenesis. Applying AK15CreER(G)T2/R26REYFP-mice we aimed to analyse if the K15 positive cell population was already active during

HF morphogenesis and could serve as an important cellular source for the formation of the SG.

3.3.1) Individual cells are labelled in tail IFE upon embryonic Tam treatment

To label individual epidermal cells at early stages of HF morphogenesis, pregnant female AK15CreER(G)T2/R26REYFP mice were injected i.p. with one single dose of 2mg Tam at E16.5. In this initial approach, we focussed on the analysis of YFP labelled cells and their progeny in tail epidermis.

To analyse the number of initially labelled cells, mice were prepared one or two days following Tam treatment (E17.5 or E18.5). Our initial data show that one day after Tam injection, almost no YFP expression was detected in tail epidermis of E17.5 embryos (Fig. 23 B). At E18.5 (two days following Tam treatment), YFP positive cells could be clearly identified (Fig. 23 C). This duration of Cre recombinase activation is consistent with previous reports using this particular Cre line (Petersson et al., 2011). As shown in Fig. 23 C, individual epidermal cells were labelled. Moreover, groups of two or three YFP positive cells were seen in close proximity to each other. One possible explanation would be that neighbouring cells randomly responded to Tamoxifen treatment individually. Another possibility is that one cell was labelled, divided and gave rise to daughter cells. Importantly, only cells in the epidermis were initially labelled and no positive cells could be detected in the already established placodes of the central HF. Thus, the experiments reveal that the K15 promoter fragment used to drive inducible Cre expression is already active at E16.5 in basal keratinocytes of the IFE.

So far, for each time point, three embryos of two different litters were analysed and similar results could be observed. To characterise the amount and distribution of labelled YFP positive cells in more detail, statistical analyses are currently performed.

However, the data show that individual cells could be targeted within the epidermis and this protocol is applicable to track YFP positive progeny during morphogenesis.

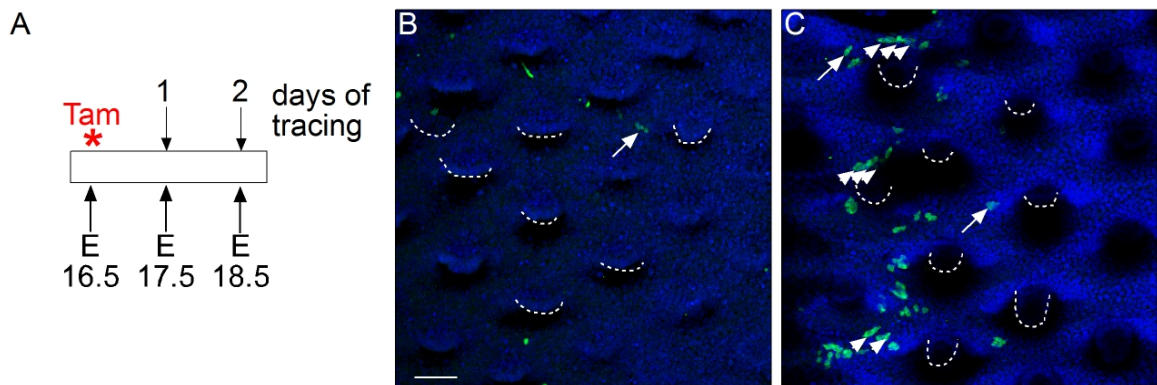


Fig. 23) Targeting of epidermal cells using AK15CreER(G)T2 mice. A) Timeline of Tamoxifen application and tissue harvesting. B-C) YFP-detection in epidermal cells at E17.5 (B) and E18.5 (C). Arrows point to YFP positive nuclei (B) and to individually labelled cells (C). Arrowheads point to small clusters of YFP positive cells. Dashed lines mark placodes of central HF. Scale bar 50 μ m.

3.3.2) Cells originating in the IFE contribute to HF and SG formation

To investigate whether individual YFP cells derived from the IFE contribute to formation of HFs and SGs, lineage tracing experiments were conducted. Therefore, later tracing time points were analysed. Tam was given at E15.5 or E16.5 to pregnant female mice and the pups were prepared at different time points shortly after birth.

Initial data suggest that labelled K15 positive cells first expanded within the epidermis. Three or four days after Tam treatment, larger YFP positive cell clusters could be detected (Fig. 24 B). Five to seven days following Tam treatment, YFP positive cells could also be detected in the developing HFs (Fig. 24 D). To characterise the distribution and localisation of labelled cell clusters in more detail, we have quantified the localisation of YFP positive cells within the pilosebaceous unit four to ten days after Tam treatment. Therefore, three different labelling patterns were defined. We grouped HFs with labelled cells at the upper part, not reaching below the SGs (termed SG). A second group comprised HFs only containing labelled cells beneath the SG (termed HF). HFs containing cells in both parts were summarised in the third group (SG/HF).

The majority of primary (central) HFs with YFP positive cells could be classified in “SG”. In these HFs, we could detect YFP positive cells surrounding Scd1 positive sebocytes (Fig. 12 D). Importantly, we also observed colocalisation of YFP and Scd1 in sebocytes (Fig. 12 K). To strengthen these observations, co

immunofluorescence stainings for Lrig1 and YFP are currently performed to analyse if K15 derived progeny contributes first to the Lrig1 positive compartment before generating sebocytes.

In secondary (side) HFs that had only reached stage 2 or 3 of HF morphogenesis, it was more difficult to distinguish between the SG and the HF pattern. Here, labelled cells localised more randomly distributed within the HG or bulbous peg (Fig. 24 C). Accordingly, most of the secondary HFs were counted in the SG/HF pattern. HFs displaying labelling according to the “HF” pattern were observed to a much lesser extent than the two other labelling patterns. This suggests that K15 derived progeny derived from the IFE preferentially localise to the SG and only occasionally contribute to the formation of HF. To strengthen these initial data, detailed statistical analyses will be performed. Moreover, co immunofluorescence stainings with markers specifically expressed in different regions of the developing HF will be performed. Thus we will be able to quantify contribution of K15 derived progeny to distinct regions within the HF.

To follow the fate of the cells labelled in the IFE, we have analysed tail skin of mice traced for a longer period of time. Analysing HF nineteen days after Tam treatment (at E15.5 or E16.5) demonstrates that K15 derived progeny can still be detected. Classifying the labelled HFs according to the above mentioned patterns revealed that an important part of the labelled HFs were among the “SG” pattern (Fig. 24 E, F). However, we also observed HF with YFP positive cells exclusively localising beneath the SG (“HF” pattern). More rarely, HFs with labelled cells in HF and SGs were detected (Fig. 24 G). In order to statistically evaluate the results obtained so far, more animals will be analysed in the near future. Our initial data strongly suggest that cells of the SG derive from the IFE and that HF and SG might be formed by different cell populations.

We have also labelled cells at E17.5, when most placodes, at least of the central HFs, are already established (Fig. 24 I-K). Similar to the results obtained before, we detected expansion of labelled cells in the IFE at two days of tracing (Fig. 24 J). When tracing was performed for seven to ten days, YFP positive cells were also detected within the HFs, mostly in the upper part. Importantly, clonal expansion of YFP positive cells from the IFE towards the SG was detected (Fig. 24 K, L).

Taken together, these initial data indicate that cells derived from the IFE contribute to HF and SG formation even after placode formation has occurred. The fact that a considerable amount of HFs contained labelled cells only at the upper part of the HF, not below the SG indicates that K15 derived progeny originating in the IFE contributes to the formation of the SG. In a majority of HFs with YFP positive cells in the “SG” pattern no YFP positive cells were detected in the HF. Therefore, it is tempting to speculate that progenitor cells of the IFE are specifically recruited to form the SG and most likely the Lrig1 positive stem cell compartment as well. This would provide a novel mechanism into the process of the formation of the SG.

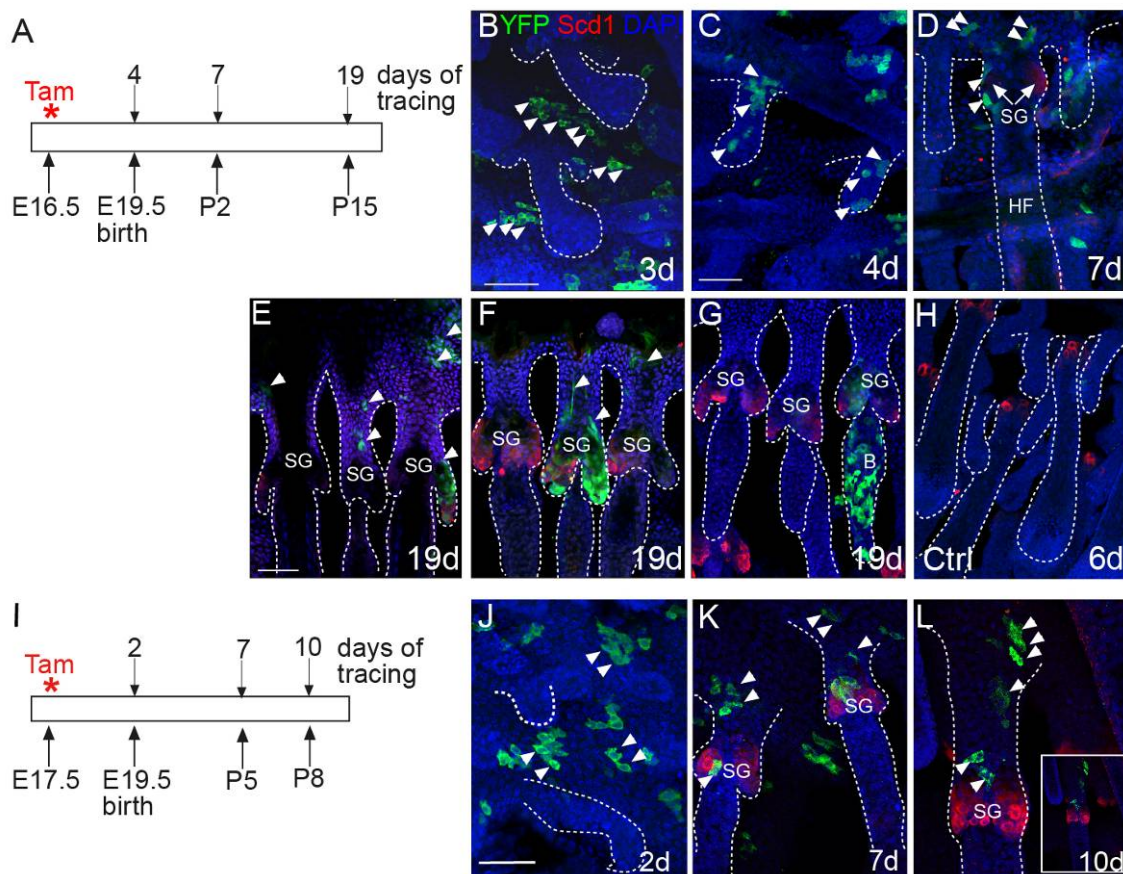


Fig. 24) Lineage tracing of IFE cells contributing to SG-development. A-G) Tracing of K15 derived progeny from E16.5 to P15. H) Oil control, I-K) Tracing of K15 derived progeny from E17.5 to P8. A, I) Timeline of Tamoxifen treatment and duration of tracing. B-H, J-K) Immunostaining of YFP (green) and Scd1 (red) on epidermal whole mounts isolated at different tracing time points. Note clonogenic expansion of labelled cells (arrowheads in B-F and I-K). Note bulge region (B) and sebaceous glands (SG) containing YFP-labelled cells in telogen HFs. Oil control (H) is clean. Scale bars: 50µm.

3.3.3) K15 derived progeny display high proliferative capacity *in vitro*

Together with previous results obtained in our laboratory, our initial lineage tracing experiments of K15 derived progeny during skin morphogenesis imply that the labelled YFP positive cells can give rise to different cell types. To evaluate labelled K15 positive cells of the IFE for their proliferative potential a colony forming assay was performed *in vitro* (Barrandon and Green, 1987; Jensen et al., 2010). In principle, a defined number of cells is plated and formation of colonies is followed for several weeks. In general, stem cells having a high proliferative capacity, form more large colonies than transit amplifying cells.

In order to investigate the proliferative capacity of K15 expressing cells and immediate progeny, we have isolated YFP positive cells at early postnatal stages of skin development. To obtain a sufficient amount of YFP labelled cells, another line of the K15CreER(G)T2 mice was applied (CK15CreER(G)T2). In this mouse line, more cells are labelled initially upon Tam treatment (Petersson et al., 2011). Prior isolating YFP positive cells, it was confirmed that initially YFP labelled keratinocytes were only detected in the IFE and not in the placodes (data not shown).

To perform the colony forming assay, embryos were treated intra uterally at E15.5 or E16.5 as for the lineage tracing experiments described before. YFP positive keratinocytes were isolated at day 5 of tracing (see 2.6.1). To increase the number of cells, back and tail skin of all pups from one litter were pooled. In order to purify basal epidermal cells, staining for Itg α 6 was performed (2.6.3). Epidermal cells were FAC-sorted for strong YFP signal and high Itg α 6 expression (Itg α 6^{high} / YFP^{positive}). As negative control, Itg α 6^{high} / YFP^{negative} cells were sorted (Fig. 25 A). 3000 YFP positive/Itg α 6^{high} and YFP^{negative}/Itg α 6^{high} epidermal cells were plated in triplicates on collagen coated culture dishes containing growth-inhibited fibroblasts (2.6.4). Additionally, 6000 and 10000 were plated as well.

Four weeks following cultivation cells were fixed and stained. Colonies were counted and the colony forming efficiency (CFE) was calculated (number of colonies/number of plated cells in %). Interestingly, CFE of YFP positive cells

was higher compared to YFP negative populations. This implies that YFP positive cells have a stronger ability to form colonies *in vitro* than YFP negative cells (Fig. 25. C, D). This indicates that YFP positive cells have a better capacity to attach to the collagen via integrins. It has been shown in human keratinocytes that enhanced adhesion is due to higher β 1-Integrin expression and this also correlates with higher proliferative capacity (Jones and Watt, 1993; Jones et al., 1995). However, the overall number of colonies formed by 3000 YFP positive cells was very low but more colonies were formed by YFP positive cells compared to YFP negative cells. When plating 6000 and 10000 cells, the CFE was higher and YFP positive cells formed more colonies than equal numbers of seeded YFP negative cells. To evaluate the proliferative potential of the plated cells we have also compared the size of colonies formed by 6000 or 10000 seeded cells (Fig. 25 E). Initial data suggest that a higher number of larger colonies is formed by YFP positive cells than by YFP negative cells. The percentage of small, abortive colonies was higher in YFP negative cells compared to YFP positive cells. To strengthen the data obtained so far and to perform statistical analysis, the assay will be repeated.

Taken together, this initial approach investigating colony forming potential of K15 derived progeny suggests that these cells have a higher proliferative capacity and form more colonies *in vitro*.

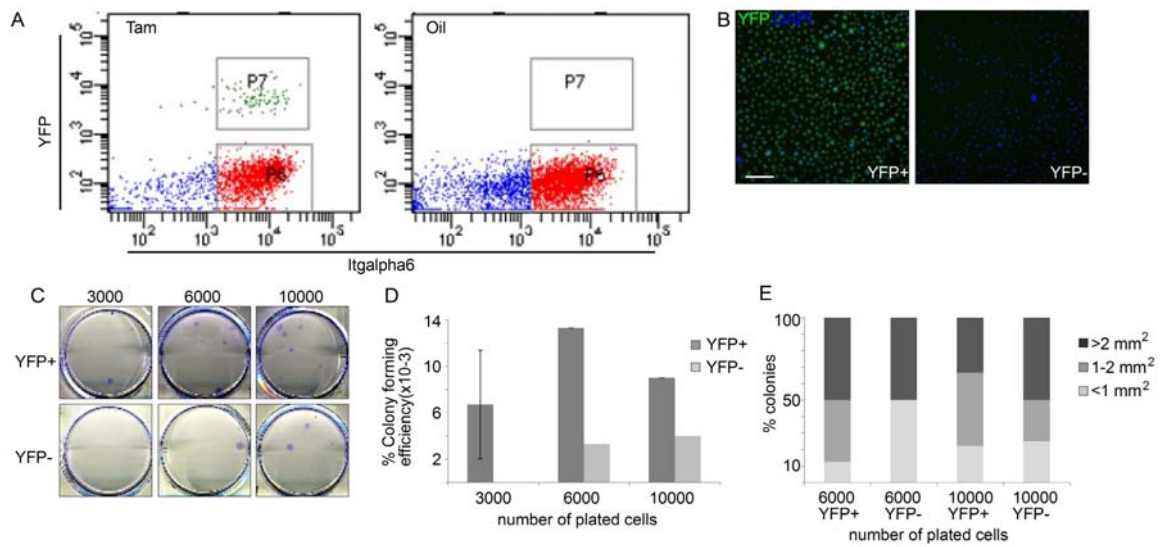


Fig. 25) YFP-positive cells have a higher potential to form colonies *in vitro*. A) FACS-plot of sorting procedure showing YFP positive (P7) and YFP negative (P6) cells. Note that Oil control is clean, not containing YFP+ cells in P7. B) YFP-expression in keratinocyte colonies. C) Crystal violet stained keratinocyte colonies from FACS-sorted YFP positive and YFP negative cells. D) Plotted colony forming efficiency of YFP positive and YFP negative cells. E) Evaluation of the colony size formed by YFP positive and negative cells. Scale bar 100 μ m

3.4) Influence of Rac1 on sebocyte differentiation in skin tumours

Together with the results of other groups, we have shown that HF stem cell populations implicated in the regeneration of the SG during adulthood also play a role in the development of this organ (Frances and Niemann, 2012; Nowak et al., 2008). It has been demonstrated that these stem and progenitor compartments are also established during ectopic SG development (Petersson et al., 2011). This appears in mice expressing N-terminally truncated Lef1 under the control of the K14 promoter (K14 Δ NLef1 mice, (Niemann et al., 2007; Niemann et al., 2002)). In K14 Δ NLef1 mice, spontaneous, well differentiated sebaceous adenomas, sebomas and squamous papillomas with sebocyte differentiation are formed (Niemann et al., 2002). These non-invasive, benign tumours can also be induced upon treatment with DMBA (Niemann et al., 2007).

In addition, the small GTPase Rac1 was previously shown to be crucial for proper maintenance of the HF stem cell compartment (Benitah et al., 2005; Chrostek et al., 2006). Activated Rac1 lead to an expansion of cells capable of clonal growth *in vitro* (Benitah et al., 2005). This indicates a potential role for Rac1 in regulating stem cell behaviour.

To investigate the effect of activated Rac1 on tumour formation, K14 Δ NLef1 mice were crossed to mice expressing L61Rac1, a constitutively active variant of the small GTPase Rac1 in epidermal cells (Tscharntke, 2006). After treatment with the carcinogen DMBA, K14 Δ NLef1/L61Rac1 mice developed sebaceous adenomas, sebomas and squameous papillomas like the K14 Δ nLef1 mice. Interestingly, also less differentiated tumours were observed (Tscharntke, 2006). To address the role of Rac1 in tumour growth, histology and invasiveness, we have analysed skin tumours of mice expressing K14 Δ NLef1 and K14L61Rac1 in epidermal cells in more detail. K14 Δ NLef1/L61Rac1 mice were compared to K14 Δ NLef1 mice. We have investigated if expression of activated Rac1 in tumours lead to alterations in the stem cell compartments. Therefore, expression of HF progenitor markers in addition to sebocyte differentiation markers was analysed within the tumours.

3.4.1) L61Rac1 alters proliferation and sebocyte differentiation in skin tumours

The incidence and frequency of skin tumours did not vary much between K14 Δ NLef1/L61Rac1 and K14 Δ NLef1 mice. L61Rac1 control mice did not form tumours (Tschardtke, 2006). The majority of the tumours of K14 Δ NLef1/L61Rac1 mice were sebaceous adenomas and squamous papillomas with sebocyte differentiation (Fig. 26). However, some of the tumours developing in K14 Δ NLef1/L61Rac1 mice showed an altered histology with a more undifferentiated character (Fig. 26).

Previously, it has been shown that K14 Δ NLef1-mice developed well differentiated benign sebaceous adenomas with lobules comprising an outer, proliferative layer of keratinocytes and differentiated sebocytes in the centre of the lobules (Niemann et al., 2007). To compare sebocyte differentiation and proliferation in K14 Δ NLef1- and K14 Δ NLef1/L61Rac1 mice, co immunofluorescence stainings for Scd1 and BrdU were carried out (Fig. 26 A). Indeed, the K14 Δ NLef1-adenomas showed well organized tumour lobules filled with Scd1 positive sebocytes. BrdU incorporating basal cells were detected at the periphery of the well organised sebocyte lobules (Fig. 26 E).

K14 Δ NLef1/L61Rac1 mice also formed well differentiated sebaceous adenomas with differentiated sebocytes in the centre and undifferentiated proliferating basal cells at the periphery of the tumour lobules (Fig. 26 B, F). Tumours of K14 Δ NLef1/L61Rac1 mice that were classified as sebomas showed less sebocyte differentiation and BrdU positive cells were not always confined to the layer of basal keratinocytes surrounding the sebaceous lobules of the tumours (Fig. 26 C, G). These tumours also contained regions with more squamous differentiation (data not shown). Another type of tumours detected in K14 Δ NLef1/L61Rac1 mice showed a very different histology. Major parts of the tumour consisted of very small, densely packed cells (Fig. 26 D). Hardly any differentiated sebocyte expressing Scd1 could be detected in these tumours. In contrast, BrdU positive cells were distributed over the tumour mass (Fig. 26 H). These tumours did not display the well organised lobular structure of an adenoma anymore and were therefore referred to as K14 Δ NLef1/L61Rac1 carcinoma.

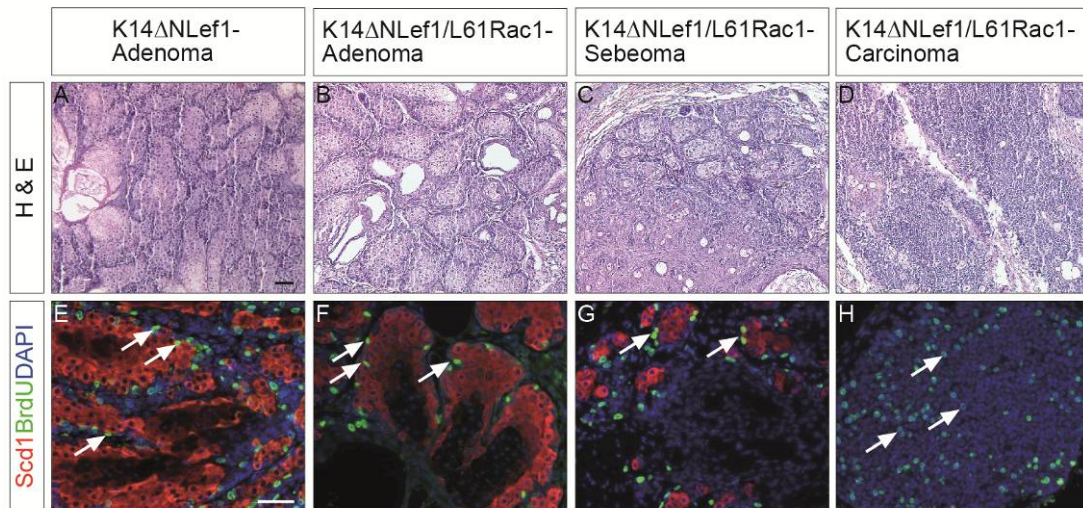


Fig. 26) Histology and proliferation of sebaceous tumours. A-D) Hematoxylin and Eosin stained sections of tumour tissue from K14 Δ NLef1 and K14 Δ NLef1/L61Rac1 -mice. E-H) Immunostaining to analyse expression of Scd1 (red), BrdU (green) in sections of skin tumours. Arrows point to proliferating cells, Scale bars: 50 μ m

The fact that some of the K14 Δ NLef1/L61Rac1 tumours displayed an undifferentiated histology lead to the hypothesis that the expression of activated Rac1 in tumours of K14 Δ NLef1 mice triggered expansion of HF progenitor cells at the expense of sebocyte differentiation. Moreover, sebocyte differentiation could be blocked. To test this, expression of HF progenitor and sebocyte differentiation markers was analysed on transcriptional and protein level, summarised in Table 14 (Sharma, 2011). Overall, immunofluorescence stainings revealed a decrease of sebocyte differentiation markers such as Scd1 and Adipophilin in K14 Δ NLef1/L61Rac1 sebeomas and K14 Δ NLef1/L61Rac1 carcinomas compared to K14 Δ NLef1- or K14 Δ NLef1/L61Rac1 adenomas. This result could be verified on a molecular level by conducting qRT-PCR. Also on transcriptional level, Scd1 expression was decreased in K14 Δ NLef1/L61Rac1 carcinomas and sebeomas versus K14 Δ NLef1/L61Rac1 and K14 Δ NLef1 adenomas. In contrast, an increase of the HF progenitor marker MTS24/Plet1 could be identified in K14 Δ NLef1/L61Rac1 sebeomas and carcinomas compared to K14 Δ NLef1/L61Rac1 adenomas and K14 Δ NLef1 adenomas by antibody staining. Stem cell marker Lrig1 was analysed on transcriptional level. Lrig1 expression was moderately elevated in K14 Δ NLef1/L61Rac1 carcinomas compared to K14 Δ NLef1/L61Rac1 adenomas and K14 Δ NLef1 adenomas. Itga6, a marker expressed by basal epithelial cells was slightly down regulated on

protein level in K14 Δ NLef1/L61Rac1 sebomas and K14 Δ NLef1/L61Rac1 carcinomas.

Taken together, these data indicate that sebocyte differentiation markers were down regulated in K14 Δ NLef1/L61Rac1 carcinomas whereas HF progenitor markers were up regulated.

Table 14) Analysis of progenitor and sebocyte differentiation marker expression in sebaceous tumours

Tumour type	SG differentiation marker			Progenitor marker		
	Scd1		Adipo-philin Protein	Plet1 Protein	Itga6 Protein	Lrig1 Transcription
	Protein	Transcription				
K14 Δ NLef1/adenoma	+++	+++	+++	+	+++	+
K14 Δ NLef1/L61Rac1 adenoma	+++	+++	+++	+	+++	+
K14 Δ NLef1/L61Rac1 seboma	++	n.d.	++	++	++	n.d.
K14 Δ NLef1/L61Rac1 carcinoma	+	+	+	++	+	++

+++ = strong expression, ++ = medium expression, + = weak expression, n.d. = not determined

3.4.2) Isolation and transcriptional profiling of distinct cell populations from sebaceous tumours

Some of the K14 Δ NLef1/L61Rac1 tumours showed less sebocyte differentiation and enhanced expression of HF progenitor markers compared to other K14 Δ NLef1/L61Rac1 tumours. Potentially, the small, densely packed cells of the K14 Δ NLef1/L61Rac1 carcinomas were undifferentiated sebocytes that were unable to undergo maturation. Besides this, it would be possible that gene expression in the K14 Δ NLef1/L61Rac1 carcinoma cells was altered. To identify potential candidate genes responsible for maintaining the cells in an undifferentiated state, we analysed the transcriptional profile of different tumour cell populations. Transcription profiles of basal cells and mature sebocytes of the K14 Δ NLef1/L61Rac1 adenomas were compared to profiles of undifferentiated cells from K14 Δ NLef1/L61Rac1 carcinomas.

To isolate distinct tumour cell populations, laser capture micro dissection approach was employed. In a first set of experiments, a pilot approach was conducted assuring accuracy of the method (see 2.4). Therefore, individual cell

populations were isolated from skin sections by laser capture micro dissection. RNA was isolated and reversely transcribed into cDNA (see 2.5.5). We have analysed marker expression by RT-PCR. Cells isolated from SGs expressed *Scd1* but did not express *K19*, known to be expressed by the HF exclusively. Also, SG-derived tissue did not show expression of *Vimentin*, a marker of the adjacent dermal cells (Fig. 10, Materials and Methods). Therefore, we concluded that micro dissection was precise enough to isolate distinct cell populations.

To compare transcriptional profiles of tumour cells, three different cell populations were isolated from the *K14 Δ NLef1/L61Rac1* tumours (Fig. 27). Basal cells and mature sebocytes were cut out from *K14 Δ NLef1/L61Rac1* adenomas (Fig. 27 A-D and E-H) and areas of undifferentiated cells were captured from *K14 Δ NLef1/L61Rac1* carcinomas (Fig. 27 I-L). Areas comprising 10-100 cells were isolated.

To determine the transcriptional profiles of the isolated cell populations, cDNA libraries were generated from 10 tissue samples of each cell type (see 2.5.6). Therefore, a novel method allowing analysing the transcriptional profile of one single cell was applied (in collaboration with the group of Christoph Klein, Regensburg, Germany). This approach involves isolation of mRNA and reverse transcription into cDNA. To amplify the amount of cDNA, PCR is conducted maintaining the relative expression levels of transcribed genes. Gene expression profiles of the different isolated cell populations were generated by oligonucleotid-arrays in collaboration with the group of Christoph Klein.



Fig. 27) Microdissection of distinct tumour cell populations. Basal cells (B) (A-D) and sebocytes (S) (E-H) from K14 Δ Nlef1/L61Rac1 adenomas and undifferentiated cells (U) (I-L) from K14 Δ Nlef1/L61Rac1 carcinomas have been isolated. Area of interest has been marked (red line in B, F, J). Laser cuts along the marked line (C, G, K) and piece of tissue is catapulted into collection tube (arrows in D, H, L). Scale bars: 50 μ m.

The expression profiles of basal cells, sebocytes and undifferentiated cells were compared to each other (in collaboration with the group of C. Klein, Regensburg, Germany). Differentially regulated genes were identified between basal cells and undifferentiated cells and sebocytes and undifferentiated cells. Table 15 summarises a selection of differentially regulated genes. Most of the genes listed in this table are associated with the lipid metabolism such as *Scd1* or *Elovl3* and 4. The majority of these genes was down regulated in undifferentiated cells captured from K14 Δ Nlef1/L61Rac1 carcinoma compared to basal cells and sebocytes isolated from K14 Δ Nlef1/L61Rac1 adenomas. This indicates a change in the gene expression profile in cells of the K14 Δ Nlef1/L61Rac1 carcinoma. A complete list of all significantly regulated genes can be found in the annex of this thesis (see 11). Interestingly, the differences detected between sebocytes and basal cells were not statistically significant. The majority of the genes up regulated in sebocytes compared to undifferentiated cells were also up regulated in basal cells compared to undifferentiated cells. This indicates that genes necessary for differentiation towards the sebocyte lineage are already

expressed when the cells are still in an undifferentiated state. Thus, basal cells of adenoma lobules are already committed towards their cell fate.

Table 15) Significantly regulated genes associated with lipid metabolism (in sebocytes and basal cells versus undifferentiated cells) derived from K14ΔNLef1/L61Rac1 mice

Gene symbol	Log2fc (compared to undifferentiated cells)		description
	Sebocytes	Basal cells	
Elovl4	6,165	5,182	Elongation of very long chain fatty acids-like 4
Elovl3	5,661	4,716	Elongation of very long chain fatty acids-like 3
Psap11	4,409	3,082	Prosaposin-like 1
Dhcr24 (Seladin-1)	3,901	3,137	24-dehydrocholesterol reductase
Adfp	3,306	1,76 (ns*)	Adipose differentiation related protein (Adipophilin)
Nupr1	3,227	-	Nuclear protein 1
Scd1	3,117	3,532	Stearoyl-Coenzyme A desaturase 1
Dgat2l6	3,027	-	Diacylglycerol O-acyltransferase 2-like 6
Pnpla5	2,846	-	Patatin-like phospholipase domain containing 5
Elovl6	1,534 (ns*)	3,522	Elongation of very long chain fatty acids-like 6
Apoa2	-	-2,991	Apolipoprotein A-II

*) ns = not significant; positive values signify up regulation of genes, negative values signify down regulation

3.4.3) Verification of selected candidate genes

The expression of the differentially regulated genes detected in the oligo nucleotide-arrays was validated by qRT-PCR. cDNA libraries applied in the array were used to verify the gene regulation. In addition, further cDNA libraries were generated from basal cells and sebocytes captured from K14ΔNLef1/L61Rac1 adenoma and undifferentiated cells isolated from K14ΔNLef1/L61Rac1 carcinoma (2.4 and 2.5.6). Fig. 28 shows exemplary results of qRT-PCR analyses. The validation results of selected candidate genes are presented in the following chapters.

In addition, we have identified interesting candidate genes playing a role in different biological functions. For example, Gankyrin has been associated with cell cycle regulation (Lozano and Zambetti, 2005). Another promising candidate gene is Prominin2, related to Prominin1, which is established as a marker for renal or prostatic epithelial stem cells (Bussolati et al., 2005; Fargeas et al.,

2003; Richardson et al., 2004). In the future, we will analyse the role of these interesting candidates in more detail.

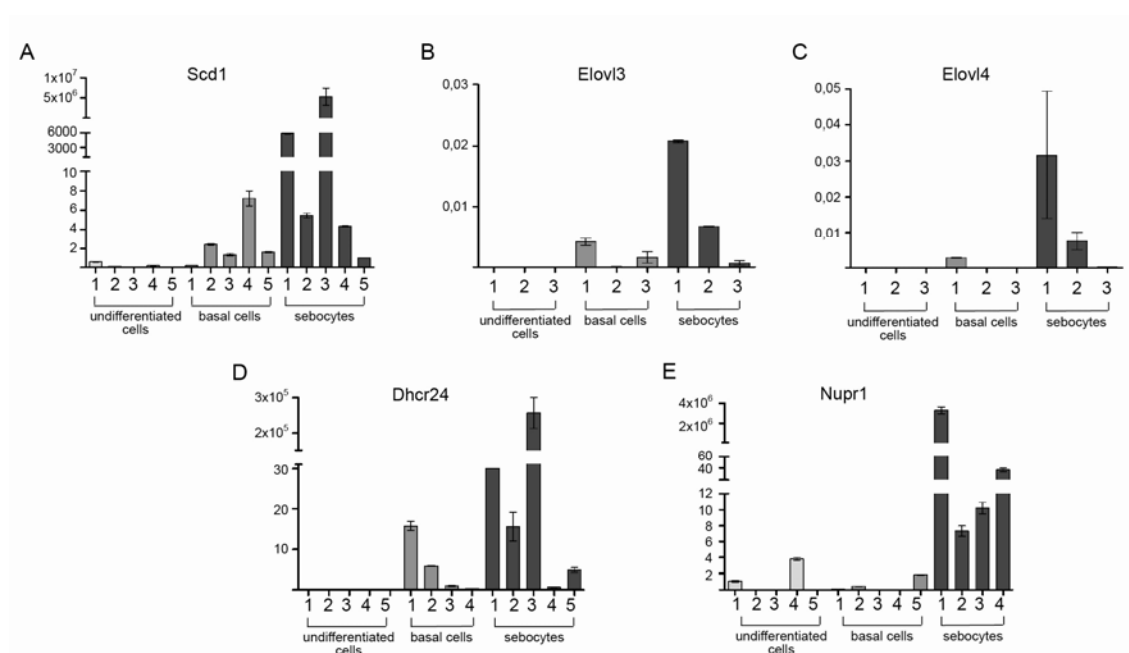


Fig. 28) Verification of selected candidate genes. A-C) qRT-PCR results verifying regulation of Scd1(TagMan-assay), Elovl3 and 4 (SYBR-green assay) in basal cell, sebocytes and undifferentiated cells of K14 Δ nLef1/KL161Rac1-tumours. D, E) qRT-PCR results (TaqMan-assay) verifying regulation of Dhcr24 and Nupr1 in basal cells, sebocytes and undifferentiated cells of K14 Δ nLef1/KL161Rac1-tumours.

3.4.3.1) Down regulation of Scd1, Elovl3 and Elovl4 in cells of K14 Δ NLef1/L61Rac1 carcinoma

We have analysed expression levels of genes known to be involved in the lipid metabolism of sebocytes as Scd1 and Elovl3 (Binczek et al., 2007; Miyazaki et al., 2001; Westerberg et al., 2004). Elovl4 was previously shown to play a role in skin barrier function (Cameron et al., 2007; Li et al., 2007).

Applying TaqMan or SYBR green assays, the regulation of Scd1, Elovl3 and Elovl4 as determined in the micro array could be confirmed. Our qRT-PCR results showed very low expression of Scd1, Elovl3 and Elovl4 in most of the samples isolated from K14 Δ NLef1/L61Rac1 carcinomas (Fig. 28 A, B, and C). In the basal cells isolated from K14 Δ NLef1/L61Rac1 adenomas, all of the tested genes were expressed to a lesser extent than in the sebocytes from the same tumours (Fig. 28). This shows that genes necessary for lipid metabolism of

sebocytes are already expressed, although to a lesser extent, when the cells are not fully differentiated.

Gene expression of *Scd1* was also analysed using RNA isolated from whole tumour lysates (Sharma, 2011). Expression levels of *Scd1* were significantly down regulated in tumours classified as K14 Δ NLef1/L61Rac1 carcinomas compared to K14 Δ NLef1/L61Rac1 adenomas. Furthermore, protein expression of *Scd1* was analysed by western blot. *Scd1* protein expression was strongly reduced in K14 Δ NLef1/L61Rac1 carcinomas compared to K14 Δ NLef1 adenomas and K14 Δ NLef1/L61Rac1 adenomas. Interestingly, the amount of *Scd1* protein was also reduced in K14 Δ NLef1/L61Rac1 adenomas compared to K14 Δ NLef adenomas. Taken together, these data indicate that micro array results for *Scd1*, *Elovl3* and *Elovl4* were reproducible. Furthermore, the results suggest that sebocyte maturation is inhibited in K14 Δ NLef1/L61Rac1 carcinomas due to changes in the gene expression profile.

3.4.3.2) Decreased expression of 24-Dehydrocholesterol-reductase in K14 Δ NLef1/L61Rac1 tumours

Furthermore, we were interested in verifying and further analysing the expression of 24-Dehydrocholesterol-reductase (*Dhcr24*, *Seladin-1*) in K14 Δ NLef1/L61Rac1 tumours. *Dhcr24* is an enzyme catalysing the conversion of desmosterol to cholesterol (Waterham et al., 2001). It was shown to be up regulated on transcriptional level in early stages of prostate cancer. In progressed stages and metastases of prostate cancer *Dhcr24* expression was down regulated (Battista et al., 2010; Hendriksen et al., 2006). To verify expression of *Dhcr24* in the cell populations isolated from K14 Δ NLef1/L61Rac1 adenomas and carcinomas, qRT-PCR was performed. Indeed, *Dhcr24* mRNA was up regulated in sebocytes and basal cells isolated from K14 Δ NLef1/L61Rac1 adenomas whereas it was down regulated in cells isolated from K14 Δ NLef1/L61Rac1 carcinomas. Analysing gene expression in whole tumour lysates showed similar results. Tumours classified as K14 Δ NLef1/L61Rac1 adenomas displayed elevated expression of *Dhcr24* compared to tumours identified as K14 Δ NLef1/L61Rac1 carcinomas. Interestingly, *Dhcr24* gene expression was significantly higher in K14 Δ NLef1

adenomas (Sharma, 2011). However, on the protein level, Dhcr24 expression was not changed between K14 Δ NLef1/L61Rac1 adenomas and K14 Δ NLef1/L61Rac1 carcinomas. Both tumour types showed low expression of Dhcr24. Nevertheless, K14 Δ NLef1 adenoma showed higher Dhcr24 protein levels than K14 Δ NLef1/L61Rac1 tumours, consistent with the results obtained on gene expression level (Sharma, 2011). This indicates that Dhcr24 expression decreases in sebaceous tumours with aberrant expression of activated Rac1. The fact that Dhcr24 expression is already down regulated in benign K14 Δ NLef1/L61Rac1 adenomas, some of which progressed into carcinomas, suggests Dhcr24 as a potential indicator for tumours susceptible to progress into undifferentiated tumours like carcinomas. Another possibility is that down regulation of Dhcr24 favours the progression of adenomas into carcinomas. In the future, it will be interesting to further characterise the role of Dhcr24 in skin tumour progression.

3.4.3.3) Reduced Nuclear protein1 expression in cells of K14 Δ NLef1/L61Rac1 carcinoma

Next, expression of Nuclear protein1 (Nupr1, also known as P8 or Com1) was validated. Nupr1 was previously shown to play a role in the cellular stress response (reviewed in (Goruppi and Iovanna, 2010)). Moreover, opposing studies were published about the role of Nupr1 in tumour biology. It was reported that Nupr1 can act as a tumour promoter also mediating metastasis in breast cancer cells (Ree et al., 2000; Ree et al., 1999). In contrast, analyses of prostate cancer suggested a tumour suppressive function for Nupr1 (Jiang et al., 2006a; Jiang et al., 2006b). So far, Nupr1 has not been implicated in formation of skin tumours. The contradictory roles of Nupr1 in tumour biology and the fact that it was not yet described to play a role in skin cancer lead us to analyse Nupr1 expression in more detail.

The results of the oligo nucleotide array suggested a down regulation of Nupr1 in cells isolated from K14 Δ NLef1/L61Rac1 carcinomas compared to sebocytes from K14 Δ NLef1/L61Rac1 adenomas. In basal cells from K14 Δ NLef1/L61Rac1 adenoma, Nupr1 was not detected in the array. Our qRT-PCR analyses of Nupr1 expression in more cDNA libraries confirm these data (Fig. 28 C). However, low

expression of Nupr1 could be detected in two out of five cDNA libraries from basal cells (K14 Δ NLef1/L61Rac1 adenoma). Analysis of Nupr1 expression in RNA isolated from whole K14 Δ NLef1/L61Rac1 tumour lysates suggested a down regulation of the gene in K14 Δ NLef1/L61Rac1 carcinomas. This is in line with the Nupr1 expression in distinct cell populations isolated from K14 Δ NLef1/L61Rac1 tumours. However, the results obtained from whole tumour lysates were not statistically significant due to the heterogeneity of the tumour material and will therefore be further investigated in the future (Sharma, 2011).

Taken together, we have compared expression profiles of three different cell populations from differentiated and undifferentiated skin tumours applying oligo nucleotide arrays. The results obtained from the arrays were reproducible. We have identified differentially regulated genes that were previously shown to play a role in tumour formation. To date, Dhcr24 and Nupr1 have not been associated with tumour formation in the skin. It will therefore be interesting to further characterise their function in tumour development.

4. Discussion

HFs and SGs are the two integral parts of the pilosebaceous unit in mammalian skin. HFs are regenerated throughout adult life by stem cells (Blanpain and Fuchs, 2009; Hardy, 1992). More recently, it was demonstrated that HF stem cells not only regenerate the HF but are also implicated in the regeneration of the SG (Petersson et al., 2011; Taylor et al., 2000). Moreover, there is evidence that HF stem cells are specified during HF morphogenesis. These stem cells were shown to be necessary for proper development of the HF stem cell niche (bulge) and the formation of functional SGs (Nowak et al., 2008; Osorio et al., 2008; Snippert et al., 2010b).

Although progress has been made during the past years in understanding mechanisms of HF morphogenesis, little is known about the process of SG development.

4.1) Differences in HF morphogenesis in mouse back and tail skin

HF morphogenesis is controlled by a network of signalling pathways (Duverger and Morasso, 2009; Fuchs, 2007). In back skin, molecular mechanisms regulating HF initiation have been well investigated during the past years (Fuchs, 2007; Millar, 2002; Paus et al., 1999; Schmidt-Ullrich and Paus, 2005; Schneider et al., 2009). Although the main morphogenetic and structural properties seem to be similar for all HFs, patterning and spatio-temporal organisation differs between HFs of back and tail skin in mice. For instance, formation of back skin HFs starts with primary guard hairs at E14.5, whereas we detect first placodes of central HFs at E16.5 in mouse tail skin. It has been shown that back skin HFs develop in waves starting at the anterior part of the mouse body and proceeding towards the posterior end (Plikus et al., 2009; Plikus et al., 2008). Therefore, waves of signals inducing HF formation would attain tail skin with a delay compared to back skin resulting in the retardation of placode formation.

Furthermore, in back skin, four different types of HFs develop in three distinct waves during skin morphogenesis (Duverger and Morasso, 2009; Schmidt-

Ullrich and Paus, 2005). In contrast, our data demonstrate that tail skin HFs are formed in two waves generating one central and two outer HFs forming a unit (triplet). Another striking difference we have observed between back and tail skin was the arrangement of the different HF types within the skin. In back skin, zigzag and awl/auchene HFs are organised circularly around primary guard HFs (Duverger and Morasso, 2009). In tail skin, we observe HF triplets organised in rows from the anterior to the posterior end of the tail.

This implies that different signals regulate the patterning in both regions of the body. It was proposed earlier by Turing (Turing, 1952) that a combination of activators and inhibitors regulates patterning in biological systems. For the skin, molecular mechanisms regulating the formation of the different types of back HFs have been well described. It was shown that Wnt and Dkk (a Wnt inhibitor) could be the activator-inhibitor pair regulating HF patterning in the skin (Sick et al., 2006). In addition, Ectodysplasin receptor (Edar) and BMP have been shown to control the initiation, the distribution and spacing at least of primary guard HFs in back skin (Mikkola, 2008; Mikkola and Thesleff, 2003; Mou et al., 2006). Secondary and tertiary HFs are induced by Noggin, a BMP-antagonist (Botchkarev et al., 2002). Furthermore, Lef1 signalling is required for formation of secondary HFs (Jamora et al., 2003). However, in these studies, the signalling pathways have not been analysed in tail skin. Therefore, it remains unclear, if distribution and spacing in tail skin is regulated by different signalling molecules than in back skin. Our data indicate that two types of HFs exist in tail skin. Central and side HFs are located in close proximity to each other and the space between two neighbouring triplets is very restricted. Therefore, signalling cues inducing the different types of HFs have to be directed very specifically.

In the future, it will be important to analyse the distribution of potential activators and inhibitors as Wnt and Dkk or Edar and BMP in mouse tail skin. Additionally, it will be important to unravel the molecular signals governing formation of the different HF types in tail skin. This would provide further insight into the molecular mechanisms regulating HF spacing in this part of the body. Moreover, it would be interesting to analyse if two different types of HFs form the triplets in murine tail skin. Analysis of hair length and number of medulla columns in the hair shafts could be done to identify potential differences.

4.2) Formation of HF progenitor compartments

During the past years, various stem and progenitor compartments within the HF have been identified (Blanpain and Fuchs, 2009; Jaks et al., 2010). However, it is not completely understood when these stem and progenitor compartments are generated and become first activated for tissue formation. First evidence for the formation of stem cell compartments during morphogenesis came from studies investigating the expression of the transcription factor Sox9. This molecule is a robust marker expressed in cells of the bulge region of HFs in adult mice (Nowak et al., 2008; Vidal et al., 2005). It was demonstrated that first Sox9 expressing cells could be detected during early HF morphogenesis. Moreover, epidermis specific depletion of Sox9 during embryogenesis resulted in a failure to form HF bulge stem cells and SGs (Nowak et al., 2008). Interestingly, Sox9 has been shown to be expressed by stem and progenitor cells of other tissues such as liver, pancreas, intestine and mammary epithelium (Furuyama et al., 2011; Guo et al., 2012; Kopp et al., 2011; van der Flier et al., 2009). These studies indicate that Sox9 is a general marker for stem cells in various tissues.

The results presented in this work demonstrate that during early HF morphogenesis, the Sox9 positive cell population initially co expresses Lrig1, a marker for stem cells of the adult HF junctional zone (Jensen et al., 2009). We show that both markers are confined to distinct regions of the developing HF at later stages of HF morphogenesis. In particular, at stage 5 of HF morphogenesis, when SGs start to form, Sox9 expression is detected below the SG (Fig. 29). This indicates that Sox9 positive cells accumulate to form the stem cell compartment of the future bulge. In contrast, Lrig1 expression is located at the upper part of the HF surrounding the first established sebocytes. To date, it is not clear why Lrig1 and Sox9 are first co expressed by the same cells and define distinct stem cell compartments later in life. Reports about the expression of the stem cell marker Lgr6 showed that this marker is also expressed during early HF morphogenesis in a similar region as Sox9 and Lrig1 (Snippert et al., 2010b). Therefore, one can speculate that one general precursor population expressing multiple stem cell markers is initially established at the earliest stages of HF morphogenesis. With proceeding development marker expression becomes confined to distinct stem cell populations as these reach their final destination

within the HF. Until now, the cellular and molecular mechanisms regulating the separation of different stem cell compartments still need to be identified. It will be very interesting to address this further in the future.

One possibility to determine if one of these marker positive stem cell pools is established first to give rise to the others could be to perform lineage tracing analysis. Using recently published *Lrig1CreERT2*-mice (Powell et al., 2012) could be useful to analyse if descendants of *Lrig1* positive cells express *Sox9* and can be detected in the future bulge region. To analyse if *Sox9* positive cells are the first stem cells to be established, lineage tracing with recently published *Sox9CreER(T2)* (Kopp et al., 2011) could be performed. Indeed, *Sox9-Cre* mice have already been used for lineage tracing during skin morphogenesis. Progeny of *Sox9* expressing cells contributed to the entire HF, indicating that *Lrig1* positive cells potentially arose from *Sox9* positive cells as well. However, co localisation of *Lrig1* with descendants of *Sox9* positive cells was not analysed in this study (Nowak et al., 2008). Another interesting point would be to analyse a potential functional interdependence of the *Sox9* and *Lrig1* stem cell compartments. Does the *Sox9* positive stem cells population form in absence of *Lrig1* and vice-versa? To address this, gene knockout studies could be combined with lineage tracing approaches applying the mouse models mentioned above.

We have also analysed the localisation of the *MTS24/Plet1* progenitor compartment. Previously, it had been demonstrated that bulge stem cell progeny transited various stem and progenitor compartments, including the *MTS24/Plet1* region of the HF before regenerating the SG (Pettersson et al., 2011). *MTS24/Plet1* positive cells are located in the upper isthmus of the adult HF and were highly clonogenic *in vitro* (Nijhof et al., 2006; Raymond et al., 2010). We wanted to address the question if progenitor cells positive for *MTS24/Plet1* could be implicated in SG formation. Our analyses revealed that during HF morphogenesis, *MTS24/Plet1* positive cells could only be detected at the upper part of the HF once a cluster of sebocytes was already established (Fig. 29). This indicates that the *MTS24/Plet1* progenitor cell compartment is dispensable for the formation of the SG. However, later in life cells positive for *MTS24/Plet1* were suggested to be necessary to maintain proper SG regeneration (Nijhof et al., 2006).

Taken together, the results presented here demonstrate that distinct stem and progenitor cell compartments of mouse HFs are formed at different time points during HF morphogenesis. The localisation of the stem and progenitor cell compartments is highly dynamic at early stages of HF development. The scheme in Fig. 29 summarises our key findings with respect to the distribution of stem and progenitor cell compartments during HF morphogenesis.

In the future, it will be important to elucidate the underlying molecular signals controlling the formation and localisation of different HF stem cell pools in more detail.

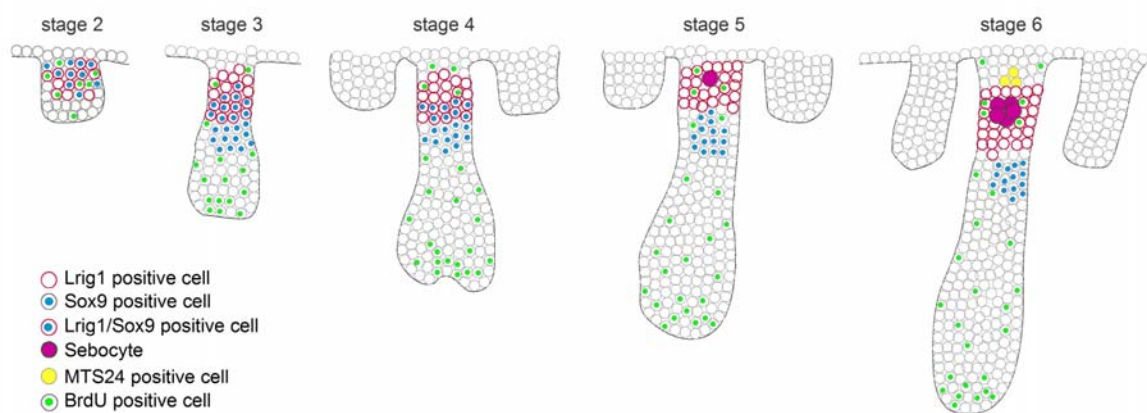


Fig. 29) Progenitor cell dynamics during HF and SG morphogenesis. Sox9 (blue dots) and Lrig1 (red circles) positive stem cells co localise at the upper part of the HF (stage 2 and 3) before marker expression becomes confined to distinct compartments (stage 4 and 5). Sebocytes (magenta circles) arise among Lrig1 positive cells. MTS24/Plet1 positive cells are detected after SG development is initiated (yellow circles, stage 6). BrdU positive cells (green dots) are distributed all over the developing HF.

4.3) Cellular and molecular mechanisms of SG morphogenesis

The SG produces lipids and sebum and has crucial function in maintaining an intact epidermal barrier (Schneider and Paus, 2009; Thody and Shuster, 1989). Moreover, the SG is indispensable for the maintenance of the HF as it has been demonstrated that HFs are degraded in absence of functional SGs. In particular, hair loss due to destruction of the pilosebaceous unit (scarring alopecia) generally starts with SG ablation (Sundberg et al., 2000). In contrast, SGs exist without being attached to a HF. Meibomian glands in the eyelids or preputial gland secreting pheromones in rodents are only two examples (Schneider and

Paus, 2009). The existence of SGs without association to HFs is one aspect supporting the idea that the SG is evolutionarily older than the HF. It was hypothesised that SGs developed during evolution as vertebrates left the water to populate dry land. To protect the body against dehydration, glandular structures producing lipids were formed within the skin. The authors of this article propose that the HF developed later to efficiently drain the sebum produced by SGs to the surface of the skin (Stenn et al., 2008). These data and hypotheses again point out how crucial the SG is for the maintenance of the HF and the epidermal barrier. However, until now little was known about the formation of the SG during embryogenesis. It has been well described that the SG forms during HF morphogenesis at the upper part of the HF (Paus et al., 1999). First sebocytes of the future SG are detected at stage 5 of HF morphogenesis by OilRedO staining. Our data have shown that single sebocytes are also detected by staining for Scd1 or adipophilin, molecules associated with lipid metabolism. Scd1 is specifically expressed by sebocytes within the epidermis and is not only useful as a marker for early sebocytes. It has been shown that ablation of Scd1 leads to SG hypoplasia (Binczek et al., 2007; Sampath et al., 2009). Moreover, Scd1 is the mutated gene in asebia-mice which are characterised by the absence of SGs due to a spontaneous mutation (Gates and Karasek, 1965; Zheng et al., 1999).

Due to the specific expression of Scd1 in sebocytes, this marker could be used for genetic manipulation selectively in the SG. Reporter genes could be expressed specifically in the SG allowing isolation of SG cells at different time points. Subsequent transcriptional profiling could help to gain further insights into genes important for SG morphogenesis, differentiation and maintenance. Moreover, gene expression could be manipulated in cells of the SG. To do so, inducible Cre recombinase in combination with EGFP (EGFP-IRES-CreERT2, (Barker et al., 2007)) could be expressed under control of the Scd1 promoter, enabling knock out of genes specifically within the SG. Furthermore, by using this construct, Scd1 positive cells would be marked by the expression of EGFP. Due to the early expression of Scd1 during SG morphogenesis, we would be able to isolate first sebocytes by FAC sorting. However, one would expect a low number of positive cells at early stages of SG morphogenesis. To overcome the challenge of isolating RNA from low amounts of cells, the single-cell cDNA library

approach applied in this thesis could be used (Hartmann and Klein, 2006). Thus, analysis of gene expression profiles of isolated sebocytes would be possible.

To date, molecular mechanisms regulating SG morphogenesis are poorly investigated. However, several signalling pathways including Hh and Wnt have been shown to be involved in differentiation and maintenance of the SG. It has been demonstrated that repression of Lef1 / β -Catenin signalling by expression of a truncated Lef1-transcription factor lacking the β -Catenin binding site leads to increased sebocyte differentiation (Niemann et al., 2002). This indicates that repression of Lef1 / β -Catenin signalling might be necessary for the formation of first sebocytes during morphogenesis. Moreover, Hh signalling influences SG development. Increased Hh signalling resulted in formation of increased size and number of SGs. In contrast, when Hh signalling was inhibited during skin morphogenesis, SGs failed to form (Allen et al., 2003; Gu and Coulombe, 2008). In addition, PPAR γ could play a role in the formation of sebocytes. PPAR γ -knockout mice die during embryogenesis. However, the influence of PPAR γ in postnatal skin was analysed in chimeras of wt and PPAR γ -null cells. These studies suggested that PPAR γ plays a role in sebocyte differentiation as SGs formed in the chimeras were generated by wt cells (Rosen et al., 1999). This is supported by a study demonstrating that PPAR γ ligands promote sebocyte differentiation *in vitro* (Rosenfield et al., 2000).

In the future, molecular mechanisms regulating early SG morphogenesis need to be further elucidated.

4.3.1) A cluster of sebocytes generates two SGs in mouse tail skin

Interestingly, our data showed that the two SGs attached to one HF in mouse tail skin arise from one cluster of sebocytes. To date, it is not clear which signals control the partitioning of the two clusters. Certainly, the tension force produced by the developing hair shaft cannot be the only reason, since other HFs also produce the hair shaft but contain only one SG.

We usually observed that the cluster of sebocytes divided into two at stage 6 or 7 of HF morphogenesis. At this stage of development, the cluster of sebocytes

may have attained a critical size triggering the segregation into two clusters. One could hypothesise that the SGs of HFs harbouring only one glandular structure never reach this critical size and therefore, only one SG is formed. This interesting questions certainly needs further investigation in the future.

Another possibility could be that branching morphogenesis is involved in splitting up the initial sebocyte cluster into two portions. So far, nothing has been reported about the involvement of branching mechanisms in SG development. However, in other epithelial appendages and organs such as the mammary gland, the salivary gland or the lung, branching is an important step during morphogenesis (Affolter et al., 2003). One candidate proposed to be involved in regulating branching in the lung or the salivary gland is Sonic Hedgehog (Shh) (Jaskoll et al., 2004; Pepicelli et al., 1998). Interestingly, Hedgehog (Hh) signalling also plays an important role in regulating the development of the SG (Gu and Coulombe, 2008). It was shown that inhibition of Hh signalling blocks SG development, whereas activation of the pathway leads to an increase in size and number of SGs (Allen et al., 2003). This is particularly interesting as one could hypothesise that increased Hh signalling leads to increased branching during the development of the SG. This could lead to the higher number of SGs observed in mutant mice displaying aberrantly activated Hh signalling (Allen et al., 2003). Besides Hh signalling, other molecules like Fibroblast Growth Factor 10 (FGF10) are suggested to be involved in regulating branching of epithelial appendages (Lu et al., 2006; Mailleux et al., 2002). FGF10 was also shown to be important for proper HF development (Petiot et al., 2003). However, much less is known about the influence of FGF10 on the development of the SG.

Taken together, our data more likely support that partitioning of the sebocyte cluster into two occurs to a due to mechanism other than branching morphogenesis. The images shown in this thesis rather suggest segregation of the cluster than forming a new branch. However, the mechanism controlling the partitioning of the sebocyte cluster remains unknown. Due to the fact that some HFs contain one SG whereas others harbour two, one can speculate that different signalling pathways regulate SG segregation at different types of HFs. Therefore, it will be very interesting in the future to analyse the underlying mechanisms regulating the formation of one or two SGs.

4.3.2) Lrig1 positive stem cells generate sebocytes

Our results clearly suggest that sebocytes are generated by Lrig1 positive stem cells at stage 5 of HF morphogenesis. Lrig1 positive cells proliferate, whereas Scd1 positive sebocytes did not incorporate BrdU or EdU labels upon short term labelling experiments, indicating that sebocytes do not divide. However, pulse-chase experiments applying EdU showed a dilution of the EdU label from Lrig1 positive cells towards Scd1 expressing sebocytes. Analyses of spindle pole orientation in the Lrig1 stem cell compartment provided evidence that asymmetric cell fate decision of Lrig1 positive cells leads to the formation of cells able to differentiate towards the sebocyte lineage. Our data shows that a majority of cell divisions in the upper part of the HF occurred perpendicularly to the basement membrane. This indicates that Lrig1 expression marks precursor cells for sebocytes during epidermal morphogenesis. Cell type specification towards the sebocyte lineage can occur after one cell division of Lrig1 positive cells, demonstrated by the EdU-experiment. To a lesser extent, Lrig1 positive cells divided in parallel to the basement indicating an expansion of the stem cell compartment. Thus, the Lrig1 positive stem cells compartment can be maintained. Moreover, one could hypothesise that Lrig1 positive cells can also provide cells for the elongating HF. A similar expression pattern was described during anagen phase of the hair cycle, where Lrig1 expression could be detected below the SG extending towards the bulge region (Jensen et al., 2009).

To further strengthen the data demonstrated here, lineage tracing experiments could be conducted. Crossing recently generated Lrig1CreERT2 (Powell et al., 2012) mice with Cre-sensitive reporter mice and activating Cre during SG morphogenesis could provide further insight into the role of Lrig1 positive stem cells in the formation of the SG and the HF. This approach would be useful to directly show that Lrig1 positive stem cells give rise to sebocytes.

Although Lrig1 positive stem cells play a crucial role in the formation of the SG, Lrig1 itself does not seem to have a functional role for SG formation and homeostasis. Lrig1 knockout mice show epidermal hyper proliferation, but no effects on the SG have been reported (Jensen et al., 2009; Suzuki et al., 2002). However, in other epithelial systems such as the intestine, Lrig1 also seems to

have functional relevance. Recently, it was described that Lrig1 is highly expressed in intestinal stem cells and controls proliferation. Knockout of Lrig1 leads to a dramatic increase of proliferation in intestinal stem cells (Wong et al., 2012). Thus, Lrig1 appears to be a more general marker for stem cells of different tissues.

4.4) Origin of cells forming HF and SG

It has been demonstrated that the HF stem cell population expressing the transcription factor Sox9 is formed during embryonic development of the skin. These stem cells were able to form HFs and give rise to SGs during morphogenesis. Ablation of Sox9 in embryonic skin lead to a failure in formation of the HF bulge region. Moreover, SGs were not detected in mice lacking Sox9 expression (Nowak et al., 2008).

To identify the origin of cells forming the SGs during embryogenesis and early postnatal development, we have performed lineage tracing experiments applying a mouse model recently established in our laboratory. This model (AK15CreER(G)T2/R26REYFP) allows to label individual stem cells in the bulge region of adult HFs. The fate of K15 positive stem cells could be traced within the HF. Interestingly, K15 derived progeny was able to regenerate the SG (Pettersson et al., 2011). In addition, expression of K15 protein could already be detected during embryogenesis at E15.5 in the IFE (Nöbel, 2009). Therefore, we used AK15CreER(G)T2/R26REYFP mice to perform lineage tracing experiments during HF and SG morphogenesis. The data provided here show that the K15 promoter driving inducible Cre indeed was already active at E15.5 in cells of the epidermis. This allowed to use AK15CreER(G)T2/R26REYFP mice to perform lineage tracing during HF morphogenesis, labelling cells in the IFE and tracing their fate during formation of HFs and SGs.

4.4.1) Specific targeting of individual IFE cells during skin morphogenesis

In a first set of experiments, we have analysed the timing of Cre recombinase activation when labelling was performed during embryogenesis. We have injected Tam at E16.5 and analysed for Cre recombinase via YFP expression one or two days later. Our results show that activation of Cre recombinase during embryogenesis (E16.5) lead to specific labelling of individual cells in the epidermis of AK15CreER(G)T2/R26REYFP mice detectable at E18.5. Importantly, cells constituting the already established placodes were not labelled within the first days following Cre activation. Thus, we could conclude that all labelled progeny of K15 positive cells is derived from the IFE. With further tracing, clusters of labelled cells were detected in the IFE indicating expansion of K15 positive cells. Infrequently, also individual YFP positive cells were detected several days after Cre activation in the IFE. This could indicate that these cells are more quiescent and have not divided yet.

To further improve our lineage tracing approach in the future, it will be important to analyse K15 promoter activity during skin morphogenesis in more detail and to optimise the experimental design for Cre recombinase activation. To date, it is only known, that K15 protein is detectable from E15.5 onwards, indicating that the promoter is active slightly before (Nöbel, 2009). To clearly state activity of the K15 promoter, in situ hybridisation of K15 mRNA needs to be conducted. Furthermore, qRT-PCR of skin samples isolated at embryonic stages could also reveal the time frame of K15 promoter activation.

Moreover, molecular characterisation of early labelled K15 positive cells is required to identify if similarities in gene expression profiles with K15 positive cells from the adult HF bulge region can be detected. This would answer the question if K15 positive cells constitute a type of epidermal progenitor cells.

4.4.2) Progeny of K15 positive IFE cells contribute to HF and SG morphogenesis

To analyse the fate of K15 positive cells labelled in the IFE, we have traced progeny of these cells till postnatal time points during HF and SG development. Interestingly, our lineage tracing experiments suggested that cells originating in the IFE are contributing to both, SG and HF formation. First, initially labelled cells expanded to form clusters in the IFE. Subsequently, clonogenic expansion of labelled cells from IFE towards the SG or further down the HF was detected. To quantify the localisation of labelled cells at later tracing time points, we have classified the labelling pattern describing the regions within the pilosebaceous units containing YFP positive cells. Our initial quantification revealed that the majority of primary HFs analysed, contained labelled cells only in the upper part of the HF and not below the SG. However, distribution of YFP positive cells in secondary HFs was less clear. Most of the analysed secondary HFs had reached only stage 2 or 3 of HF morphogenesis. Here, we detected labelled cells randomly distributed within the developing HFs and it was not possible to distinguish between different regions of the HF. One possible explanation for this random labelling pattern could be the different time point of Cre-activation compared to the primary HF. Potentially, the mechanism of HF and SG formation differs between primary and secondary HFs. To investigate this in more detail, more mice will be analysed in the future. In addition, labelling at later time points during morphogenesis will to be performed. In the future, we plan to perform co immunofluorescence studies to better distinguish between different regions within the HF. Additionally, we also observed HFs with labelled cells located below the SG. Certainly, K15 derived progeny contributed here to the formation of the hair shaft, the IRS or the ORS.

To investigate the ultimate fate of progeny derived from K15 positive cells of the IFE, we have also analysed later time points of tracing. Importantly, the majority of labelled P15 HFs (induced at E16.5) contain YFP positive cells in the infundibulum or the SG but not below these compartments. Interestingly, this pattern was also observed in secondary HFs, where initially labelled cells could not be attributed to a distinct region of the developing HF. This suggests that

cells derived from the IFE are recruited to the infundibulum and or subsequently to the SG and contribute to HFs more rarely.

However, at P15 we also detected HFs containing labelled cells in the SG and in the HF. Moreover, HFs with labelled cells only below the SG were observed. These data propose that progeny of K15 positive cell in the IFE are able to form HFs and SGs. Our data obtained so far suggest that contribution to SGs occurs more frequently than involvement in HF formation. However, we cannot rule out that YFP positive cells in the SGs at P15 are derived from K15 progeny that first populated the HF bulge region and later contributed to SG (re)generation.

Taken together, our initial data suggest that mostly, K15 derived progeny contribute to the upper part of the HF, the infundibulum or the SG. To a lesser extent, cells localise to the HF and are detected in the bulge region when HFs are in the first resting phase of the hair cycle. In order to evaluate the data statistically, more mice are currently analysed. However, these initial results suggest that K15 positive cells in the IFE constitute a population of stem or progenitor cells able to give rise to all lineages of the epidermis. In contrast to Sox9 positive cells that localise to placodes and gave rise to cells of HFs and SG, K15 positive cells are derived from the IFE. When IFE cells were labelled at E17, when HGs (stage 2) of primary HFs are already established, progeny of K15 positive cells also contributed to HFs and SGs. This suggests that the recruitment of cells from the IFE seems to be a permanent process during HF and SG development. The data that we show here provide novel insights into the process of HF and SG development.

Recently, reporter mice allowing multiple colour lineage tracing have been described. Stochastically, one out of four fluorescent proteins is expressed in cells with active Cre recombinase (R26R-Confetti, (Snippert et al., 2010a)). These mice allow distinguishing between progeny of different stem cells of the same niche. By crossing these mice with our AK15CreER(G)T2-mice we would be able to trace different stem cells to their eventual fate. One can imagine that different stem cells, marked by different fluorescent proteins, contribute to the HF or the SG. More precisely, one would be able to discriminate if labelled cells in the SG and the bulge region of one HF are derived from the same “cell of origin”. This would help understanding the process of the formation of HFs and SGs by cells originating in the IFE.

4.4.3) Test for proliferative capacity of K15 derived progeny

We have analysed proliferative capacity of K15 derived YFP positive progeny by performing colony forming assays. Our initial results indicate that YFP positive cells isolated from newborn AK15CreER(G)T2/YFP+/+ mice formed a higher number of colonies *in vitro* than YFP negative cells. This indicates that K15 derived progeny have a higher self renewing potential. However, these initial experiments need to be repeated.

Assuming that K15 derived progeny have stem or progenitor cell properties, we expect YFP positive cells to form more colonies larger than 2mm² (representing holoclones) compared to YFP negative cells. To address if K15 derived progeny have the capacity to generate all lineages of the skin, transplantation assays could be performed. Following Cre activation in K15 positive cells, YFP positive and negative cells would be isolated via FAC sorting. Subsequently, epidermal cells would be mixed with primary dermal fibroblast and transplanted onto the back of Nude mice in silicone chambers (Fusenig et al., 1983; Weinberg et al., 1993). Grafts would be monitored for several weeks to analyse potential hair growth. It will be important to compare the regenerative potential of YFP positive and negative epidermal cells.

4.5) Role of Rac1 in tumour formation

Rac1 was previously shown to be important for the maintenance of the adult HF stem cell region. In absence of Rac1, the cycling part of the HF could not be maintained resulting in a progressive hair loss (Chrostek et al., 2006). In a similar study, it was demonstrated that in absence of Rac1, HFs morphogenesis was impaired and HFs never formed properly. Moreover, grafted Rac1 deficient keratinocytes were not able to reconstitute HFs and SGs although formation of the IFE was not impaired (Castilho et al., 2007). In contrast, activation of Rac1 lead to an expansion of keratinocytes capable of clonal growth (Benitah et al., 2005). Altogether, these studies indicate that Rac1 has crucial function in regulating stem cell behaviour.

In addition, over expression of the small GTPase Rac1 has been implicated in the progression of several tumours such as breast, testicular or gastric cancer (Gomez del Pulgar et al., 2005; Kamai et al., 2004; Pan et al., 2004; Schnelzer et al., 2000). Moreover, it was reported that depletion of Rac1 in epidermal cells prevented mice from DMBA/TPA induced skin tumour formation (Wang et al., 2010). These reports propose an important role for Rac1 in tumour formation and progression. However, the role of Rac1 in skin tumours was insufficiently addressed.

We have analysed the effect of activated Rac1 (L61Rac1) in benign skin tumours. Therefore, K14 Δ NLef1/L61Rac1 mice were generated. In a one step carcinogenesis experiment, K14 Δ NLef1/L61Rac1 mice did not develop significantly more tumours than K14 Δ NLef1 control mice. This indicates that active Rac1 does not regulate frequency of tumour formation.

Supporting the data mentioned above about Rac1 function in HF stem cells, we found increased expression of Lrig1 and MTS24/Plet1 in K14 Δ NLef1/L61Rac1 seboma and carcinoma compared to K14 Δ NLef1/L61Rac1 adenoma and K14 Δ NLef1 adenoma (Sharma, 2011).

4.5.1) Activation of Rac1 leads to decreased sebocyte differentiation in skin tumours

Interestingly, in addition to adenomas and sebomas K14 Δ NLef1/L61Rac1 mice developed undifferentiated tumours (carcinomas). K14 Δ NLef1/L61Rac1 adenomas resembled K14 Δ NLef1 adenomas. Undifferentiated, proliferative basal cells at the periphery of the adenoma lobules surrounded mature, Scd1 positive sebocytes in the centre. Distribution and amount of sebocytes were comparable between the adenomas of these two mouse strains. K14 Δ NLef1/L61Rac1 sebomas showed less expression of the sebocyte differentiation marker Scd1 on transcriptional and on protein level. A further decrease in Scd1 expression was observed in K14 Δ NLef1/L61Rac1 carcinomas. Similar results were obtained for expression of adipophilin, another sebocyte differentiation marker (Ostler et al., 2010; Sharma, 2011). The gradual decrease of Scd1 was accompanied by an increase in BrdU positive cells. In both, K14 Δ NLef1/L61Rac1 and K14 Δ NLef1 adenomas, BrdU positive cells were

confined to the outer layer of undifferentiated cells at the periphery of the tumour lobules that are filled with differentiated sebocytes. In K14 Δ NLef1/L61Rac1 sebomas, BrdU positive cells were observed slightly more randomly distributed within the tumour tissue. This effect was even stronger in K14 Δ NLef1/L61Rac1 carcinomas, where BrdU positive cells were distributed all over the tumour mass. Our data indicate that active Rac1 leads to a decrease in differentiation in sebaceous tumours. More undifferentiated, proliferative cells are detected. To date, the role of Rac1 in regulating differentiation is not well investigated. However, it has been suggested that active Rac1 inhibits differentiation of muscle cells *in vitro* (Heller et al., 2001). Also, it was proposed by analysing samples of human urinary cancer that high Rac1 activity was associated with low grades of differentiation (Kamai et al., 2010). Interestingly, Rac1 has been implicated in regulating the cell cycle (Coleman et al., 2004). Activation of Rac1 was associated with stimulation of cell cycle progression (Olson et al., 1995). Furthermore, it was reported that Rac1 can promote G1-S transition in the cell cycle by increasing CyclinD1 (Klein et al., 2007). In line with that, we have detected elevated proliferation in K14 Δ NLef1/L61Rac1 tumours. However, the mechanism through which active Rac1 stimulates cell cycle progression and proliferation are still largely unknown.

4.5.2) Gene expression profile is altered in cells of K14 Δ NLef1/L61Rac1 carcinomas

In order to dissect the molecular mechanisms underlying the altered histology of the K14 Δ NLef1/L61Rac1 carcinomas compared to K14 Δ NLef1/L61Rac1 adenomas, micro array analyses were performed. We have compared expression profiles of basal cells and sebocytes isolated from K14 Δ NLef1/L61Rac1 adenomas with expression profiles of undifferentiated cells from K14 Δ NLef1/L61Rac1 carcinomas. Our results show significant alterations in gene expression between cells from K14 Δ NLef1/L61Rac1 adenomas and carcinomas. Among the regulated candidates, we found members of the lipid metabolism such as Scd1 or adipophilin, up regulated in sebocytes of K14 Δ NLef1/L61Rac1 adenomas compared to undifferentiated cells from

K14 Δ NLef1/L61Rac1 carcinomas. This supported the data we have obtained in immunofluorescence analysis before ((Sharma, 2011) and this work).

Moreover, three members of the Elovl-family, namely Elovl3, 4 and 6 were up regulated in sebocytes of K14 Δ NLef1/L61Rac1 adenomas. Elovl3 and 4 have been previously associated with lipid metabolism of sebocytes and maintenance of an intact epidermal barrier function (Cameron et al., 2007; Li et al., 2007; Westerberg et al., 2004). Interestingly, our qRT-PCR results showed that these genes of the lipid metabolism were already expressed in the basal cells of K14 Δ NLef1/L61Rac1 adenomas. Basal cells at the periphery of the sebocyte lobules within adenomas are proliferative and undifferentiated. They give rise to maturing sebocytes. Our data indicate that these cells might already be committed to their ultimate sebocyte cell fate. The fact that the expression of genes associated with lipid metabolism was down regulated in the cells isolated from K14 Δ NLef1/L61Rac1 carcinoma indicates that these cells had lost the ability to differentiate towards the sebocyte lineage.

Another interesting candidate gene, differentially regulated among sebocytes of K14 Δ NLef1/L61Rac1 adenoma and undifferentiated cells of K14 Δ NLef1/L61Rac1 carcinomas was Dhcr24. Dhcr24 is an enzyme converting desmosterol to cholesterol. It has been demonstrated that knock out of Dhcr24 in mice leads to severe skin barrier defects in mice (Mirza et al., 2009; Mirza et al., 2008; Mirza et al., 2006). We found Dhcr24 up regulated in sebocytes and basal cells of K14 Δ NLef1/L61Rac1 adenoma compared to K14 Δ NLef1/L61Rac1 carcinoma. This was particularly interesting because Dhcr24 had been shown to be over expressed at early stages of prostate cancer but was down regulated in more progressed stages and metastasis of this cancer type (Battista et al., 2010). This correlates with our data if we assume that K14 Δ NLef1/L61Rac1 seboma and carcinoma are progressive stages of K14 Δ NLef1/L61Rac1 adenoma. One could speculate that carcinomas develop from adenomas due to down regulated Dhcr24 expression. Moreover it would be utile to use Dhcr24 as a marker for progression of sebaceous adenomas towards sebaceous carcinomas. Interestingly, our data demonstrate that expression of Dhcr24 protein was significantly decreased in K14 Δ NLef1/L61Rac1 tumours compared to K14 Δ NLef1 adenoma. A similar regulation was also observed on transcriptional level when analysing RNA from whole tumour lysates (Sharma,

2011). As Dhcr24 expression is lower in K14 Δ NLef1 adenoma compared to K14 Δ NLef1/L61Rac1 adenoma (Sharma, 2011), it is tempting to speculate that Dhcr24 expression might be regulated via active Rac1.

Besides genes involved in lipid metabolism, some cell cycle associated genes e.g. Gankyrin were up regulated in undifferentiated cells from K14 Δ NLef1/L61Rac1 carcinomas compared to sebocytes and basal cells from K14 Δ NLef1/L61Rac1 adenomas. Gankyrin was shown to be up regulated in oesophageal squamous cell carcinoma (Ortiz et al., 2008) and has anti apoptotic effects. More recently, it was proposed that levels of Gankyrin were closely associated with dedifferentiation of tumours in hepatoma patients (Sun et al., 2011). These studies together with our result render Gankyrin an interesting candidate for further analysis.

Furthermore, we identified Prominin2 (Prom2) to be regulated among the different tumour cell populations. Prom2 is a glycoprotein expressed in epithelial cells (Florek et al., 2007) and was up regulated in undifferentiated cells of K14 Δ NLef1/L61Rac1 carcinoma to basal cells from K14 Δ NLef1/L61Rac1 adenoma. Prom2 is highly similar to Prominin1, established as surface marker of renal or prostatic epithelial stem cells (Bussolati et al., 2005; Fargeas et al., 2003; Richardson et al., 2004). This provokes the question, if Prom2 could also be a useful marker for cells with stem cell characteristics in the skin or in skin tumours. Up regulated Prom2 in cells from K14 Δ NLef1/L61Rac1 carcinoma could indicate that these cells might be stem or progenitor cells. Analysing the expressing of Prom2 in skin and tumour samples and performing clonogenicity assays with tumour-cells will help to evaluate its utility as a potential stem-cell marker.

Interestingly, no significantly regulated genes were found when comparing the profiles of basal cells and differentiated sebocytes both isolated from K14 Δ NLef1/L61Rac1 adenoma. This indicates that genes needed for the function of differentiated sebocytes are already expressed in earlier stages of differentiation. Therefore, expression profiles of basal cells and sebocytes from K14 Δ NLef1/L61Rac1 adenoma showed strong overlap. Another potential explanation could be the limitations of the cell isolation method. Basal cells are localised in close proximity to sebocytes in K14 Δ NLef1/L61Rac1 adenoma. Therefore, it is possible that during laser micro dissection of basal cells, parts of

sebocytes were also catapulted into the collection tube. This would explain why not significant differences in gene expression were detected between sebocytes and basal cells.

To gain insights into genes which are regulated by Rac1 signalling, we will proceed to analyse these initial data using real-time PCR. Comparing the expression profile of cells isolated from K14 Δ NLef1/L61Rac1 tumours with profiles of cells from K14 Δ NLef1 adenomas could help to identify genes that are specifically regulated by activated Rac1.

Taken together, the data obtained from oligo nucleotide arrays revealed interesting candidate genes regulated in cells of differentiated and undifferentiated sebaceous tumours in K14 Δ NLef1/L61Rac1 mice. Further investigation will potentially lead to the identification of novel target genes for skin tumour therapy.

4.6) Perspectives

The data presented here provide novel insights into the establishment of stem and progenitor cell compartments during skin morphogenesis. We propose the existence of a common progenitor population giving rise to HF stem cells and SGs. The principle of a common progenitor cell population could apply to the development of other organs and tissues as well, especially because the analysed markers are also expressed in other tissues.

Our data from the lineage tracing approach suggest that SGs are directly formed by cells of the IFE. For the future, it will be interesting to investigate whether HFs and SGs are formed by the same stem cells. Alternatively, stem cells could already be primed for different cell fates during early morphogenesis of the pilosebaceous unit. By using a multi colour lineage tracing approach one could distinguish between the progeny of individually labelled different stem cells and track their fate during HF and SG morphogenesis

Our results identifying the cellular processes and progenitor compartments involved in SG development could be of major importance for skin tumour biology as it was proposed that during tumour formation, basic steps of morphogenesis are recapitulated. Understanding the dynamics of stem cell

behaviour during skin development will help to unravel cellular processes of early tumour formation and might have relevant diagnostic and therapeutic value.

Furthermore, the lineage tracing approach together with the identification of different stem and progenitor compartments demonstrate that mouse tail skin constitutes an excellent model system to study important general processes such as cell type specification and stem cell function in a three dimensional fashion

In addition, we provide new insights into the role of Rac1 in skin tumour formation. In a sebaceous tumour model, activated Rac1 leads to the formation of undifferentiated tumours, accompanied by a decrease in sebaceous differentiation. This is reflected by a change in gene expression. Genes implicated in lipid metabolism are down regulated in undifferentiated tumour cells. Moreover we have identified progenitor markers and cell cycle regulators. Further analysis of these candidates could lead to the identification of novel target genes for therapy of skin tumours.

5) Summary

Hair follicles (HFs) and sebaceous glands (SGs) constitute the two essential parts of the pilosebaceous unit in mammalian skin, substantially contributing to the formation of an intact epidermal barrier. Over the past decades, considerable progress has been made in understanding the cellular and molecular mechanisms of HF formation and various stem cell (SC) and progenitor compartments have been described within the HF. Although promising initial studies exist, the formation of the diverse HF SC and progenitor compartments during morphogenesis still remains to be elucidated. In particular, cellular mechanisms of SG morphogenesis occurring in close association with HF development are not well understood.

Here, we investigate the spatio-temporal organisation of HF SC and progenitor compartments during HF and SG morphogenesis. HF SC compartments of the future bulge region (Sox9 positive) and the junctional zone of the upper adult HF (Lrig1 positive) are detectable prior SG formation. Our studies reveal that Sox9 and Lrig1 are initially co expressed by cells of the HF. Once the SG starts to form, expression of each marker is localised to distinct cell compartments. Importantly, Lrig1 positive SCs at the upper part of the HF proliferate and give rise to sebocytes by asymmetric cell fate decision. Sox9 positive SCs localise to the future bulge region. In contrast, progenitor cells of the HF isthmus region, expressing MTS24/Plat1 were not detected before SG formation was initiated indicating that these cells are dispensable for SG development.

To decipher the origin of cells forming the SG, lineage tracing of basal keratinocytes was performed during HF and SG morphogenesis. Importantly, our data suggest that progeny of multipotent cells labelled in the IFE during embryogenesis can contribute to SG formation independently of HF development.

Previously, it has been shown that the small GTPase Rac1 is crucial for maintaining the SC compartment of the HF. Therefore, we have addressed the role of activated Rac1 in tumour formation, differentiation and progression. Interestingly, in addition to sebaceous adenomas, less differentiated tumours (“carcinomas”) were formed upon expression of active Rac1 in mouse epidermis.

Expression of HF SC and progenitor markers was increased at the expense of sebocyte differentiation in these tumours. To identify differentially regulated genes in the carcinomas, we have compared sebocytes and basal cells from adenomas with undifferentiated cells from carcinomas. Genes down regulated in carcinoma cells mainly comprise candidates involved in lipid metabolism associated with sebocytes. Interestingly, regulated genes also involve candidates regulating the cell cycle or previously implicated in tumour formation in other tissues.

These results suggest that activated Rac1 in sebaceous adenomas influences differentiation and proliferation leading to more progressive tumours.

6) Zusammenfassung

Haarfollikel (HF) und assoziierte Talgdrüsen (TD) tragen maßgeblich zur Entstehung und Erhaltung der Hautbarriere bei. Zelluläre und molekulare Mechanismen, die an der Entstehung des HFs beteiligt sind, wurden in den letzten Jahren gut charakterisiert und diverse Stammzell (SZ)- und Progenitorpopulationen wurden im HF beschrieben. Erste Untersuchungen zeigen, dass einzelne SZ Marker bereits in der frühen HF-Morphogenese detektiert werden. Bisher ist jedoch noch nicht ausreichend verstanden, wann die verschiedenen SZ- und Progenitorpopulationen des HFs entstehen und ob sie maßgeblich an der Morphogenese von HF und TD beteiligt sind.

Im Rahmen dieser Arbeit wurde die zeitliche und räumliche Anordnung von SZ- und Progenitorpopulationen während der HF-Morphogenese analysiert. Die SZ-Kompartimente der späteren „bulge“-Region (Sox9 positiv) und der „junctional“ Region des oberen adulten HFs (Lrig1 positiv) entstehen noch vor der Entwicklung der TD. Unsere Daten zeigen, dass Sox9 und Lrig1 zunächst gleichzeitig von Zellen des HFs exprimiert werden. Sobald erste Zellen der TD erkennbar waren, wurde Lrig1 Expression im oberen Teil des HFs um die ersten Sebozyten detektiert. Außerdem wurde gezeigt, dass bei der Teilung von Lrig1-positiven SZ durch asymmetrische Zelldeterminierung Sebozyten gebildet werden. Sox9-exprimierende SZ hingegen wurden unterhalb der entstehenden TD, in der zukünftigen HF-„bulge“ detektiert. Im Gegensatz zu den Lrig1- und Sox9-exprimierenden SZ-Populationen wurde die MTS24/Plet1 positive Progenitorpopulation der Isthmus-Region des HFs erst detektiert, nachdem bereits Sebozyten erkennbar waren.

Um den Ursprung der Zellen, die die TD bilden zu identifizieren, wurden „lineage“ Analysen während der frühen Hautmorphogenese durchgeführt. Interessanterweise konnten die Abkömmlinge von basalen Zellen der IFE nicht nur in die SZ Region des adulten HFs, sondern unabhängig davon, auch in die TD verfolgt werden.

In vorangegangenen Studien wurde gezeigt, dass die kleine GTPase Rac1 eine wichtige Rolle in der Erhaltung des HF SZ Kompartiments spielt. Um nun die Rolle von Rac1 in der Entstehung, Differenzierung und Progression von

Hauttumoren zu untersuchen, wurde konstitutiv aktives Rac1 in gutartig differenzierten TD-Tumoren exprimiert. Interessanterweise entstanden neben gutartigen TD-Adenomen auch weniger differenzierte Karzinome. Die Expression von HF SZ Markern war in diesen undifferenzierten Karzinomen erhöht, wohingegen Sebozytendifferenzierung unterdrückt war. Um Änderungen der Genexpression in Karzinomen festzustellen und die Auswirkungen der Aktivierung von Rac1 zu untersuchen, wurden Genexpressionsprofile von Sebozyten und Basalzellen aus Adenomen mit undifferenzierten Zellen aus Karzinomen verglichen. In Karzinomzellen waren vor allem Gene des mit Sebozytendifferenzierung assoziierten Lipidmetabolismus herunter reguliert. Zusätzlich konnten wir auch Gene identifizieren, die der Zellzyklusregulation eine Rolle spielen oder bereits mit der Tumorentstehung in anderen Geweben in Verbindung gebracht wurden. Diese Ergebnisse zeigen, dass konstitutiv aktives Rac1 in TD-Tumoren die Differenzierung und Proliferation beeinflusst und zur Bildung von progressiveren Tumoren führt.

7) References

- Affolter M., Bellusci S., Itoh N., Shilo B., Thiery J.P., Werb Z. (2003) Tube or not tube: remodeling epithelial tissues by branching morphogenesis. *Dev Cell* 4:11-8. DOI: S1534580702004100 [pii].
- Allen M., Grachtchouk M., Sheng H., Grachtchouk V., Wang A., Wei L., Liu J., Ramirez A., Metzger D., Chambon P., Jorcano J., Dlugosz A.A. (2003) Hedgehog signaling regulates sebaceous gland development. *Am J Pathol* 163:2173-8. DOI: S0002-9440(10)63574-2 [pii]
- Andl T., Reddy S.T., Gaddapara T., Millar S.E. (2002) WNT signals are required for the initiation of hair follicle development. *Dev Cell* 2:643-53.
- Arnold I., Watt F.M. (2001) c-Myc activation in transgenic mouse epidermis results in mobilization of stem cells and differentiation of their progeny. *Curr Biol* 11:558-68. DOI: S0960-9822(01)00154-3 [pii].
- Barker N., van Es J.H., Kuipers J., Kujala P., van den Born M., Cozijnsen M., Haegebarth A., Korving J., Begthel H., Peters P.J., Clevers H. (2007) Identification of stem cells in small intestine and colon by marker gene *Lgr5*. *Nature* 449:1003-7.
- Barker N., Huch M., Kujala P., van de Wetering M., Snippert H.J., van Es J.H., Sato T., Stange D.E., Begthel H., van den Born M., Danenberg E., van den Brink S., Korving J., Abo A., Peters P.J., Wright N., Poulsom R., Clevers H. (2010) *Lgr5*(+ve) stem cells drive self-renewal in the stomach and build long-lived gastric units in vitro. *Cell Stem Cell* 6:25-36.
- Barrandon Y., Green H. (1987) Three clonal types of keratinocyte with different capacities for multiplication. *Proc Natl Acad Sci U S A* 84:2302-6.
- Battista M.C., Guimond M.O., Roberge C., Doueik A.A., Fazli L., Gleave M., Sabbagh R., Gallo-Payet N. (2010) Inhibition of DHCR24/seladin-1 impairs cellular homeostasis in prostate cancer. *Prostate* 70:921-33. DOI: 10.1002/pros.21126.
- Behrendt K., Klatter J., Pofahl R., Bloch W., Smyth N., Tschardt M., Krieg T., Paus R., Niessen C., Niemann C., Brakebusch C., Haase I. (2012) A function for *Rac1* in the terminal differentiation and pigmentation of hair. *J Cell Sci*. DOI: jcs.091868 [pii]
- Benitah S.A., Frye M., Glogauer M., Watt F.M. (2005) Stem cell depletion through epidermal deletion of *Rac1*. *Science* 309:933-5.
- Binczek E., Jenke B., Holz B., Gunter R.H., Thevis M., Stoffel W. (2007) Obesity resistance of the stearoyl-CoA desaturase-deficient (*scd1*^{-/-}) mouse results from disruption of the epidermal lipid barrier and adaptive thermoregulation. *Biol Chem* 388:405-18. DOI: 10.1515/BC.2007.046.
- Blanpain C., Fuchs E. (2009) Epidermal homeostasis: a balancing act of stem cells in the skin. *Nat Rev Mol Cell Biol* 10:207-17.
- Blanpain C., Lowry W.E., Geoghegan A., Polak L., Fuchs E. (2004) Self-renewal, multipotency, and the existence of two cell populations within an epithelial stem cell niche. *Cell* 118:635-48.
- Botchkarev V.A., Paus R. (2003) Molecular biology of hair morphogenesis: development and cycling. *J Exp Zool B Mol Dev Evol* 298:164-80. DOI: 10.1002/jez.b.33.

- Botchkarev V.A., Botchkareva N.V., Sharov A.A., Funa K., Huber O., Gilchrist B.A. (2002) Modulation of BMP signaling by noggin is required for induction of the secondary (nonylotoch) hair follicles. *J Invest Dermatol* 118:3-10. DOI: 1645 [pii]
- Botchkarev V.A., Botchkareva N.V., Roth W., Nakamura M., Chen L.H., Herzog W., Lindner G., McMahon J.A., Peters C., Lauster R., McMahon A.P., Paus R. (1999) Noggin is a mesenchymally derived stimulator of hair-follicle induction. *Nat Cell Biol* 1:158-64. DOI: 10.1038/11078.
- Braun K.M., Niemann C., Jensen U.B., Sundberg J.P., Silva-Vargas V., Watt F.M. (2003) Manipulation of stem cell proliferation and lineage commitment: visualisation of label-retaining cells in wholemounts of mouse epidermis. *Development* 130:5241-55.
- Burgeson R.E., Christiano A.M. (1997) The dermal-epidermal junction. *Curr Opin Cell Biol* 9:651-8. DOI: S0955-0674(97)80118-4 [pii].
- Bussolati B., Bruno S., Grange C., Buttiglieri S., Deregibus M.C., Cantino D., Camussi G. (2005) Isolation of renal progenitor cells from adult human kidney. *Am J Pathol* 166:545-55. DOI: S0002-9440(10)62276-6 [pii]
- Cameron D.J., Tong Z., Yang Z., Kaminoh J., Kamiyah S., Chen H., Zeng J., Chen Y., Luo L., Zhang K. (2007) Essential role of Elovl4 in very long chain fatty acid synthesis, skin permeability barrier function, and neonatal survival. *Int J Biol Sci* 3:111-9.
- Candi E., Schmidt R., Melino G. (2005) The cornified envelope: a model of cell death in the skin. *Nat Rev Mol Cell Biol* 6:328-40. DOI: nrm1619 [pii]
- Carmon K.S., Lin Q., Gong X., Thomas A., Liu Q. (2012) LGR5 Interacts and Co-Internalizes with Wnt Receptors to Modulate Wnt/beta-catenin Signaling. *Mol Cell Biol*. DOI: MCB.00272-12 [pii]
- Carroll J.M., Romero M.R., Watt F.M. (1995) Suprabasal integrin expression in the epidermis of transgenic mice results in developmental defects and a phenotype resembling psoriasis. *Cell* 83:957-68.
- Castilho R.M., Squarize C.H., Patel V., Millar S.E., Zheng Y., Molinolo A., Gutkind J.S. (2007) Requirement of Rac1 distinguishes follicular from interfollicular epithelial stem cells. *Oncogene* 26:5078-85. DOI: 1210322 [pii]
- Chan E.F., Gat U., McNiff J.M., Fuchs E. (1999) A common human skin tumour is caused by activating mutations in beta-catenin. *Nat Genet* 21:410-3.
- Chen W., Kelly M.A., Opitz-Araya X., Thomas R.E., Low M.J., Cone R.D. (1997) Exocrine gland dysfunction in MC5-R-deficient mice: evidence for coordinated regulation of exocrine gland function by melanocortin peptides. *Cell* 91:789-98. DOI: S0092-8674(00)80467-5 [pii].
- Chrostek A., Wu X., Quondamatteo F., Hu R., Sanecka A., Niemann C., Langbein L., Haase I., Brakebusch C. (2006) Rac1 is crucial for hair follicle integrity but is not essential for maintenance of the epidermis. *Mol Cell Biol* 26:6957-70. DOI: 26/18/6957 [pii]
- Clevers H. (2006) Wnt/beta-catenin signaling in development and disease. *Cell* 127:469-80. DOI: S0092-8674(06)01344-4 [pii]
- Coleman M.L., Marshall C.J., Olson M.F. (2004) RAS and RHO GTPases in G1-phase cell-cycle regulation. *Nat Rev Mol Cell Biol* 5:355-66. DOI: 10.1038/nrm1365

- Cotsarelis G., Sun T.T., Lavker R.M. (1990) Label-retaining cells reside in the bulge area of pilosebaceous unit: implications for follicular stem cells, hair cycle, and skin carcinogenesis. *Cell* 61:1329-37.
- DasGupta R., Fuchs E. (1999) Multiple roles for activated LEF/TCF transcription complexes during hair follicle development and differentiation. *Development* 126:4557-68.
- de Lau W., Barker N., Low T.Y., Koo B.K., Li V.S., Teunissen H., Kujala P., Haegebarth A., Peters P.J., van de Wetering M., Stange D.E., van Es J.E., Guardavaccaro D., Schasfoort R.B., Mohri Y., Nishimori K., Mohammed S., Heck A.J., Clevers H. (2011) Lgr5 homologues associate with Wnt receptors and mediate R-spondin signalling. *Nature* 476:293-7. DOI: nature10337 [pii]
- Depreter M.G., Blair N.F., Gaskell T.L., Nowell C.S., Davern K., Pagliocca A., Stenhouse F.H., Farley A.M., Fraser A., Vrana J., Robertson K., Morahan G., Tomlinson S.R., Blackburn C.C. (2008) Identification of Plet-1 as a specific marker of early thymic epithelial progenitor cells. *Proc Natl Acad Sci U S A* 105:961-6.
- Duverger O., Morasso M.I. (2009) Epidermal patterning and induction of different hair types during mouse embryonic development. *Birth Defects Res C Embryo Today* 87:263-72. DOI: 10.1002/bdrc.20158.
- Enoch H.G., Catala A., Strittmatter P. (1976) Mechanism of rat liver microsomal stearyl-CoA desaturase. Studies of the substrate specificity, enzyme-substrate interactions, and the function of lipid. *J Biol Chem* 251:5095-103.
- Enshell-Seiffers D., Lindon C., Kashiwagi M., Morgan B.A. (2010) beta-catenin activity in the dermal papilla regulates morphogenesis and regeneration of hair. *Dev Cell* 18:633-42.
- Fargeas C.A., Florek M., Huttner W.B., Corbeil D. (2003) Characterization of prominin-2, a new member of the prominin family of pentaspan membrane glycoproteins. *J Biol Chem* 278:8586-96. DOI: 10.1074/jbc.M210640200
- Fehrenschild D., Galli U., Breiden B., Bloch W., Schettina P., Brodesser S., Michels C., Gunschmann C., Sandhoff K., Niessen C.M., Niemann C. (2012) TCF/Lef1-mediated control of lipid metabolism regulates skin barrier function. *J Invest Dermatol* 132:337-45. DOI: jid2011301 [pii]
- Florek M., Bauer N., Janich P., Wilsch-Braeuning M., Fargeas C.A., Marzesco A.M., Ehninger G., Thiele C., Huttner W.B., Corbeil D. (2007) Prominin-2 is a cholesterol-binding protein associated with apical and basolateral plasmalemmal protrusions in polarized epithelial cells and released into urine. *Cell Tissue Res* 328:31-47. DOI: 10.1007/s00441-006-0324-z.
- Forde A., Constien R., Grone H.J., Hammerling G., Arnold B. (2002) Temporal Cre-mediated recombination exclusively in endothelial cells using Tie2 regulatory elements. *Genesis* 33:191-7. DOI: 10.1002/gene.10117.
- Frances D., Niemann C. (2012) Stem cell dynamics in sebaceous gland morphogenesis in mouse skin. *Dev Biol* 363:138-46. DOI: S0012-1606(11)01448-5 [pii]
- Fuchs E. (2007) Scratching the surface of skin development. *Nature* 445:834-42. DOI: nature05659 [pii]
- Fuchs E., Green H. (1980) Changes in keratin gene expression during terminal differentiation of the keratinocyte. *Cell* 19:1033-42.

- Furuyama K., Kawaguchi Y., Akiyama H., Horiguchi M., Kodama S., Kuhara T., Hosokawa S., Elbahrawy A., Soeda T., Koizumi M., Masui T., Kawaguchi M., Takaori K., Doi R., Nishi E., Kakinoki R., Deng J.M., Behringer R.R., Nakamura T., Uemoto S. (2011) Continuous cell supply from a Sox9-expressing progenitor zone in adult liver, exocrine pancreas and intestine. *Nat Genet* 43:34-41. DOI: ng.722 [pii]
- Fusenig N.E., Breitkreutz D., Dzarlieva R.T., Boukamp P., Bohnert A., Tilgen W. (1983) Growth and differentiation characteristics of transformed keratinocytes from mouse and human skin in vitro and in vivo. *J Invest Dermatol* 81:168s-75s.
- Gandarillas A., Watt F.M. (1995) Changes in expression of members of the fos and jun families and myc network during terminal differentiation of human keratinocytes. *Oncogene* 11:1403-7.
- Gat U., DasGupta R., Degenstein L., Fuchs E. (1998) De Novo hair follicle morphogenesis and hair tumors in mice expressing a truncated beta-catenin in skin. *Cell* 95:605-14.
- Gates A.H., Karasek M. (1965) Hereditary Absence of Sebaceous Glands in the Mouse. *Science* 148:1471-3. DOI: 148/3676/1471 [pii]
- Ghazizadeh S., Taichman L.B. (2001) Multiple classes of stem cells in cutaneous epithelium: a lineage analysis of adult mouse skin. *Embo J* 20:1215-22.
- Gill J., Malin M., Hollander G.A., Boyd R. (2002) Generation of a complete thymic microenvironment by MTS24(+) thymic epithelial cells. *Nat Immunol* 3:635-42.
- Glinka A., Dolde C., Kirsch N., Huang Y.L., Kazanskaya O., Ingelfinger D., Boutros M., Cruciat C.M., Niehrs C. (2011) LGR4 and LGR5 are R-spondin receptors mediating Wnt/beta-catenin and Wnt/PCP signalling. *EMBO Rep* 12:1055-61. DOI: embor2011175 [pii]
- Gomez del Pulgar T., Benitah S.A., Valeron P.F., Espina C., Lacal J.C. (2005) Rho GTPase expression in tumorigenesis: evidence for a significant link. *Bioessays* 27:602-13. DOI: 10.1002/bies.20238.
- Goruppi S., Iovanna J.L. (2010) Stress-inducible protein p8 is involved in several physiological and pathological processes. *J Biol Chem* 285:1577-81. DOI: R109.080887 [pii]
- Greco V., Chen T., Rendl M., Schober M., Pasolli H.A., Stokes N., Dela Cruz-Racelis J., Fuchs E. (2009) A two-step mechanism for stem cell activation during hair regeneration. *Cell Stem Cell* 4:155-69.
- Gu L.H., Coulombe P.A. (2008) Hedgehog signaling, keratin 6 induction, and sebaceous gland morphogenesis: implications for pachyonychia congenita and related conditions. *Am J Pathol* 173:752-61.
- Guo W., Keckesova Z., Donaher J.L., Shibue T., Tischler V., Reinhardt F., Itzkovitz S., Noske A., Zurrer-Hardi U., Bell G., Tam W.L., Mani S.A., van Oudenaarden A., Weinberg R.A. (2012) Slug and Sox9 cooperatively determine the mammary stem cell state. *Cell* 148:1015-28. DOI: S0092-8674(12)00165-1 [pii]
- Handjiski B.K., Eichmuller S., Hofmann U., Czarnetzki B.M., Paus R. (1994) Alkaline phosphatase activity and localization during the murine hair cycle. *Br J Dermatol* 131:303-10.
- Hardy M.H. (1951) The development of pelage hairs and vibrissae from skin in tissue culture. *Ann N Y Acad Sci* 53:546-61.
- Hardy M.H. (1992) The secret life of the hair follicle. *Trends Genet* 8:55-61.

- Hartmann C.H., Klein C.A. (2006) Gene expression profiling of single cells on large-scale oligonucleotide arrays. *Nucleic Acids Res* 34:e143. DOI: gkl740 [pii]
- Hebert J.M., Rosenquist T., Gotz J., Martin G.R. (1994) FGF5 as a regulator of the hair growth cycle: evidence from targeted and spontaneous mutations. *Cell* 78:1017-25. DOI: 0092-8674(94)90276-3 [pii].
- Heid H.W., Moll R., Schwetlick I., Rackwitz H.R., Keenan T.W. (1998) Adipophilin is a specific marker of lipid accumulation in diverse cell types and diseases. *Cell Tissue Res* 294:309-21.
- Heller H., Gredinger E., Bengal E. (2001) Rac1 inhibits myogenic differentiation by preventing the complete withdrawal of myoblasts from the cell cycle. *J Biol Chem* 276:37307-16. DOI: 10.1074/jbc.M103195200
- Hendriksen P.J., Dits N.F., Kokame K., Veldhoven A., van Weerden W.M., Bangma C.H., Trapman J., Jenster G. (2006) Evolution of the androgen receptor pathway during progression of prostate cancer. *Cancer Res* 66:5012-20. DOI: 66/10/5012 [pii]
- Horsley V., Aliprantis A.O., Polak L., Glimcher L.H., Fuchs E. (2008) NFATc1 balances quiescence and proliferation of skin stem cells. *Cell* 132:299-310.
- Horsley V., O'Carroll D., Tooze R., Ohinata Y., Saitou M., Obukhanych T., Nussenzweig M., Tarakhovskiy A., Fuchs E. (2006) Blimp1 defines a progenitor population that governs cellular input to the sebaceous gland. *Cell* 126:597-609.
- Hsu Y.C., Pasolli H.A., Fuchs E. (2011) Dynamics between stem cells, niche, and progeny in the hair follicle. *Cell* 144:92-105. DOI: S0092-8674(10)01371-1 [pii]
- Huber O., Krohn M., Kemler R. (1997) A specific domain in alpha-catenin mediates binding to beta-catenin or plakoglobin. *J Cell Sci* 110 (Pt 15):1759-65.
- Huelsken J., Birchmeier W., Behrens J. (1994) E-cadherin and APC compete for the interaction with beta-catenin and the cytoskeleton. *J Cell Biol* 127:2061-9.
- Huelsken J., Vogel R., Erdmann B., Cotsarelis G., Birchmeier W. (2001) beta-Catenin controls hair follicle morphogenesis and stem cell differentiation in the skin. *Cell* 105:533-45.
- Hurlin P.J., Foley K.P., Ayer D.E., Eisenman R.N., Hanahan D., Arbeit J.M. (1995) Regulation of Myc and Mad during epidermal differentiation and HPV-associated tumorigenesis. *Oncogene* 11:2487-501.
- Indra A.K., Warot X., Brocard J., Bornert J.M., Xiao J.H., Chambon P., Metzger D. (1999) Temporally-controlled site-specific mutagenesis in the basal layer of the epidermis: comparison of the recombinase activity of the tamoxifen-inducible Cre-ER(T) and Cre-ER(T2) recombinases. *Nucleic Acids Res* 27:4324-7.
- Ito M., Liu Y., Yang Z., Nguyen J., Liang F., Morris R.J., Cotsarelis G. (2005) Stem cells in the hair follicle bulge contribute to wound repair but not to homeostasis of the epidermis. *Nat Med* 11:1351-4.
- Jaks V., Kasper M., Toftgard R. (2010) The hair follicle-a stem cell zoo. *Exp Cell Res*.

- Jaks V., Barker N., Kasper M., van Es J.H., Snippert H.J., Clevers H., Toftgard R. (2008) Lgr5 marks cycling, yet long-lived, hair follicle stem cells. *Nat Genet* 40:1291-9.
- Jamora C., DasGupta R., Kocieniewski P., Fuchs E. (2003) Links between signal transduction, transcription and adhesion in epithelial bud development. *Nature* 422:317-22. DOI: 10.1038/nature01458
- Janich P., Pascual G., Merlos-Suarez A., Battle E., Ripperger J., Albrecht U., Cheng H.Y., Obrietan K., Di Croce L., Benitah S.A. (2011) The circadian molecular clock creates epidermal stem cell heterogeneity. *Nature* 480:209-14. DOI: nature10649 [pii]
- Jaskoll T., Leo T., Witcher D., Ormestad M., Astorga J., Bringas P., Jr., Carlsson P., Melnick M. (2004) Sonic hedgehog signaling plays an essential role during embryonic salivary gland epithelial branching morphogenesis. *Dev Dyn* 229:722-32. DOI: 10.1002/dvdy.10472.
- Jensen K.B., Jones J., Watt F.M. (2008a) A stem cell gene expression profile of human squamous cell carcinomas. *Cancer Lett* 272:23-31.
- Jensen K.B., Driskell R.R., Watt F.M. (2010) Assaying proliferation and differentiation capacity of stem cells using disaggregated adult mouse epidermis. *Nat Protoc* 5:898-911.
- Jensen K.B., Collins C.A., Nascimento E., Tan D.W., Frye M., Itami S., Watt F.M. (2009) Lrig1 expression defines a distinct multipotent stem cell population in mammalian epidermis. *Cell Stem Cell* 4:427-39.
- Jensen U.B., Yan X., Triel C., Woo S.H., Christensen R., Owens D.M. (2008b) A distinct population of clonogenic and multipotent murine follicular keratinocytes residing in the upper isthmus. *J Cell Sci* 121:609-17.
- Jiang W.G., Davies G., Kynaston H., Mason M.D., Fodstad O. (2006a) Does the PGC-1/PPARgamma pathway play a role in Com-1/p8 mediated cell growth inhibition in prostate cancer? *Int J Mol Med* 18:1169-75.
- Jiang W.G., Davies G., Martin T.A., Kynaston H., Mason M.D., Fodstad O. (2006b) Com-1/p8 acts as a putative tumour suppressor in prostate cancer. *Int J Mol Med* 18:981-6.
- Jones P.H., Watt F.M. (1993) Separation of human epidermal stem cells from transit amplifying cells on the basis of differences in integrin function and expression. *Cell* 73:713-24.
- Jones P.H., Harper S., Watt F.M. (1995) Stem cell patterning and fate in human epidermis. *Cell* 80:83-93.
- Josefowicz W.J., Hardy M.H. (1978) The expression of the gene *asebia* in the laboratory mouse. I. Epidermis and dermis. *Genet Res* 31:53-65.
- Kamai T., Yamanishi T., Shirataki H., Takagi K., Asami H., Ito Y., Yoshida K. (2004) Overexpression of RhoA, Rac1, and Cdc42 GTPases is associated with progression in testicular cancer. *Clin Cancer Res* 10:4799-805. DOI: 10.1158/1078-0432.CCR-0436-03
- Kamai T., Shirataki H., Nakanishi K., Furuya N., Kambara T., Abe H., Oyama T., Yoshida K. (2010) Increased Rac1 activity and Pak1 overexpression are associated with lymphovascular invasion and lymph node metastasis of upper urinary tract cancer. *BMC Cancer* 10:164. DOI: 1471-2407-10-164 [pii]
- Kazanskaya O., Glinka A., del Barco Barrantes I., Stannek P., Niehrs C., Wu W. (2004) R-Spondin2 is a secreted activator of Wnt/beta-catenin signaling

- and is required for *Xenopus* myogenesis. *Dev Cell* 7:525-34. DOI: S1534580704002813 [pii]
- Kim K.A., Wagle M., Tran K., Zhan X., Dixon M.A., Liu S., Gros D., Korver W., Yonkovich S., Tomasevic N., Binnerts M., Abo A. (2008) R-Spondin family members regulate the Wnt pathway by a common mechanism. *Mol Biol Cell* 19:2588-96. DOI: E08-02-0187 [pii]
- Klein E.A., Yang C., Kazanietz M.G., Assoian R.K. (2007) NFkappaB-independent signaling to the cyclin D1 gene by Rac. *Cell Cycle* 6:1115-21. DOI: 4147 [pii].
- Knop E., Knop N., Schirra F. (2009) [Meibomian glands. Part II: physiology, characteristics, distribution and function of meibomian oil]. *Ophthalmologie* 106:884-92. DOI: 10.1007/s00347-009-2019-9.
- Knop N., Knop E. (2009) [Meibomian glands. Part I: anatomy, embryology and histology of the Meibomian glands]. *Ophthalmologie* 106:872-83. DOI: 10.1007/s00347-009-2006-1.
- Kobielak K., Stokes N., de la Cruz J., Polak L., Fuchs E. (2007) Loss of a quiescent niche but not follicle stem cells in the absence of bone morphogenetic protein signaling. *Proc Natl Acad Sci U S A* 104:10063-8.
- Kopp J.L., Dubois C.L., Schaffer A.E., Hao E., Shih H.P., Seymour P.A., Ma J., Sander M. (2011) Sox9+ ductal cells are multipotent progenitors throughout development but do not produce new endocrine cells in the normal or injured adult pancreas. *Development* 138:653-65. DOI: 138/4/653 [pii]
- Krause K., Foitzik K. (2006) Biology of the hair follicle: the basics. *Semin Cutan Med Surg* 25:2-10.
- Kretzschmar K., Watt F.M. (2012) Lineage tracing. *Cell* 148:33-45. DOI: S0092-8674(12)00003-7 [pii]
- Lavker R.M., Sun T.T., Oshima H., Barrandon Y., Akiyama M., Ferraris C., Chevalier G., Favier B., Jahoda C.A., Dhouailly D., Panteleyev A.A., Christiano A.M. (2003) Hair follicle stem cells. *J Invest Dermatol Symp Proc* 8:28-38.
- Levy V., Lindon C., Zheng Y., Harfe B.D., Morgan B.A. (2007) Epidermal stem cells arise from the hair follicle after wounding. *Faseb J* 21:1358-66.
- Li W., Sandhoff R., Kono M., Zerfas P., Hoffmann V., Ding B.C., Proia R.L., Deng C.X. (2007) Depletion of ceramides with very long chain fatty acids causes defective skin permeability barrier function, and neonatal lethality in ELOVL4 deficient mice. *Int J Biol Sci* 3:120-8.
- Liu Y., Lyle S., Yang Z., Cotsarelis G. (2003) Keratin 15 promoter targets putative epithelial stem cells in the hair follicle bulge. *J Invest Dermatol* 121:963-8.
- Lloyd C., Yu Q.C., Cheng J., Turksen K., Degenstein L., Hutton E., Fuchs E. (1995) The basal keratin network of stratified squamous epithelia: defining K15 function in the absence of K14. *J Cell Biol* 129:1329-44.
- Lo Celso C., Prowse D.M., Watt F.M. (2004) Transient activation of beta-catenin signalling in adult mouse epidermis is sufficient to induce new hair follicles but continuous activation is required to maintain hair follicle tumours. *Development* 131:1787-99.
- Lowry W.E., Blanpain C., Nowak J.A., Guasch G., Lewis L., Fuchs E. (2005) Defining the impact of beta-catenin/Tcf transactivation on epithelial stem cells. *Genes Dev* 19:1596-611.

- Lozano G., Zambetti G.P. (2005) Gankyrin: an intriguing name for a novel regulator of p53 and RB. *Cancer Cell* 8:3-4. DOI: S1535-6108(05)00200-X [pii]
- Lu P., Sternlicht M.D., Werb Z. (2006) Comparative mechanisms of branching morphogenesis in diverse systems. *J Mammary Gland Biol Neoplasia* 11:213-28. DOI: 10.1007/s10911-006-9027-z.
- Lüllmann-Rauch R. (2003) Taschenlehrbuch Histologie Thieme.
- Lyle S., Christofidou-Solomidou M., Liu Y., Elder D.E., Albelda S., Cotsarelis G. (1998) The C8/144B monoclonal antibody recognizes cytokeratin 15 and defines the location of human hair follicle stem cells. *J Cell Sci* 111 (Pt 21):3179-88.
- Lyle S., Christofidou-Solomidou M., Liu Y., Elder D.E., Albelda S., Cotsarelis G. (1999) Human hair follicle bulge cells are biochemically distinct and possess an epithelial stem cell phenotype. *J Invest Dermatol Symp Proc* 4:296-301.
- Mailleux A.A., Spencer-Dene B., Dillon C., Ndiaye D., Savona-Baron C., Itoh N., Kato S., Dickson C., Thiery J.P., Bellusci S. (2002) Role of FGF10/FGFR2b signaling during mammary gland development in the mouse embryo. *Development* 129:53-60.
- McMillan J.R., Akiyama M., Shimizu H. (2003) Epidermal basement membrane zone components: ultrastructural distribution and molecular interactions. *J Dermatol Sci* 31:169-77. DOI: S0923181103000458 [pii].
- Merrill B.J., Gat U., DasGupta R., Fuchs E. (2001) Tcf3 and Lef1 regulate lineage differentiation of multipotent stem cells in skin. *Genes Dev* 15:1688-705.
- Mikkola M.L. (2008) TNF superfamily in skin appendage development. *Cytokine Growth Factor Rev* 19:219-30. DOI: S1359-6101(08)00041-5 [pii]
- Mikkola M.L., Thesleff I. (2003) Ectodysplasin signaling in development. *Cytokine Growth Factor Rev* 14:211-24. DOI: S1359610103000200 [pii].
- Millar S.E. (2002) Molecular mechanisms regulating hair follicle development. *J Invest Dermatol* 118:216-25.
- Mirza R., Qiao S., Murata Y., Seo H. (2009) Requirement of DHCR24 for postnatal development of epidermis and hair follicles in mice. *Am J Dermatopathol* 31:446-52. DOI: 10.1097/DAD.0b013e318196f10c
- Mirza R., Hayasaka S., Kambe F., Maki K., Kaji T., Murata Y., Seo H. (2008) Increased expression of aquaporin-3 in the epidermis of DHCR24 knockout mice. *Br J Dermatol* 158:679-84. DOI: BJD8424 [pii]
- Mirza R., Hayasaka S., Takagishi Y., Kambe F., Ohmori S., Maki K., Yamamoto M., Murakami K., Kaji T., Zadworny D., Murata Y., Seo H. (2006) DHCR24 gene knockout mice demonstrate lethal dermopathy with differentiation and maturation defects in the epidermis. *J Invest Dermatol* 126:638-47. DOI: 5700111 [pii]
- Miyazaki M., Man W.C., Ntambi J.M. (2001) Targeted disruption of stearoyl-CoA desaturase1 gene in mice causes atrophy of sebaceous and meibomian glands and depletion of wax esters in the eyelid. *J Nutr* 131:2260-8.
- Montagna W. (1974a) An introduction to sebaceous glands. *J Invest Dermatol* 62:120-3.
- Montagna W.a.P., P. (1974b) The structure and function of skin Academic press, New York.

- Morris R.J., Tacker K.C., Baldwin J.K., Fischer S.M., Slaga T.J. (1987) A new medium for primary cultures of adult murine epidermal cells: application to experimental carcinogenesis. *Cancer Lett* 34:297-304.
- Morris R.J., Liu Y., Marles L., Yang Z., Trempus C., Li S., Lin J.S., Sawicki J.A., Cotsarelis G. (2004) Capturing and profiling adult hair follicle stem cells. *Nat Biotechnol* 22:411-7.
- Mou C., Jackson B., Schneider P., Overbeek P.A., Headon D.J. (2006) Generation of the primary hair follicle pattern. *Proc Natl Acad Sci U S A* 103:9075-80. DOI: 0600825103 [pii]
- Muller-Rover S., Handjiski B., van der Veen C., Eichmuller S., Foitzik K., McKay I.A., Stenn K.S., Paus R. (2001) A comprehensive guide for the accurate classification of murine hair follicles in distinct hair cycle stages. *J Invest Dermatol* 117:3-15.
- Narhi K., Jarvinen E., Birchmeier W., Taketo M.M., Mikkola M.L., Thesleff I. (2008) Sustained epithelial beta-catenin activity induces precocious hair development but disrupts hair follicle down-growth and hair shaft formation. *Development* 135:1019-28. DOI: dev.016550 [pii]
- Nelson W.G., Sun T.T. (1983) The 50- and 58-kdalton keratin classes as molecular markers for stratified squamous epithelia: cell culture studies. *J Cell Biol* 97:244-51.
- Nguyen H., Rendl M., Fuchs E. (2006) Tcf3 governs stem cell features and represses cell fate determination in skin. *Cell* 127:171-83.
- Niemann C. (2009) Differentiation of the sebaceous gland. *Dermato-Endocrinology* 1:64-67.
- Niemann C., Owens D.M., Schettina P., Watt F.M. (2007) Dual role of inactivating Lef1 mutations in epidermis: tumor promotion and specification of tumor type. *Cancer Res* 67:2916-21.
- Niemann C., Owens D.M., Hulsken J., Birchmeier W., Watt F.M. (2002) Expression of DeltaN_{Lef1} in mouse epidermis results in differentiation of hair follicles into squamous epidermal cysts and formation of skin tumours. *Development* 129:95-109.
- Niemann C., Unden A.B., Lyle S., Zouboulis Ch C., Toftgard R., Watt F.M. (2003) Indian hedgehog and beta-catenin signaling: role in the sebaceous lineage of normal and neoplastic mammalian epidermis. *Proc Natl Acad Sci U S A* 100 Suppl 1:11873-80.
- Nijhof J.G., Braun K.M., Giangreco A., van Pelt C., Kawamoto H., Boyd R.L., Willemze R., Mullenders L.H., Watt F.M., de Gruijl F.R., van Ewijk W. (2006) The cell-surface marker MTS24 identifies a novel population of follicular keratinocytes with characteristics of progenitor cells. *Development* 133:3027-37.
- Nöbel H. (2009) Analysen zur Regulation und Manipulation von epithelialen Progenitorzellen. Universität zu Köln.
- Nowak J.A., Fuchs E. (2009) Isolation and culture of epithelial stem cells. *Methods Mol Biol* 482:215-32. DOI: 10.1007/978-1-59745-060-7_14.
- Nowak J.A., Polak L., Pasolli H.A., Fuchs E. (2008) Hair follicle stem cells are specified and function in early skin morphogenesis. *Cell Stem Cell* 3:33-43.
- Nusse R. (2005) Wnt signaling in disease and in development. *Cell Res* 15:28-32.

- Olson M.F., Ashworth A., Hall A. (1995) An essential role for Rho, Rac, and Cdc42 GTPases in cell cycle progression through G1. *Science* 269:1270-2.
- Ortiz C.M., Ito T., Tanaka E., Tsunoda S., Nagayama S., Sakai Y., Higashitsuji H., Fujita J., Shimada Y. (2008) Gankyrin oncoprotein overexpression as a critical factor for tumor growth in human esophageal squamous cell carcinoma and its clinical significance. *Int J Cancer* 122:325-32. DOI: 10.1002/ijc.23106.
- Oshimori N., Fuchs E. (2012) Paracrine TGF-beta signaling counterbalances BMP-mediated repression in hair follicle stem cell activation. *Cell Stem Cell* 10:63-75. DOI: S1934-5909(11)00533-9 [pii]
- Osorio K.M., Lee S.E., McDermitt D.J., Waghmare S.K., Zhang Y.V., Woo H.N., Tumber T. (2008) Runx1 modulates developmental, but not injury-driven, hair follicle stem cell activation. *Development* 135:1059-68.
- Ostler D.A., Prieto V.G., Reed J.A., Deavers M.T., Lazar A.J., Ivan D. (2010) Adipophilin expression in sebaceous tumors and other cutaneous lesions with clear cell histology: an immunohistochemical study of 117 cases. *Mod Pathol* 23:567-573.
- Pan Y., Bi F., Liu N., Xue Y., Yao X., Zheng Y., Fan D. (2004) Expression of seven main Rho family members in gastric carcinoma. *Biochem Biophys Res Commun* 315:686-91. DOI: 10.1016/j.bbrc.2004.01.108
- Panteleyev A.A., Jahoda C.A., Christiano A.M. (2001) Hair follicle predetermination. *J Cell Sci* 114:3419-31.
- Panteleyev A.A., Rosenbach T., Paus R., Christiano A.M. (2000) The bulge is the source of cellular renewal in the sebaceous gland of mouse skin. *Arch Dermatol Res* 292:573-6.
- Paus R., Foitzik K. (2004) In search of the "hair cycle clock": a guided tour. *Differentiation* 72:489-511.
- Paus R., Muller-Rover S., Van Der Veen C., Maurer M., Eichmuller S., Ling G., Hofmann U., Foitzik K., Mecklenburg L., Handjiski B. (1999) A comprehensive guide for the recognition and classification of distinct stages of hair follicle morphogenesis. *J Invest Dermatol* 113:523-32.
- Pepicelli C.V., Lewis P.M., McMahan A.P. (1998) Sonic hedgehog regulates branching morphogenesis in the mammalian lung. *Curr Biol* 8:1083-6. DOI: S0960-9822(98)70446-4 [pii].
- Petersson M., Brylka H., Kraus A., John S., Rappl G., Schettina P., Niemann C. (2011) TCF/Lef1 activity controls establishment of diverse stem and progenitor cell compartments in mouse epidermis. *Embo J* 30:3004-18. DOI: emboj2011199 [pii]
- Petiot A., Conti F.J., Grose R., Revest J.M., Hodivala-Dilke K.M., Dickson C. (2003) A crucial role for Fgfr2-IIIb signalling in epidermal development and hair follicle patterning. *Development* 130:5493-501. DOI: 10.1242/dev.00788
- Plikus M.V., Widelitz R.B., Maxson R., Chuong C.M. (2009) Analyses of regenerative wave patterns in adult hair follicle populations reveal macro-environmental regulation of stem cell activity. *Int J Dev Biol* 53:857-68. DOI: 072564mp [pii]
- Plikus M.V., Mayer J.A., de la Cruz D., Baker R.E., Maini P.K., Maxson R., Chuong C.M. (2008) Cyclic dermal BMP signalling regulates stem cell

- activation during hair regeneration. *Nature* 451:340-4. DOI: nature06457 [pii]
- Poulson N.D., Lechler T. (2010) Robust control of mitotic spindle orientation in the developing epidermis. *The Journal of Cell Biology* 191:915-922. DOI: 10.1083/jcb.201008001.
- Powell A.E., Wang Y., Li Y., Poulin E.J., Means A.L., Washington M.K., Higginbotham J.N., Juchheim A., Prasad N., Levy S.E., Guo Y., Shyr Y., Aronow B.J., Haigis K.M., Franklin J.L., Coffey R.J. (2012) The Pan-ErbB Negative Regulator Lrig1 Is an Intestinal Stem Cell Marker that Functions as a Tumor Suppressor. *Cell* 149:146-58. DOI: S0092-8674(12)00280-2 [pii]
- Raymond K., Richter A., Kreft M., Frijns E., Janssen H., Slijper M., Praetzel-Wunder S., Langbein L., Sonnenberg A. (2010) Expression of the Orphan Protein Plet-1 during Trichilemmal Differentiation of Anagen Hair Follicles. *J Invest Dermatol*.
- Ree A.H., Pacheco M.M., Tvermyr M., Fodstad O., Brentani M.M. (2000) Expression of a novel factor, com1, in early tumor progression of breast cancer. *Clin Cancer Res* 6:1778-83.
- Ree A.H., Tvermyr M., Engebraaten O., Rooman M., Rosok O., Hovig E., Meza-Zepeda L.A., Bruland O.S., Fodstad O. (1999) Expression of a novel factor in human breast cancer cells with metastatic potential. *Cancer Res* 59:4675-80.
- Rendl M., Polak L., Fuchs E. (2008) BMP signaling in dermal papilla cells is required for their hair follicle-inductive properties. *Genes Dev* 22:543-57.
- Rhee H., Polak L., Fuchs E. (2006) Lhx2 maintains stem cell character in hair follicles. *Science* 312:1946-9.
- Rheinwald J.G. (1989) Human epidermal keratinocyte cell culture and xenograft systems: applications in the detection of potential chemical carcinogens and the study of epidermal transformation. *Prog Clin Biol Res* 298:113-25.
- Rheinwald J.G., Green H. (1975) Serial cultivation of strains of human epidermal keratinocytes: the formation of keratinizing colonies from single cells. *Cell* 6:331-43.
- Richardson G.D., Robson C.N., Lang S.H., Neal D.E., Maitland N.J., Collins A.T. (2004) CD133, a novel marker for human prostatic epithelial stem cells. *J Cell Sci* 117:3539-45. DOI: 10.1242/jcs.01222
- Rogers G.E. (2004) Hair follicle differentiation and regulation. *Int J Dev Biol* 48:163-70.
- Rosen E.D., Sarraf P., Troy A.E., Bradwin G., Moore K., Milstone D.S., Spiegelman B.M., Mortensen R.M. (1999) PPAR gamma is required for the differentiation of adipose tissue in vivo and in vitro. *Mol Cell* 4:611-7. DOI: S1097-2765(00)80211-7 [pii].
- Rosenfield R.L., Deplewski D., Greene M.E. (2000) Peroxisome proliferator-activated receptors and skin development. *Horm Res* 54:269-74. DOI: 53270 [pii].
- Rosenfield R.L., Deplewski D., Kentsis A., Ciletti N. (1998) Mechanisms of androgen induction of sebocyte differentiation. *Dermatology* 196:43-6. DOI: drm96043 [pii].
- Rosenfield R.L., Kentsis A., Deplewski D., Ciletti N. (1999) Rat preputial sebocyte differentiation involves peroxisome proliferator-activated

- receptors. *J Invest Dermatol* 112:226-32. DOI: 10.1046/j.1523-1747.1999.00487.x.
- Sampath H., Flowers M.T., Liu X., Paton C.M., Sullivan R., Chu K., Zhao M., Ntambi J.M. (2009) Skin-specific deletion of stearyl-CoA desaturase-1 alters skin lipid composition and protects mice from high fat diet-induced obesity. *J Biol Chem* 284:19961-73.
- Schmidt-Ullrich R., Paus R. (2005) Molecular principles of hair follicle induction and morphogenesis. *Bioessays* 27:247-61. DOI: 10.1002/bies.20184 [doi].
- Schneider M.R., Paus R. (2009) Sebocytes, multifaceted epithelial cells: Lipid production and holocrine secretion. *Int J Biochem Cell Biol*.
- Schneider M.R., Schmidt-Ullrich R., Paus R. (2009) The hair follicle as a dynamic miniorgan. *Curr Biol* 19:R132-42.
- Schnelzer A., Prechtel D., Knaus U., Dehne K., Gerhard M., Graeff H., Harbeck N., Schmitt M., Lengyel E. (2000) Rac1 in human breast cancer: overexpression, mutation analysis, and characterization of a new isoform, Rac1b. *Oncogene* 19:3013-20. DOI: 10.1038/sj.onc.1203621.
- Schweizer J., Marks F. (1977) A developmental study of the distribution and frequency of Langerhans cells in relation to formation of patterning in mouse tail epidermis. *J Invest Dermatol* 69:198-204.
- Sellheyer K., Krahl D. (2009) Blimp-1: a marker of terminal differentiation but not of sebocytic progenitor cells. *J Cutan Pathol*.
- Sharma N. (2011) Characterization of sebaceous tumors and analyzing expression of epidermal progenitor and differentiation markers, CMMC, University of Bonn, Cologne.
- Shubbar E., Vegfors J., Carlstrom M., Petersson S., Enerback C. (2011) Psoriasis (S100A7) increases the expression of ROS and VEGF and acts through RAGE to promote endothelial cell proliferation. *Breast Cancer Res Treat*. DOI: 10.1007/s10549-011-1920-5.
- Sick S., Reinker S., Timmer J., Schlake T. (2006) WNT and DKK determine hair follicle spacing through a reaction-diffusion mechanism. *Science* 314:1447-50. DOI: 1130088 [pii]
- Simpson C.L., Patel D.M., Green K.J. (2011) Deconstructing the skin: cytoarchitectural determinants of epidermal morphogenesis. *Nat Rev Mol Cell Biol* 12:565-80. DOI: nrm3175 [pii]
- Snippert H.J., van der Flier L.G., Sato T., van Es J.H., van den Born M., Kroon-Veenboer C., Barker N., Klein A.M., van Rheenen J., Simons B.D., Clevers H. (2010a) Intestinal crypt homeostasis results from neutral competition between symmetrically dividing Lgr5 stem cells. *Cell* 143:134-44. DOI: S0092-8674(10)01064-0 [pii]
- Snippert H.J., Haegebarth A., Kasper M., Jaks V., van Es J.H., Barker N., van de Wetering M., van den Born M., Begthel H., Vries R.G., Stange D.E., Toftgard R., Clevers H. (2010b) Lgr6 marks stem cells in the hair follicle that generate all cell lineages of the skin. *Science* 327:1385-9.
- Srinivas S., Watanabe T., Lin C.S., Williams C.M., Tanabe Y., Jessell T.M., Costantini F. (2001) Cre reporter strains produced by targeted insertion of EYFP and ECFP into the ROSA26 locus. *BMC Dev Biol* 1:4.
- Stachelscheid H., Ibrahim H., Koch L., Schmitz A., Tschardt M., Wunderlich F.T., Scott J., Michels C., Wickenhauser C., Haase I., Bruning J.C., Niessen C.M. (2008) Epidermal insulin/IGF-1 signalling control

- interfollicular morphogenesis and proliferative potential through Rac activation. *EMBO J* 27:2091-101. DOI: emboj2008141 [pii]
- Stenn K.S., Paus R. (2001) Controls of hair follicle cycling. *Physiol Rev* 81:449-494.
- Stenn K.S., Zheng Y., Parimoo S. (2008) Phylogeny of the hair follicle: the sebogenic hypothesis. *J Invest Dermatol* 128:1576-8. DOI: 5701200 [pii]
- Stolt C.C., Lommes P., Sock E., Chaboissier M.C., Schedl A., Wegner M. (2003) The Sox9 transcription factor determines glial fate choice in the developing spinal cord. *Genes Dev* 17:1677-89. DOI: 10.1101/gad.259003 [doi]
- Sun W., Ding J., Wu K., Ning B.F., Wen W., Sun H.Y., Han T., Huang L., Dong L.W., Yang W., Deng X., Li Z., Wu M.C., Feng G.S., Xie W.F., Wang H.Y. (2011) Gankyrin-mediated dedifferentiation facilitates the tumorigenicity of rat hepatocytes and hepatoma cells. *Hepatology* 54:1259-72. DOI: 10.1002/hep.24530.
- Sundberg. (1994) Hair types and subtypes in the laboratory mouse, in: S. JP (Ed.), *Handbook of mouse mutations with skin and hair abnormalities: animal models and biochemical tools*, CRC Press, Boca Raton.
- Sundberg J.P., Boggess D., Sundberg B.A., Eilertsen K., Parimoo S., Filippi M., Stenn K. (2000) Asebia-2J (Scd1(ab2J)): a new allele and a model for scarring alopecia. *Am J Pathol* 156:2067-75. DOI: S0002-9440(10)65078-X [pii]
- Suzuki Y., Miura H., Tanemura A., Kobayashi K., Kondoh G., Sano S., Ozawa K., Inui S., Nakata A., Takagi T., Tohyama M., Yoshikawa K., Itami S. (2002) Targeted disruption of LIG-1 gene results in psoriasiform epidermal hyperplasia. *FEBS Lett* 521:67-71. DOI: S0014579302028247 [pii].
- Takeda H., Lyle S., Lazar A.J., Zouboulis C.C., Smyth I., Watt F.M. (2006) Human sebaceous tumors harbor inactivating mutations in LEF1. *Nat Med*.
- Taylor G., Lehrer M.S., Jensen P.J., Sun T.T., Lavker R.M. (2000) Involvement of follicular stem cells in forming not only the follicle but also the epidermis. *Cell* 102:451-61.
- Thiboutot D. (2004) Regulation of human sebaceous glands. *J Invest Dermatol* 123:1-12. DOI: 10.1111/j.1523-1747.2004.t01-2-x
- Thody A.J., Shuster S. (1989) Control and function of sebaceous glands. *Physiol Rev* 69:383-416.
- Trempus C.S., Morris R.J., Bortner C.D., Cotsarelis G., Faircloth R.S., Reece J.M., Tennant R.W. (2003) Enrichment for living murine keratinocytes from the hair follicle bulge with the cell surface marker CD34. *J Invest Dermatol* 120:501-11.
- Tscharntke M. (2006) Funktionale Charakterisierung von Rac1 in der epidermalen Wundheilung in vivo und in vitro, Universität zu Köln, Köln.
- Tumbar T., Guasch G., Greco V., Blanpain C., Lowry W.E., Rendl M., Fuchs E. (2004) Defining the epithelial stem cell niche in skin. *Science* 303:359-63.
- Turing A. (1952). *Philos. Trans. R. Soc. London B Biol.* 237.
- van der Flier L.G., van Gijn M.E., Hatzis P., Kujala P., Haegebarth A., Stange D.E., Begthel H., van den Born M., Guryev V., Oving I., van Es J.H., Barker N., Peters P.J., van de Wetering M., Clevers H. (2009) Transcription factor achaete scute-like 2 controls intestinal stem cell fate. *Cell* 136:903-12. DOI: S0092-8674(09)00079-8 [pii]

- Van Mater D., Kolligs F.T., Dlugosz A.A., Fearon E.R. (2003) Transient activation of beta -catenin signaling in cutaneous keratinocytes is sufficient to trigger the active growth phase of the hair cycle in mice. *Genes Dev* 17:1219-24.
- Vidal V.P., Chaboissier M.C., Lutzkendorf S., Cotsarelis G., Mill P., Hui C.C., Ortonne N., Ortonne J.P., Schedl A. (2005) Sox9 is essential for outer root sheath differentiation and the formation of the hair stem cell compartment. *Curr Biol* 15:1340-51.
- Waikel R.L., Kawachi Y., Waikel P.A., Wang X.J., Roop D.R. (2001) Deregulated expression of c-Myc depletes epidermal stem cells. *Nat Genet* 28:165-8. DOI: 10.1038/88889
- Wang Z., Pedersen E., Basse A., Lefever T., Peyrollier K., Kapoor S., Mei Q., Karlsson R., Chrostek-Grashoff A., Brakebusch C. (2010) Rac1 is crucial for Ras-dependent skin tumor formation by controlling Pak1-Mek-Erk hyperactivation and hyperproliferation in vivo. *Oncogene* 29:3362-73. DOI: onc201095 [pii]
- Waterham H.R., Koster J., Romeijn G.J., Hennekam R.C., Vreken P., Andersson H.C., FitzPatrick D.R., Kelley R.I., Wanders R.J. (2001) Mutations in the 3beta-hydroxysterol Delta24-reductase gene cause desmosterolosis, an autosomal recessive disorder of cholesterol biosynthesis. *Am J Hum Genet* 69:685-94. DOI: S0002-9297(07)61125-2 [pii]
- Watt F.M. (2002) Role of integrins in regulating epidermal adhesion, growth and differentiation. *Embo J* 21:3919-26.
- Weinberg W.C., Goodman L.V., George C., Morgan D.L., Ledbetter S., Yuspa S.H., Lichti U. (1993) Reconstitution of hair follicle development in vivo: determination of follicle formation, hair growth, and hair quality by dermal cells. *J Invest Dermatol* 100:229-36.
- Westerberg R., Tvrdik P., Uden A.B., Mansson J.E., Norlen L., Jakobsson A., Holleran W.H., Elias P.M., Asadi A., Flodby P., Toftgard R., Capecchi M.R., Jakobsson A. (2004) Role for ELOVL3 and fatty acid chain length in development of hair and skin function. *J Biol Chem* 279:5621-9. DOI: 10.1074/jbc.M310529200
- Wong V.W., Stange D.E., Page M.E., Buczacki S., Wabik A., Itami S., van de Wetering M., Poulsom R., Wright N.A., Trotter M.W., Watt F.M., Winton D.J., Clevers H., Jensen K.B. (2012) Lrig1 controls intestinal stem-cell homeostasis by negative regulation of ErbB signalling. *Nat Cell Biol* 14:401-8. DOI: ncb2464 [pii]
- Zhang L., Li W.H., Anthonavage M., Eisinger M. (2006) Melanocortin-5 receptor: a marker of human sebocyte differentiation. *Peptides* 27:413-20.
- Zhang Y., Andl T., Yang S.H., Teta M., Liu F., Seykora J.T., Tobias J.W., Piccolo S., Schmidt-Ullrich R., Nagy A., Taketo M.M., Dlugosz A.A., Millar S.E. (2008) Activation of beta-catenin signaling programs embryonic epidermis to hair follicle fate. *Development* 135:2161-72. DOI: dev.017459 [pii]
- Zheng Y., Eilertsen K.J., Ge L., Zhang L., Sundberg J.P., Prouty S.M., Stenn K.S., Parimoo S. (1999) Scd1 is expressed in sebaceous glands and is disrupted in the asebia mouse. *Nat Genet* 23:268-70. DOI: 10.1038/15446.

8) Figure index

Fig. 1) The structure of the skin	1
Fig. 2) The interfollicular epidermis	2
Fig. 3) The hair follicle	4
Fig. 4) Morphogenesis of the HF	6
Fig. 5) The hair cycle	8
Fig. 6) K15CreER(G)T2 mouse model	10
Fig. 7) Stem and progenitor cell populations of the adult HF	11
Fig. 8) The Sebaceous gland (SG)	14
Fig. 9) The canonical Wnt-signalling pathway	17
Fig. 10) Isolation of small tissue pieces and RT-PCR	31
Fig. 11) Generation of cDNA libraries	38
Fig. 12) HF morphogenesis in tail skin proceeds in two distinct waves	45
Fig. 13) Timeline of HF morphogenesis in mouse back and tail skin	46
Fig. 14) Comparison of HF patterning in back and tail skin	47
Fig. 15) Development of the SG in mouse tail skin	49
Fig. 16) Localisation of proliferating cells during HF morphogenesis	50
Fig. 17) Expression of stem and progenitor markers during HF morphogenesis	52
Fig. 18) Dynamic expression of progenitor markers Lrig1 and Sox9 during HF morphogenesis	53
Fig. 19) Sebocytes arise next to Lrig1 positive stem cells	55
Fig. 20) Lrig1 positive cells generate sebocytes by asymmetric cell fate decision	57
Fig. 21) Lrig1 positive cells proliferate to generate sebocytes	59
Fig. 22) Lrig1 positive cells proliferate and give rise to sebocytes	60
Fig. 23) Targeting of epidermal cells using AK15CreER(G)T2 mice	63
Fig. 24) Lineage tracing of IFE cells contributing to SG-development	65
Fig. 25) YFP-positive cells have a higher potential to form colonies <i>in vitro</i>	68
Fig. 26) Histology and proliferation of sebaceous tumours	71

Fig. 27) Microdissection of distinct tumour cell populations	74
Fig. 28) Verification of selected candidate genes	76
Fig. 29) Progenitor cell dynamics during HF and SG morphogenesis	84

9) Table index

Table 1) Chemicals	21
Table 2) Solutions and buffers	22
Table 3) Primary antibodies	23
Table 4) Secondary antibodies	23
Table 5) Kits	23
Table 6) Mouse models applied in this study	24
Table 7) Blocking solutions for immunofluorescence stainings on cryo sections	28
Table 8) Genotyping primers	33
Table 9) PCR primers for cDNA samples (conventional and real time PCR)	33
Table 10) TaqMan probes	35
Table 11) Primers used for cDNA library generation	37
Table 12) Solutions for library generation	37
Table 13) Solutions for Oligonucleotide array hybridisation	39
Table 14) Analysis of progenitor and sebocyte differentiation marker expression in sebaceous tumours	72
Table 15) Significantly regulated genes associated with lipid metabolism (in sebocytes and basal cells versus undifferentiated cells) derived from K14 Δ NLef1/L61Rac1 mice	75
Table 16) Significantly regulated candidate genes identified by oligonucleotid arrays	123

10) List of abbreviations

APC	adenomatous polyposis coli
AP	alkaline phosphatase
BCIP	5-Bromo-4-chloro-3-indolyl phosphate
BMP	bone morphogenetic protein
BrdU	5-bromo-2'-deoxyuridine
cDNA	complementary desoxyribonucleic acid
CFE	Colony forming efficiency
CK1- α	casein kinase 1alpha
DAPI	4',6-Diamidin-2-phenylindol
DEPC	Diethylpyrocarbonate
dH ₂ O	distilled water
Dhcr24	24-Dehydrocholesterol reductase (Seladin1)
DMBA	7,12-Dimethylbenz(a)anthracene
DP	dermal papillae
DTT	Dithiothreitol
E	embryonic day
EDTA	Ethylenediaminetetraacetic acid
EdU	5-Ethynyl-2'-deoxyuridine
EGF	epiderma growth factor
Elovl 3 (4, 6)	Elongation of very long fatty acids like 3 (4, 6)
ER	Oestrogen receptor
EtOH	Ethanol
EYFP	enhanced yellow fluorescent protein
FACS	Fluorescence activated cell sorting
FCS	fetal calf serum
FGF	fibroblast growth factor
Fig	Figure
GapDH	glyceraldehyde-3-phosphate dehydrogenase
gDNA	genomic desoxyribo nucleic acid
GFP	green fluorescent protein
GSK3 β	Glycogen synthase kinase 3 beta
h	hour
H&E	Hematoxylin and Eosin
HF	hair follicle
HG	hair germ
Hh	Hedgehog (Indian-, Sonic-)
HRP	horseradish peroxidase
i.p.	intra peritoneal
IF	immunofluorescence
IFE	interfollicular epidermis
IRS	inner root sheath
Itga6	Integrin alpha 6
K	keratin
K ₂ HPO ₄	Dipotassium phosphate
kg	kilogramm
Lef1	Lymphoid enhancer-binding factor 1 (LEF1)
LGR 4 (5, 6)	leucine-rich repeat containing G protein-coupled receptor 4 (5,6)
Lhx2	LIM/homeobox protein Lhx2
Lrig1	leucine-rich repeats and immunoglobulin-like domains 1

LRP	Low Density Lipoprotein Receptor-related Proteins
M	molar
m	milli
MC5R	melanocortin 5 receptor
MeOH	methanol
mg	milligramm
MgCl ₂	magnesium chloride
min	minute
mRNA	messenger ribonucleic acid
MTS24	mouse thymic stroma 24
NBT	nitro blue tetrazolium
NFATc1	nuclear factor of activated T-cells
NGS	normal goat serum
NGS	normal donkey serum
nt	nucleotide
Nupr1	nuclear protein 1 (P8)
ORS	outer root sheath
P	postnatal day
PBS	phosphate buffered saline
Pcad	P-Cadherin
PCR	polymerase chain reaction
PFA	paraformaldehyde
Plet1	placenta expressed transcript 1
pmol	picomol
PNA	peptide nucleic acid
PPAR γ	peroxisome proliferator-activated receptor gamma
Prom2	Prominin2
rpm	revolutions per minute
RT	room temperature
Scd1	Stearoyl CoA-desaturase 1
SD	sebaceous duct
sec	second
SG	sebaceous gland
sHG	secondary hair germ
Sox9	SRY-box containing gene 9
TAE	Tris-acetate-EDTA
Tam	Tamoxifen
Tcf3	T-cell factor 3
TdT	Terminal deoxynucleotidyl transferase
TGF β R	Transforming growth factor beta receptor
UV	ultra violet
V	Volt
WT	wild type
3'	three prime end of DANN sequence
5'	five prime end of DANN sequence
Δ	deleted / mutated allele
°C	degree Celsius
μ l	micro litre
μ m	micro metre

11) Annex

Table 16) Significantly regulated candidate genes identified by oligonucleotid arrays

Gene symbol	Log2fc (compared to undifferentiated cells)		description
	Sebocytes	Basal cells	
Elovl4	6,1647	5,1824	elongation of very long chain fatty acids (FEN1/Elo2, SUR4/Elo3, yeast)-like 4
Elovl3	5,6606	4,7161	elongation of very long chain fatty acids (FEN1/Elo2, SUR4/Elo3, yeast)-like 3
BLAST: Psapl1	4,4094	3,0819	Prosaposin-like 1
Dhcr24	3,9011	3,1366	24-dehydrocholesterol reductase
Mxd3	-3,589	-3,3542	Max dimerization protein 3
Sfxn1	3,5248	3,331	sideroflexin 1
4632417N05 Rik BLAST: Sdr42e1	3,4086	-	short chain dehydrogenase/reductase family 42E, member 1
Adfp	3,3058	1,76 ns	adipose differentiation related protein
Nupr1	3,227	-	nuclear protein 1
BLAST: Echdc1	3,1871	-	enoyl Coenzyme A hydratase domain containing 1
Scd1	3,117	3,5322	stearoyl-Coenzyme A desaturase 1
Lass4	3,0503	2,3217 ns	longevity assurance homolog 4 (<i>S. cerevisiae</i>)
BLAST: Airn	3,0354	0,0259	antisense Igf2r RNA
Dgat2l6	3,0271	-	diacylglycerol O-acyltransferase 2-like 6
Cdx2	2,874	2,419 ns	caudal type homeo box 2
Upk1b	-2,8714	-1.6053 ns	uroplakin 1B
Pnpla5	2,8461	-	patatin-like phospholipase domain containing 5
Krt79	2,7713	3,4061	keratin 79
BLAST: Whsc1	-2,7636	-1.,3335 ns	Wolf-Hirschhorn syndrome candidate1
4930422G04 Rik	-2,7279	-1,1666 ns	RIKEN cDNA 4930422G04 gene
BLAST:PERP,	2,7252	3,141	TP53 apoptosis effector
BLAST: hypothetical protein	-2,6624	-1,092 ns	-
BLAST: Chr14 genomic contig	-2,6528	-1,4895 ns	-
Dhrs7	2,6066	2,1764 ns	dehydrogenase/reductase (SDR family) member 7
Zfand2b	-2,5674	-1,4192 ns	zinc finger, AN1 type domain 2B
Hmnr	-2,5535	-1,3565 ns	hyaluronan mediated motility receptor (RHAMM)
BLAST: Chr6 genomic contig	-2,52	-1,1593 ns	-

Psm10= Gankyrin	-2,5013	-1,5286 ns	proteasome (prosome, macropain) 26S subunit, non-ATPase, 10
Ttc3	-2,4928	-1,3378 ns	tetratricopeptide repeat domain 3
Chr12 genomic contig	-1,6643 ns	-4,3754	-
BLAST: Prom2	-1,5813 ns	n	Prominin2
Cdc123	-1,7725 ns	-3,6574	cell division cycle 123 homolog (S. cerevisiae)
Elovl6	1,5336 ns	3,5222	ELOVL family member 6, elongation of long chain fatty acids (yeast)
Hbb-b1	-1,2656 ns	-3,5128	hemoglobin, beta adult major chain
Hbb-b2	-	-3,3775	Hemoglobin beta minor chain
Abcb1a	-1,4427 ns	-3,1921	ATP-binding cassette, sub-family B (MDR/TAP), member 1A
Ttr	-	-3,0938	transthyretin
Apoa2	-	-2,9905	apolipoprotein A-II
2610016E04Rik, BLAST: Mup	-	-2,9725	Predicted: Mus musculus similar to Major urinary Protein1
1810011O16Rik	-	-2,9383	RIKEN cDNA 1810011O16 gene
Hba-a1	-1,2302 ns	-2,8858	hemoglobin alpha, adult chain 1
-	-	2,8661	-
Alb1	-	-2,8545	albumin 1
Immt	1,6446 ns	2,8526	inner membrane protein, mitochondrial
Trf	-	-2,8336	transferrin
Sftpc	-1,1951 ns	-2,8333	surfactant associated protein C
Nrl	-	-2,8149	neural retina leucine zipper gene
Hbb-b1	-1,2656 ns	-2,77	hemoglobin, beta adult major chain
Apoa1	-	-2,7663	apolipoprotein A-I
Teddm1	2,0997 ns	2,7459	transmembrane epididymal protein 1
A430005L14Rik	-1,445 ns	-2,7371	RIKEN cDNA A430005L14 gene
Chr2 genomic contig	-	2,7309	-
Hamp1	-	-2,6407	hepcidin antimicrobial peptide 1
Csn3	-	-2,6267	casein kappa

*) ns = not significant; positive values signify up regulation of genes, negative values signify down regulation

Acknowledgements

First of all, I would like to thank Catherin Niemann for the excellent supervision and support during my PhD-thesis and for giving me the opportunity to work on this interesting project.

I would like to thank Prof. Dr. Matthias Hammerschmidt, Prof. Dr. Carien Niessen and Prof. Dr. Günter Plickert for agreeing to build my thesis committee.

Furthermore, I would like to thank all the former and present members of the AG Niemann: Andreas, Claudia, Dagmar, Gilles, Heike B., Heike N., Karen, Monika, Neha, Parisa, Peter, Ramona, Susan and Vera for continuous support, helpful discussions and nice times in the lab and in private life.

Special thanks to Karen and Moni for critically reading the thesis and for continuous encouragement during the writing process.

Furthermore, I would like to thank Wilhelm Bloch (Deutsche Sporthochschule) and his group for giving me the opportunity to use the Laser-Microdissection device. I am grateful to the AG Klein (University Of Regensburg) for teaching me the cDNA-library method and helping evaluating the micro arrays.

Finally, I would like to thank my parents, brother, sister and my friends for their constant support. Finalement, je remercie Cédric pour son soutien constant et sa patience durant ma thèse.

Eidesstattliche Erklärung

Ich versichere, daß ich die von mir vorgelegte Dissertation selbständig angefertigt, die benutzten Quellen und Hilfsmittel vollständig angegeben und die Stellen der Arbeit – einschließlich Tabellen, Karten und Abbildungen-, die anderen Werken im Wortlaut oder dem Sinn nach entnommen sind, in jedem Einzelfall als Entlehnung kenntlich gemacht habe; daß diese Dissertation noch keiner anderen Fakultät oder Universität zur Prüfung vorgelegen hat; daß sie – abgesehen von unten angegebenen Teilpublikationen – noch nicht veröffentlicht worden ist sowie, daß ich eine solche Veröffentlichung vor Abschluß des Promotionsverfahrens nicht vornehmen werde.

Die Bestimmungen dieser Promotionsordnung sind mir bekannt. Die von mir vorgelegte Dissertation ist von Herrn Prof. Dr. Matthias Hammerschmidt betreut worden.

Köln im Mai 2013

Daniela Frances

Nachfolgende Teilpublikationen liegen vor:

Frances. D., Niemann, C. (2012) Stem cell dynamics in sebaceous gland morphogenesis in mouse skin. Dev Biol. 363:138-46.

12) Curriculum vitae

Bildungsweg

03/2008 bis heute	Doktorarbeitsprojekt "Cellular and molecular mechanisms of sebaceous gland morphogenesis and sebaceous tumour formation "im Labor von Dr. Catherin Niemann (CMMC) in Köln
12/2005 – 11/2006	Diplomarbeit im Labor von Prof. Wolfgang Liebl (Genomische und angewandte Mikrobiologie, Universität zu Göttingen)
09/2003 – 11/2005	Hauptstudium in Mikrobiologie, Humangenetik und Botanik an der GEORG AUGUST Universität in Göttingen, Abschluss: Diplom
08/2002 – 07/2003	Hauptstudium an der PAUL SABATIER Universität in Toulouse, Frankreich (ERASMUS-Programm)
10/2000 – 07/2002	Grundstudium in Biologie an der GEORG AUGUST Universität in Göttingen
06/2000	Abitur in Kassel, Note 2,4

Wissenschaftliche Kongresse

09/2010	Teilnahme am „European Workshop on skin stem cells“ (Cambridge, Groß-Britannien)
09/2011	ausgewählt für eine Präsentation auf dem Kongress der „European society of dermatological research“ (Barcelona, Spanien)
11/2011	ausgewählt für eine Präsentation auf der Jahrestagung der deutschen Gesellschaft für Stammzellforschung (GSZ) in Düsseldorf

Publikationen / Preise

- 2012 Frances. D., Niemann, C. (2012) Stem cell dynamics in sebaceous gland morphogenesis in mouse skin. Dev Biol. 363:138-46
- 2012 Gewinnerin des ersten Posterpreises auf dem internationalen Studentensymposium „Crossroads in Biology“ in Köln
- 2012 Mitautorin des Buchkapitels „Lineage tracing of hair follicle stem cells in epidermal whole mounts“ erscheint Ende 2012 in „Skin Stem Cells-Methods and Protocols“ im Springer Verlag